Dissertation

The translation of IP_3-triggered Ca^{2+} release from the ER to the Mitochondria points out the tight connection of the two organelles

Submitted by

MSc, BSc

Olaf Arne Georg Stefan Bachkönig

For the Academic Degree of

Doctor of Philosophy

(PhD)

At the

Medical University of Graz

Institute of Biochemistry and Molecular Biology

Under the Supervision of

Univ.-Prof. Mag.pharm. Dr.rer.nat. Wolfgang F. Graier

2025

Declaration of Academic Integrity

I hereby confirm that the present diploma thesis is the result of my own independent scholarly work. I also confirm that in all cases, where material from the work of others (in books, articles, essays, dissertations, and on the internet) is acknowledged, quotations and paraphrases are clearly indicated. No material other than that cited in the reference list has been used. I have read and understood the Medical University's regulations and procedures concerning plagiarism.

Furthermore, I hereby declare that if artificial intelligence (AI) tools were used for the generation and/or correction of certain text passages in the creation of this work, such employment was conducted in compliance with ethical principles, academic integrity, and the regulations of my university. Additionally, it was ensured that this usage was transparently disclosed and appropriately attributed.

Graz, 11.09.2025 Olaf Bachkönig BSc MSc

Disclosures

Parts of this work have been previously published in:
Bachkoenig O.A., Gottschalk B., Malli R., Graier W.F., 2022. An unexpected effect of risperidone reveals a nonlinear relationship between cytosolic Ca2+ and mitochondrial Ca2+ uptake. pp. 13–35. https://doi.org/10.1016/bs.ctm.2022.09.001

The following co-authors contributed to my first-author publication:

Benjamin Gottschalk[1], Roland Malli[1], Wolfgang F. Graier[1]

[1]Gottfried Schatz Research Center, Molecular Biology and Biochemistry, Medical University of Graz, Neue Stiftingtalstraße 6/6, 8010 Graz, Austria

I confirm that all authors agreed to use their data in my dissertation. Further, Elsevier granted me the rights to reproduce the figures previously published in Bachkoenig et al. (2022).

Danksagung:

An dieser Stelle möchte ich mich bei den Menschen bedanken, die mich in den letzten Jahren unterstützt haben.

Mein größter Dank gilt Wolfgang Graier. Du hast mir ermöglicht mich mit ganzem Herzen der Biologie zu widmen, das bedeutet mir sehr viel. Ich möchte dir auch für deine Unterstützung bei meiner Arbeit danken, und dass du immer ein offenes Ohr für mich hattest.

Auch meiner Familie gilt ein großes Dankeschön. Allen voran meiner Mutter, die mir mit ihrer Resilienz, Ausdauer und Rationalität als immenses Vorbild gilt. Danke dass du mich in jeder erdenklichen Art und Weise, zu jeder Zeit unterstützt hast, und immer tun wirst. Natürlich gilt dies auch für meine Tochter, meine Geschwister und meine Tante. Ohne euch alle wäre dies nicht möglich.

Ich bin auch äußerst dankbar für die Menschen die nicht nur Kollegen, sondern auch meine Freunde sind. Besonders möchte ich hier Helmut Bischof erwähnen, der mich nun schon seit 14 Jahren durch das Laborleben begleitet, ich hoffe es werden noch viele weitere. Ich möchte hier auch Melly, Benni, Martin, Tony, René, Katharina und Corina erwähnen. Danke euch für die interessanten und unterhaltsamen Gespräche, und für die gemeinsame Zeit voller Spaß an unserer Arbeit und abseits davon! Ihr habt mir dabei geholfen nicht nur als Wissenschaftler, sondern auch als Mensch zu wachsen. Danke auch für die gemeinsamen täglichen Trainingseinheiten am Wuzzler, diese waren sehr unterhaltsam und spannend. Ich werde sie vermissen.

Ich möchte mich auch bei Karin Osibow bedanken. Danke für deine endlose Geduld, dein umfassendes Wissen und deine unerschöpfliche Bereitschaft die Studenten des DK-MCD zu unterstützen.

Natürlich möchte ich mich auch bei meinen Freunden abseits des Laboralltags bedanken. Danke für die schönen gemeinsamen Campingurlaube und die sommerlichen Grillabende. Ich habe diese immer sehr genossen, und freue mich auf die kommenden. Danke an meinen Bruder Gunnar, und unsere Freunde Michael und Jürgen für die Konzerte die wir gemeinsam besucht haben. Das waren immer Highlights an die ich sehr gerne zurück denke. Mögen noch viele weitere folgen.

Des Weiteren möchte ich mich bei meinem Biologielehrer, Bernhard Schleich bedanken. Sie waren der erste der meine bedingungslose Liebe für die Biologie und andere Wissenschaften geweckt und genährt hat.

Danke an euch alle für eure Ermutigungen, eure Bekräftigungen und eure Unterstützung.

Acknowledgements

During my work as a student, I received support from the Austrian Science Fund (FWF) (DK-MCD W1226 to W.F.G.), the MEFO Graz (to W.F.G.), and Nikon Austria (to W.F.G.)

I want to express my appreciation for the international PhD program “Metabolic and Cardiovascular Diseases”.

Table of contents

Zusammenfassung

Mitochondrien spielen eine wesentliche Rolle in der zellulären Ca^{2+}-Regulation. Sie dienen als Ca^{2+}-Puffer, initiieren apoptotischen Zelltod, und sind ein zentrales Element des Stoffwechsels. Die Aufnahme von Ca^{2+} in die mitochondriale Matrix wird stark durch den mitochondrialen Calcium-Uniporter, einem Multiproteinkomplex in der inneren Mitochondrienmembran, reguliert. Dieser Komplex besteht aus dem porenbildenden Protein MCU, der dominanten negativen Untereinheit MCUb, seinem essenziellen Regulator EMRE, den sogenannten Torwächtern MICU1 und 2, dem Gerüstprotein MCUR1 und, unter bestimmten Umständen wie in Krebs oder Altern, die Entkopplungsproteinen UCP2/3. Die Öffnung des MCUC wird durch lokale Ca^{2+}-Erhöhungen erreicht, die zur Ca^{2+}-Bindung an die Ca^{2+}-Bindungs-Domänen der MICUs und zu einer anschließenden Konformationsänderung und MCU Aktivierung führen. In dieser Arbeit haben wir die Übertragung von zytosolischen Ca^{2+}-Signalen zu den Mitochondrien aus verschiedenen Quellen, dem endoplasmatischen Retikulum (ER) und dem Speicher-regulierten Ca^{2+} Einstrom (SOCE), untersucht. Wir verwendeten verschiedene Konzentrationen des IP_3-erzeugenden Mittels Histamin und des Antipsychotikums Risperidon, das neben seiner Hauptwirkung auch eine antihistaminische Wirkung am H1-Histamin-Rezeptor hat, und korrelierten die Veränderungen der Signale im Zytosol mit denen in den Mitochondrien. Wir fanden eine Bestätigung für einen notwendigen zytosolischen Ca^{2+}-Schwellenwert zur Aktivierung der mitochondrialen Ca^{2+}-Aufnahme und Unterstützung für die Hypothese quellabhängiger mitochondrialer Ca^{2+}-Sensitivität.

Abstract

Mitochondria play an essential role in cellular Ca^{2+} signaling. They serve as Ca^{2+} buffers, initiate apoptotic cell death, and are a central hub for cellular metabolism. The uptake of Ca^{2+} into the mitochondrial matrix is highly regulated by the mitochondrial calcium uniporter complex (MCUC), a multiprotein complex in the inner mitochondrial membrane. The MCUC consists of the pore-forming protein MCU, the dominant negative subunit MCUb, its essential regulator EMRE, the so-called gatekeepers MICU1 and 2, the assembly factor MCUR1, and, under certain conditions like cancer or aging, the uncoupling proteins UCP2/3. Opening of the MCUC is facilitated by local Ca^{2+} hotspots, which lead to Ca^{2+} binding to the EF-hand domains of the MICUs and a subsequent conformational change. In this work, I studied the translation of cytosolic Ca^{2+} signals from different sources, including the endoplasmatic reticulum (ER) and extracellular space via the store-operated Ca^{2+} entry (SOCE), to the mitochondrial matrix. I used different concentrations of the IP_3-generating agent histamine and the antipsychotic drug risperidone, which exhibits antihistaminic side effects, and correlated the changes in cytosolic Ca^{2+} signals with those in the mitochondrial matrix. My results confirm the necessity of a cytosolic Ca^{2+} threshold for achieving activation of mitochondrial Ca^{2+} uptake and support the hypothesis of source-dependent mitochondrial Ca^{2+} uptake.

1 Introduction

The general perception of the role of mitochondria in regulating the Ca^{2+} homeostasis of the cell changed dramatically over the years. During the 1960s it was shown that mitochondria isolated from liver, heart, and kidney tissue accumulate Ca^{2+} in dependence on ATP or substrates of the tricarboxylic acid (TCA) cycle, and it was thought that mitochondria serve as cellular Ca^{2+} deposit (Brierley et al., 1964; Carafoli Ernesto et al., 1965; Vasington and Murphy, 1962). Even though it was published that sarcoplasmic reticulum (SR) fractions isolated from cardiac and uterine muscle cells free of mitochondria also show an ATP- and Mg^{2+}- dependent uptake of Ca^{2+} that exceeded the mitochondrial Ca^{2+} uptake (Carsten, 1969, 1964), in 1983 the endoplasmic reticulum (ER) was identified as the primary Ca^{2+} store of cells, when Streb et al. showed in their groundbreaking work that inositol-1,4,5-triphosphate (IP_3) leads to non-mitochondrial Ca^{2+} release (Streb et al., 1983). A few years later, Putney et al were able to show that the release of Ca^{2+} from the ER also stimulates the influx of Ca^{2+} into the cell (Putney, 1986; Takemura et al., 1989). This led to the conclusion that the signal molecule IP_3 does not only control ER Ca^{2+} release but also cellular Ca^{2+} uptake. When the release of Ca^{2+} from the ER by IP_3 receptors was studied, people described different events of Ca^{2+} release into the cytosol. The smallest, so-called blips, were described as single activated channels, while puffs were created by several receptors that accumulate in close proximity. The biggest IP_3-triggered events are global Ca^{2+} signals that affect the whole cell. (Bootman and Berridge, 1996; Horne and Meyer, 1997; Parker et al., 1996; Parker and Yao, 1996) Independent of the size of the Ca^{2+} signal, the IP_3-receptor needs IP_3 and Ca^{2+} to be activated. The first release of Ca^{2+} from an IP_3 receptor leads to propagation of the signal by local increases of cytosolic Ca^{2+}, which is why the Ca^{2+} rise in the cytosol happens with a short delay after IP_3 generation (Matsu-ura et al., 2019a). But Ca^{2+} is not only reported as a necessary ligand for IP_3 mediated Ca^{2+} release. High Ca^{2+} concentrations are also reported to have an inhibitory effect on IP_3 receptors. (Emily A Schmitz et al., 2022)

When the ER was identified as the primary Ca^{2+} deposit, it was already known that Ca^{2+} played a crucial role in the regulation of mitochondrial metabolism, especially in the activity of enzymes of the TCA cycle. The knowledge of the importance of mitochondrial Ca^{2+} for the cellular metabolism raised the question of the molecular basis of mitochondrial Ca^{2+} uptake, and the search for the pore-forming protein MCU. Today, we know several proteins that participate in individual roles in the facilitation and regulation of the multi-protein complex MCUC. The structure of this multi-protein complex allows precise fine-tuning of the mitochondrial Ca^{2+}

homeostasis via several different mechanisms, like changes in the Stoichiometry of the proteins or posttranslational modifications. One protein that is famous for its role in the regulation of mitochondrial Ca^{2+} uptake is MICU1 (Giacomello et al., 2010; Gottschalk et al., 2022b; Mallilankaraman et al., 2012b; Xing et al., 2019), since it establishes a threshold that needs to be exceeded to allow Ca^{2+} to enter the mitochondrial matrix. This is achieved by local Ca^{2+} hotspots at the interface of mitochondria with the ER, commonly known as Mitochondria – ER contacts.

Apart from its role as a regulator of mitochondrial activity, Ca^{2+} ions participate in the induction of apoptotic cell death. There are several reports that connect mitochondrial Ca^{2+} overload with mitochondrial permeability transition pore (mPTP) formation, mitochondrial swelling and cytochrome C release into the cytosol, thus inducing the intrinsic pathway of apoptosis. This explains as well the importance of the tight regulation of Ca^{2+} uptake into the mitochondrial matrix.

The research on mitochondrial Ca^{2+} homeostasis and the molecular basis for the uptake of Ca^{2+} ions into the mitochondrial matrix revealed not only the sophisticated regulation of the MCUC, but also its participation and changes under pathologies. The knowledge about the importance of mitochondrial Ca^{2+} homeostasis in physiological processes and their changes under pathological conditions points out fundamental causes of diseases and new targets for therapies.

In this work, I studied the transport of Ca^{2+} from the ER and the extracellular space into the mitochondrial matrix. To do this, I compared Ca^{2+} signals stimulated with different concentrations of an IP_3-generating agent versus the inhibition of the corresponding G-protein coupled receptor in the cytosol and the mitochondrial matrix in the endothelial cell line EA.hy926.

1.1 Mitochondria, Ca^{2+} and apoptosis

Mitochondria play a central role in controlling cell death pathways. In apoptotic cell death, the formation of the mitochondrial permeability transition pore (mPTP) plays a crucial role. Opening of the mPTP leads to mitochondrial swelling, dissipation of the mitochondrial membrane potential ($\Delta\psi_M$) and release of cytochrome C and other components of the mitochondrial matrix into the cytosol, which further activates initiator caspase 9. Caspase 9 subsequently activates the executioner caspases 3/7, leading to apoptosis (D'Arcy, 2019).

The molecular components of the mPTP have long been under discussion. One protein that needs to be mentioned in this regard is cyclophilin D (CpD) (Nakagawa et al., 2005), which is a Ca^{2+}-sensitive protein that regulates mPTP formation and is thus called mPTP sensitizer. The inhibition of mPTP formation by CsA is mediated by its interaction with CypD (Connern and Halestrap, 1992). Since it was already known that this protein is involved in the regulation of mPTP formation, CypD was used to look for interaction partners that form the pore. The first protein that was identified was the Adenine nucleotide translocator (ANT) (Brustovetsky and Klingenberg, 1996; Halestrap and Brenner, 2003; Halestrap, 2004; Halestrap and Davidson, 1990; WOODFIELD et al., 1998). Leading to the generell view that the ANT in the IMM forms with VDAC in the OMM the mPTP. But since Bongkrekic acid, an inhibitor of the ANT, and CsA inhibited Ca^{2+} induced swelling of mitochondria, which is a sign for mPTP opening, doubt was raised about ANT as the molecular basis for the mPTP. Since it was shown that ANT ko cells were still able to perform CsA-sensitive mPTP opening, this doubt was reinforced (Halestrap and Davidson, 1990; Kokoszka et al., 2004).

Later it was shown that the F_OF_1-ATP Synthase participates in mPTP formation. (Bonora et al., 2013; Carraro et al., 2014; Giorgio et al., 2013; Mnatsakanyan et al., 2019; Morciano et al., 2018; Neginskaya et al., 2019). While multiple reports confirmed the contribution of the ATP Synthase to mPTP, it remains unclear whether the whole complex contributes to the pore as a monomer (Mnatsakanyan et al., 2019), dimer (Carraro et al., 2014; Giorgio et al., 2013) or multimers of the c-subunit (Bonora et al., 2013; Morciano et al., 2018; Neginskaya et al., 2019). Regardless of the exact nature of the participation of ATP Synthase in mPTP formation, it explains the occurrence of CsA-sensitive apoptosis in VDAC and ANT double ko (Zorov et al., 2009), since the inhibition of CypD allowed the prevention of mPTP opening and the subsequent initiation of apoptotic cell death.

Frequently, simplifications about the causality between mitochondrial Ca^{2+} overload as a trigger of mPTP opening and apoptotic cell death are found in the literature (Baumgartner et al., 2009; Zhou et al., 2022). However, several publications show that a supramaximal stimulation with IP_3-mobilizing agents does not cause initiation of apoptosis (Bachkoenig et al., 2022; Madreiter-Sokolowski et al., 2016b; Waldeck-Weiermair et al., 2010b) and even an increase of the mitochondrial calcium uptake (mtCU) with resveratrol did not change that (Madreiter-Sokolowski et al., 2016a). On the contrary, it has been published that the fertilization of mouse oocytes results in strong repetitive Ca^{2+} oscillations, which play an important role in the activation of the cell (Matsu-ura et al., 2019a; Swann and Yu, 2008). Moreover, shRNA-mediated knockdown of MICU1, the gatekeeper of mitochondrial Ca^{2+} uptake, does not lead to cell death despite a strong increase in mitochondrial Ca^{2+} levels under

basal conditions, but the susceptibility of the cells was increased towards proapoptotic stimuli (Mallilankaraman et al., 2012b). These data go along with the viability data of MICU1-ko mice (Antony et al., 2016). Antony et al. showed that MICU1-ko mice died shortly after birth, and as the genotype of the born animals followed a Mendelian distribution, intrauterine mortality could be excluded (Antony et al., 2016). In 2001 Pacher and Hajnóczky showed that they could induce apoptosis by mobilizing Ca^{2+} from the SR in cardiac myotubes using 30µM $CaCl_2$ after they treated the cells with C2 ceramide or ethanol to induce proapoptotic signals. These studies nicely showed that Ca^{2+} signaling alone is not sufficient to induce mPTP opening and apoptosis alone, but essentially requires the presence of yet unknown proapoptotic signals, like possibly Bax/Bak proteins which are needed to establish mitochondrial outer membrane permeabilization, mitochondrial swelling and rupture (Karch et al., 2013).

1.2 Ca^{2+} and the mitochondrial metabolism

The most prominent metabolic pathway in the mitochondrial matrix is the tricarboxylic acid cycle (TCA cycle). Compared to other pathways, there is not one enzyme-mediated rate-limiting step that is crucial for the kinetics of metabolite throughput, but the concentrations of adenosine-5'-diphosphate (ADP)/ATP, redox equivalents, including $NADH^+$, $H^{+,}$ or $FADH_2$, the availability of acetyl-Coenzyme A (acetyl-CoA) and the matrix Ca^{2+} concentration regulate the pace. It gets fueled by metabolites from carbohydrate-, amino acid-, and lipid-degradation, and its energetic outputs are GTP, $FADH_2$, and NADH + H^+. The latter two are subsequently used in the electron transport chain to establish the electrochemical gradient, known as membrane potential ($\Delta\psi_M$), which is essential for ATP production (MITCHELL, 1961).

The connecting step between glycolysis and the TCA cycle is the conversion of pyruvate to acetyl-CoA. This is catalyzed by the multienzyme complex, the pyruvate dehydrogenase (PDH), which is under the control of cytosolic Ca^{2+} that controls its phosphorylation status and, thus, its activity (**fig. 1**). The PDH is dephosphorylated by the Pyruvate dehydrogenase phosphatase (PDP), leading to its activation. The activity of PDP was shown to be dependent on extracellular Ca^{2+} in multiple tissues, including the heart, liver, and brain (Denton, 2009; Huang et al., 1998). By a high activity of PDP, a high activity of PDH is assured. Pyruvate that is generated in glycolysis is directly transformed to acetyl-CoA and transported into the mitochondrial matrix, where it fuels the TCA cycle, thus representing one way how mitochondrial metabolism is controlled by cytosolic Ca^{2+}.

One of the enzymes of the TCA cycle that is directly dependent on Ca^{2+} is the isocitrate dehydrogenase (IDH). It converts isocitrate to α-Ketoglutarate while producing CO_2 and reducing NAD^+ to NADH (**fig. 1**). In 1978, Denton et al. showed in isolated mitochondria from the rat heart that this enzymes activity depends on the availability of Ca^{2+} (Denton et al., 1978). This was confirmed and refined later by Rutter et al., who showed that the enzymes affinity for Ca^{2+} depends on the ADP/ATP ratio and increases with rising ADP levels. Since it has no Ca^{2+} binding domain like EF-hands, it is likely that Ca^{2+} directly bind in the catalytic domain of the protein (Rutter and Denton, 1989, 1988a).

Similar results were found when α-Ketoglutarate dehydrogenase, another enzyme of the TCA cycle. Its activity was found to be increased with high ADP/ATP ratios. The availability of NAD^+ lowers the K_d for Ca^{2+}, and Ca^{2+} lowered the K_M value of the enzyme in isolated mitochondria from rat adipose tissue, liver, and kidney (Lawlis and Roche, 1981; McCormack and Denton, 1979; Rutter and Denton, 1988b) (**fig. 1**). Altogether, these findings indicate that the enzyme is activated at reduced energy status and stimulated Ca^{2+} signaling.

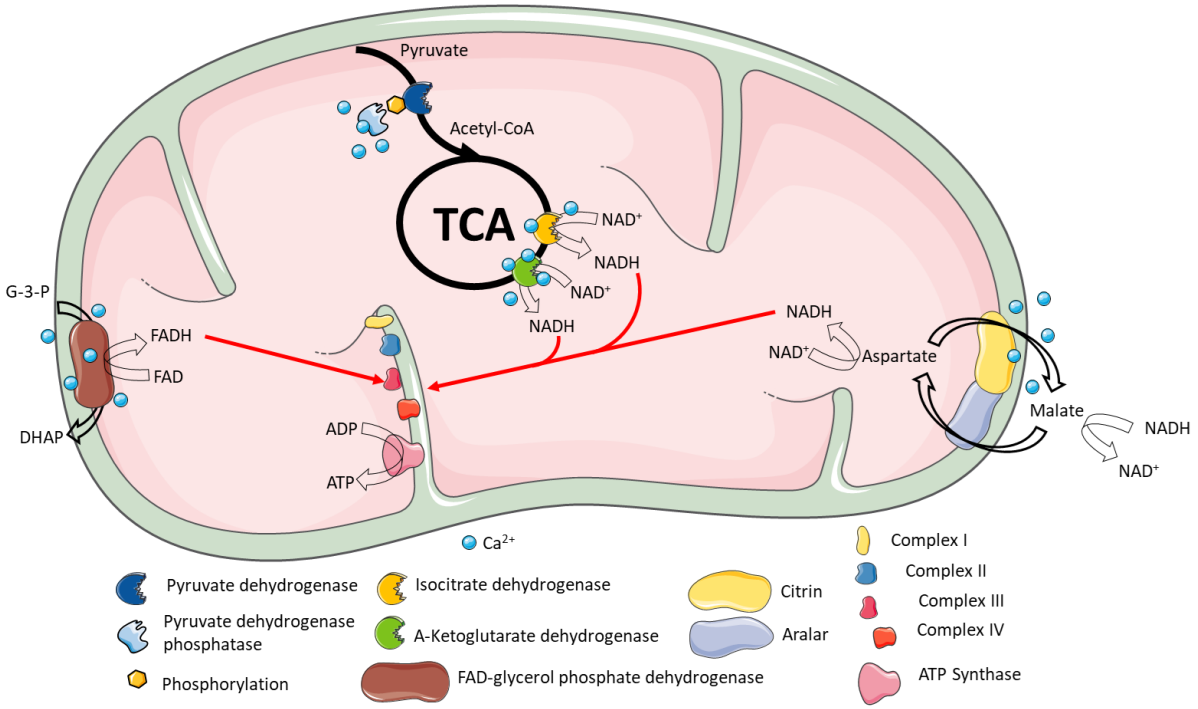

Figure 1 mitochondrial activity and Ca^{2+} In this scheme the Ca^{2+} dependent steps in mitochondrial metabolism are depicted, Acetyl-Coenzyme A (acetyl-CoA), Nicotinamide Adenine Dinucleotoide (NAD^+/NADH), Adenosin-5´-diphosphate (ADP), Adenosin-5´-triphosphate (ATP), flavin adenine dinucleotide (FAD/$FADH_2$), glycerol 3-phosphate (G-3-P), dihydroxyacetone phosphate (DHAP), tricarboxylic acid cycle (TCA), figures were generated in Microsoft PowerPoint with images from Servier Medical Art (https://smart.servier.com/)

But not only enzymes of the TCA cycle have been shown to depend on Ca^{2+} in their activity. The FAD-glycerol phosphate dehydrogenase (GPD2) is located at the outside of the IMM and catalyzes the conversion of glycerol 3-phosphate to dihydroxyacetone phosphate. In this reaction, also FAD/$FADH_2$ is needed. GPD2 uses FAD as a coenzyme and provides $FADH_2$ to fuel the electron transport chain (Ou et al., 2006) (**fig. 1**). GPD2 has been shown to have EF-hand domains, and mutations that diminish Ca^{2+} binding have a severe effect on its functionality (Novials et al., 1997) while its cytosolic isoform seems to be independent of Ca^{2+}.

Other proteins in the IMM that have been shown to be Ca^{2+} sensitive are the glutamate–aspartate shuttles, citrin and aralar (Contreras et al., 2007; Koshenov et al., 2022; Mármol et al., 2009) (**fig. 1**). These transporters connect cytosolic with mitochondrial NAD^+/NADH levels. While it restores NAD^+ in the cytosol, where it is needed for glycolysis, it ensures that malate in the mitochondrial matrix can be converted to oxaloacetate, a step in which NAD^+ is converted to NADH, which can subsequently be used to fuel the electron transport chain. Koshenov et al showed that this shuttle is sensitive to minor changes in intermembrane space (IMS) Ca^{2+} levels, leading to metabolic rewiring, which can be rescued with pyruvate supplementation (Koshenov et al., 2022). Consequently, bypassing the NAD^+-dependent steps of glycolysis and directly fueling the TCA with substrates restored the metabolic phenotype, pointing towards a need for efficient glucose utilization in epithelial cells under basal conditions. Since other steps in the TCA cycle were not affected in the nominal absence of extracellular Ca^{2+}, it can be concluded that the dependency of mitochondrial dehydrogenases on Ca^{2+} does not play a pivotal role under basal conditions, but may be important under stimulation i.e. IP_3 induced Ca^{2+} release from the ER.

In sum, Ca^{2+} plays an important role in the modulation of mitochondrial metabolism, by fine-tuning the activity of several proteins depicted in **figure 1**. In this way, the whole cells energy homeostasis and metabolite turnover is controlled.

1.3 The mitochondrial Calcium uniporter complex –MCUC

1.3.1The Pore-forming proteins: Component A: The Mitochondrial Calcium Uniporter (MCU)

Despite mitochondrial Ca^{2+} signaling being investigated for a long time, the protein that forms the pore and thus allows Ca^{2+} to pass the IMM was not identified until 2011, but then by two independent groups in the same issue of the renowned journal Nature (Baughman et al., 2011; De Stefani et al., 2011). Both groups used MICU1, which was already known to regulate mitochondrial Ca^{2+} uptake, to find potential candidates for the pore-forming MCU protein. In both papers, it was shown that the knockdown of MCU abolished mitochondrial Ca^{2+} uptake after stimulation with an IP_3-generating agent, while the membrane potential was unchanged. While Baughman et al. supported their findings via calcium green measurements, identified three amino acids that are essential for MCUs function, and proved that the inhibition of mitochondrial Ca^{2+} uptake by Ruthenium 360 depends on MCU (Baughman et al., 2011), De Stefani et al. used overexpression to show increased mtCU, used patch clamp measurements to investigate the opening of MCU and demonstrated its inhibition by ruthenium red (De Stefani et al., 2011). Moreover, they also found changes of mitochondrial Ca^{2+} uptake mediated by two point-mutations in the loop between MCUs' two transmembrane domains. Two years later, Pan et al. created an MCU knockout mouse and characterized it (Pan et al., 2013). The body weight of the mice did not change, and the weight of the organs relative to the body weight remained unchanged. Interestingly, MCU KO mice, however, showed a reduced skeletal muscle peak performance in physical exercises. Moreover, when they investigated ischemia-reperfusion injuries in the heart, they found no significant differences between WT and KO animals in the rate-pressure product nor the infarct area, but the hearts of KO mice were immune to the rescuing effect of CsA (Pan et al., 2013).

In 2013, a dominant negative subunit of MCU was found and named MCUb. Raffaello et al found that MCU forms multimers that can be homogenously formed by MCU or heterogeneously together with MCUb (Raffaello et al., 2013). The study of the expression of the two proteins in different tissues showed that there can be vast differences between different cell and tissue types (e.g. higher ratios of MCU to MCUb in skeletal muscle, lower ratios in heart and lung), which fit the computational model of tetrameric MCU pores. This model was later confirmed in multiple structural studies (Baradaran et al., 2018; Fan et al., 2018; Nguyen et al., 2018; Yoo et al., 2018). In general, MCU shows higher expression than MCUb. Sequence comparison between the sequences of the transmembrane domains and the loop unravelled amino acids that are fundamental for the function of the MCU protein. These amino acids were unchanged in MCUb, but they found two other amino acids that were different in seven different species of vertebrates. When MCUbs effect on mtCU was studied opposite effects for MCUb compared to MCU in knockdown and overexpression were found. An exchange of the two amino acids at positions D251 and E256 yielded effects comparable to the mutations used in their first paper on MCU, as mtCU was decreased

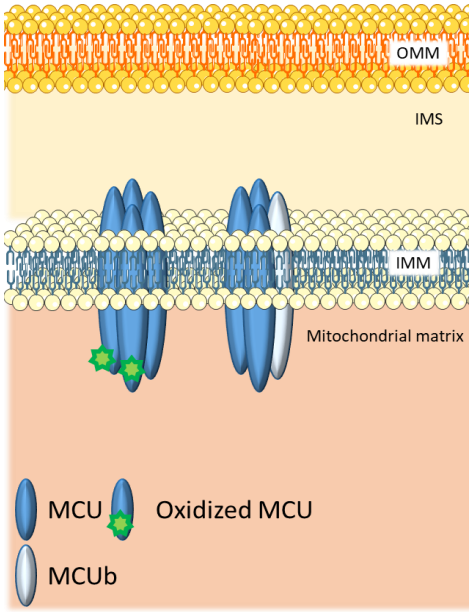

Figure 2 the pore-forming protein MCU is located in the IMM where it forms either homotetramers or heterotetramers with MCUb, during high mitochondrial activity MCU gets oxidized which is associated with increased mitochondrial Ca2+ uptake.
Adapted from (Baughman et al., 2011; De Stefani et al., 2011; Dong et al., 2017) figures were generated in Microsoft PowerPoint with images from Servier Medical Art (https://smart.servier.com/)

Regulation of MCU via oxidation

Since mitochondrial Ca^{2+} levels and their metabolic activity are tightly connected, Dong et al. investigated the regulation of the MCUC in the oxidative milieu. (Dong et al., 2017) They screened the proteins known to participate in the formation of the complex and found MCU as the sole target for oxidation. When they treated the cells with LPS or H_2O_2 they saw an increase in mitochondrial Ca^{2+} uptake, while the cytosolic signals remained unchanged. This effect could be reversed by overexpression of mangan superoxid dismutase or peroxiredoxin 3. Moreover, they identified the cysteine residue 97, in the N-terminal domain, which is located

in the matrix, to be the locus for reversible S-gluthathionylation. This posttranslational modification was identified as a positive feedback loop, where proinflammatory signals lead to increased mitochondrial ROS production, which stimulated MCU oxidation followed by increased mtCU. This increased mitochondrial activity led to mitochondrial swelling, translocation of the MCU to the IBM and sensitization towards cell death.

1.3.2 The Pore-forming proteins: Component B: The essential MCU regulator – EMRE

The protein termed essential MCU regulator, EMRE, is a small 10 kDa protein that has a transmembrane domain, is located in the IMM, interacts with MCU and is required for the proper formation of the channels pore and its further interaction with MICU1 proteins. Moreover, its downregulation abolishes mtCU efficiently (Sancak et al., 2013). Wang et al showed, that four molecules of EMRE are found in each MCU channel. (Wang et al., 2019) They found that MCU and EMRE interact in the transmembrane domain (TMD) of the two proteins, and additionally with the N-terminal β-hairpin of EMRE which interacts with the coiled-coil domain of a different MCU molecule in the pore. In a later study, it was revealed that the number of EMRE molecules in the MCUC varies in many tissues. (Watanabe et al., 2022) Experiments to identify the orientation of EMRE in the IMM showed that its C-terminal domain faces the IMS, and the N-terminal domain faces the mitochondrial matrix. Moreover, it has been shown that EMRE participates in the connection between MCU and MICU1 via the conserved C-terminal polyaspartate region (Tsai et al., 2016)

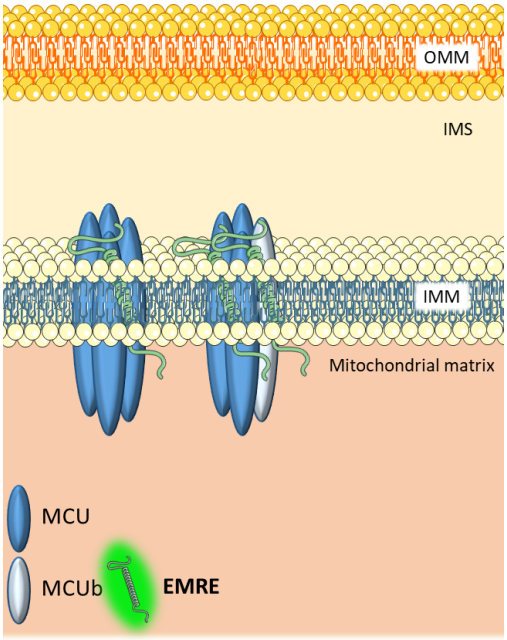

Figure 3 EMRE is a small single membrane pass protein that interacts with MCU and MICU1
adapted from (Wang et al., 2019; Watanabe et al., 2022) figures were generated in Microsoft PowerPoint with images from Servier Medical Art (https://smart.servier.com/)

1.3.3 Mitochondrial Calcium Uniporter Regulator 1 – MCUR1

In 2012, an RNAi screen of mitochondrial membrane proteins identified MCUR1 as an important protein for mtCU (Mallilankaraman et al., 2012a). The screening showed that its knockdown did not alter cytosolic Ca^{2+} signals, but strongly diminished the translation of cytosolic Ca^{2+} into the mitochondrial matrix. Interestingly, downregulation of MCUR1 increased the expression of MCU in HeLa cells, but the increased presence of MCU could not rescue histamine-induced mitochondrial Ca^{2+} signals, nor could the overexpression of MCUR1 rescue the MCU-KD diminished mitochondrial Ca^{2+} transients (Mallilankaraman et al., 2012a). This shows that both proteins are essential proteins to allow Ca^{2+} to pass the IMM, and that proper mtCU can only happen in the presence of both proteins. These findings were further supported by cellular bioenergetic studies (Chaudhuri et al., 2016; Tomar et al., 2016). The knockdown of MCUR1 shifted the adenosine-5'-monophosphate (AMP)/ATP ratio in HeLa cells towards AMP, and the basal oxygen consumption rate (OCR) was reduced, while the maximal rate was unchanged. Moreover, phosphorylation of AMPK was strongly increased in MCUR1-shRNA-expressing cells, which is a strong indicator for low cellular energy levels. These findings were later also supported by patch clamp measurements of MCU activity in mitoplasts, as MCU conductance strongly depended on MCUR1 expression (Tomar et al., 2016; Vais et al., 2015). In a subsequent study, tissue-specific MCUR1-KO mice were created, where the KO of MCUR1 in cardiomyocytes and endothelial cells led to a reduced Ca^{2+} uptake into the mitochondrial matrix. Moreover, the proliferation and migration rate of endothelial cells were reduced (Tomar et al., 2016). Further, they investigated the interaction of MCUR1 with other proteins of the MCUC and found that MCUR1 did not only pull down MCU but also EMRE (Tomar et al., 2016). Also, the MCU multimers were investigated, and it was shown that the absence of MCUR1 led to a shift towards lower molecular weight, i.e. complexes with a lower number of MCU molecules. Based on these data, the authors concluded that MCUR1 acts in the MCUC as a scaffolding protein, ensuring proper MCUC structure and function. Even

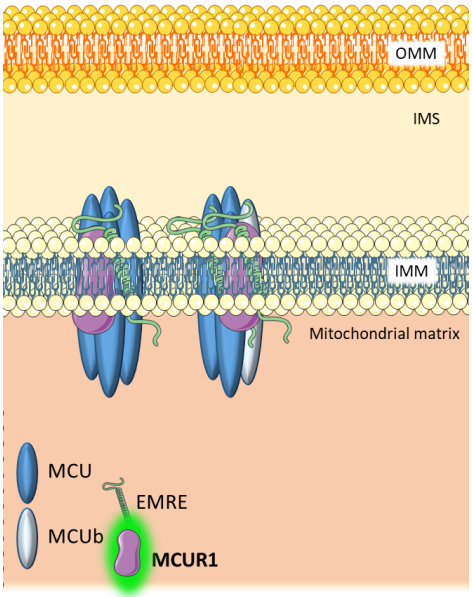

Figure 4 MCUR1 is a scaffolding protein that contributes to MCUC structure and function
Adapted from (Mallilankaraman et al., 2012a; Tomar et al., 2016) figures were generated in Microsoft PowerPoint with images from Servier Medical Art (https://smart.servier.com/)

though the $\Delta\psi_M$ was not changed in MCUR1-KO cells, this protein plays an important role in the cells bioenergetics, since ATP levels and OCR were altered (Tomar et al., 2016).

1.3.4 The Gatekeepers of mitochondrial Ca^{2+} Uptake – MICU 1,2 and 3

One of the most intensely studied proteins that is part of the MCUC is the mitochondrial calcium uptake protein 1 (MICU1). In 2010, Perrochi et al reported to have identified a protein that is located in the mitochondria, has two EF-hand domains and its knockdown abolishes Ca^{2+} uptake into the mitochondria from both, active Ca^{2+} release from the ER and upon inhibition of the sarcoplasmic/ endoplasmic reticulum Ca^{2+} ATPase (SERCA). MICU1 is expressed in a broad range of tissues and cells (Perocchi et al., 2010).

In the following studies MICU1 was shown to act in the MCUC as a kind of gatekeeper, allowing Ca^{2+} inflow in a concentration-dependent way. This is mediated by its EF-hand domains, which, by their affinity for Ca^{2+}, define a threshold that needs to be overcome to initiate mtCU. To overcome this threshold, subcellular Ca^{2+} release happens in a spatially limited way, so-called hotspots, that create microdomains with high concentrations of Ca^{2+}, ultimately allowing mtCU (Giacomello et al., 2010). Through studying its crystalline structure, it has been revealed that MICU1 forms hexamers in the absence of Ca^{2+}, which are dissipated into homo- or heterodimers with MICU2 and MICU3 upon Ca^{2+} binding to the EF hands of MICU1 (Wang et al., 2014). With this change in the oligmeric stoichiometry, also a functional change goes along. While in the hexameric form, MICU1 participates in the formation of the cristae junction, it colocalizes with

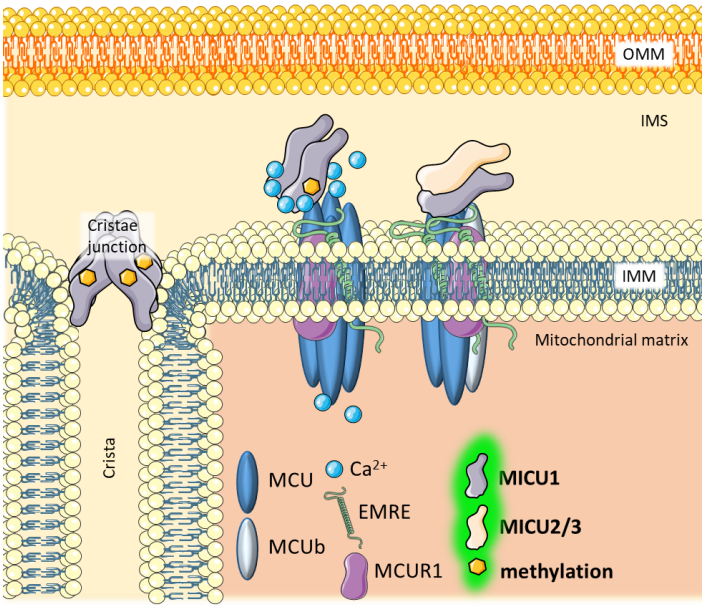

Figure 5 the gatekeeping proteins MICU1, 2 and 3 are located in the IMS and associate as homo- or heterodimers with MCU. Binding to their EF-hand domains facilitate opening of the pore and allow Ca2+ influx, when no Ca2+ is bound MICU1 forms hexameres and participate in CJ formation, adapted from (Perocchi et al., 2010; Gottschalk et al., 2022) figures were generated in Microsoft PowerPoint with images from Servier Medical Art (https://smart.servier.com/)

MCU in the inner boundary membrane in its dimeric form (Gottschalk et al., 2022b, 2019; Petrungaro et al., 2015). In 2016 Madreiter-Sokolowski et al showed that an asymmetric dimethylation of MICU1 by PRMT1 led to a change of MICU1s Ca^{2+} affinity from an EC_{50} of 4.4 µM towards 18.5 µM, which was rescued by the interaction with the uncoupling proteins 2 and 3 (UCP2/ UCP3). (Bachkoenig et al., 2022; Madreiter-Sokolowski et al., 2016b; Waldeck-Weiermair et al., 2015) The knowledge about MICU1s role in proper mitochondrial function was further broadened by Gottschalk et al in 2019 (Gottschalk et al., 2019). The authors showed the dynamic changes in the localization of MICU1 and other proteins of the MCUC and their dependency on changes in intracellular Ca^{2+} levels. Moreover, they presented data that show the importance of MICU1 for the stability of the cristae junction (CJ) and that the loss of MICU1 leads to a widening of it, which was associated with a change in cytochrome c localization from the cristae lumen (CL) to the IBM. Later on, this was further refined, showing that MICU1s participation in the CJ controls the restriction of the membrane potential to the CL, and the dynamic process of MCU translocation from the CL to the IBM explains the different kinetics in mtCU in HeLa cells (Gottschalk et al., 2022b).

Like MICU1, MICU2 is expressed in various tissues. It has been identified by its homology to MICU1. MICU1 interacts with MCU by electrostatic charges. While MCU has negative charges in the D-ring of its DIME domain, MICU1 has positive charges in the DIME-interacting domain. MICU2 lacks these residues, which fits with the reports that MICU2 depends on dimerization with MICU1 to interact with MCU (Paillard et al., 2018; Phillips et al., 2019a).

MICU3 is expressed only in a few tissues, and most prominently in the central nervous system. Like the two other paralogs, it has two EF-hand domains and resides in the IMS. While MICU1 was characterized as a regulator of mtCU with a rather decreasing effect, MICU3 has been shown to increase the uptake of Ca^{2+} into the mitochondrial matrix, and to accelerate the translation of cytosolic to mitochondrial Ca^{2+} transients (Patron et al., 2019a).

Regulation of MICU1 by phosphorylation

Besides the methylation of MICU1 at arginine 455, its phosphorylation on serine 124 is a posttranslational modification allowing to adjust the mitochondrial Ca^{2+} homeostasis. (Marchi et al., 2019) Marchi et al. showed that a phosphomimetic mutant of MICU1 allowed a similar mitochondrial Ca^{2+} uptake as observed in MICU1 knockdown cells under SERCA inhibition, pointing towards a lower threshold for mtCU. Interestingly the Ca^{2+} signals during histamine stimulation were unchanged. Further they demonstrated in their work that the overexpression

of a constitutively active form of AKT leads to a shift from mature MICU1 towards a precursor/intermediate form of MICU1, which lacked proteolytic cleavage steps in the protein's maturation. Moreover, it was shown that the half-life of the immature MICU1 was strongly reduced. When these changes in the maturation and stability of MICU1 were prevented with the non-phosphorylatable mutant of MICU1 in xenograft tumours, the number, volume and weight of tumours was reduced, pointing towards a higher susceptibility for proapoptotic signals This idea is further supported by the observed increased basal Ca^{2+} levels in cells expressing the phosphomimetic mutant of MICU1

1.3.5 The uncoupling proteins 2 and 3 – UCP

The first proteins that were identified to participate in mtCU were UCP2 and UCP3 in 2007 by Trenker et al (Trenker et al., 2007). Since they were annotated due to their sequence similarity to their paralog UCP1, these proteins were expected to function in a similar way, uncoupling the electron transport chain (ETC) from ATP synthesis. But instead of the expected negative effect of UCP2/3 overexpression on the mtCU, the opposite was found, and the downregulation of the two proteins strongly decreased the histamine induced Ca^{2+} transients in EA.hy926 cells. Interestingly, the intermembrane loop 2 which is identical in UCP2 and UCP3, was identified as the domain that mediates this effect. In 2010 these findings were further refined, showing that UCP3-knock down decelerated the mitochondrial kinetics of Ca^{2+} transients, and the specific amino acids, at the positions 167, 171 and 172, that mediate this effect were identified (Waldeck-Weiermair et al., 2010a, 2010c). In the following years several members of the MCUC were identified as described above, and the growing knowledge of the structure of this multiprotein complex allowed the creation of new hypotheses how the UCPs

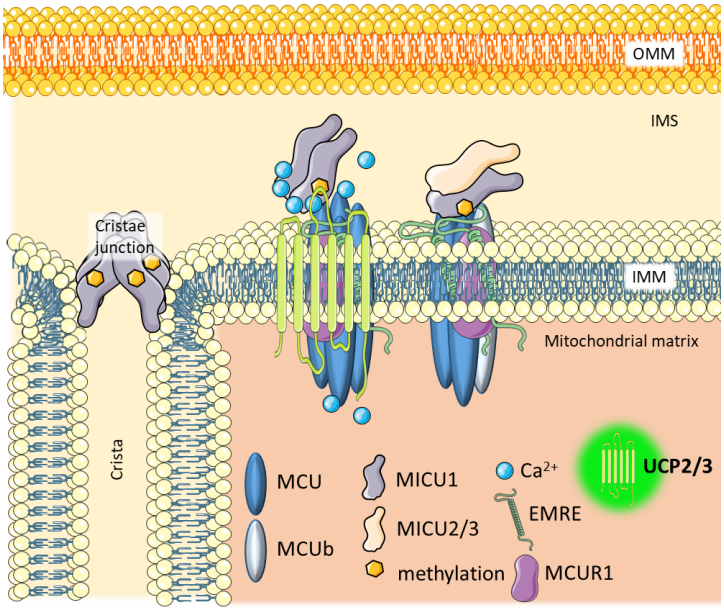

Figure 6 the IML2 of UCP2/3 interact with methylated MICU1 and support mtCU, adapted from Madreiter-Sokolwski et al., 2016, figures were generated in Microsoft PowerPoint with images from Servier Medical Art (https://smart.servier.com/)

modify mtCU. Madreiter-Sokolowski et al. found in 2016 that the asymmetric arginine methylation of MICU1 at position 455 by methyl transferase activity of PRMT1 is the prerequisite posttranslational modification that switches the opening of the MCUC from a solely Ca^{2+} dependent way towards a dependency on the presence and expression level of UCP2/3 (Madreiter-Sokolowski et al., 2016b). High activity of PRMT1 has been shown to be associated with aging and cancer, the effect of UCP2/3-knock down seems to be specific for cell types exhibiting a high asymmetric dimethylarginine (aDMA) status. Moreover, it has been shown that high expression levels of PRMT1 and UCP2/3 are poor prognostic markers for patients suffering from lung and gastric cancer (Koshenov et al., 2020; Madreiter-Sokolowski et al., 2017).

The understanding of UCP2/3s effect on the mitochondrial Ca^{2+} homeostasis was changed when cristae dynamics were studied with high resolution microscopy in living cells (Gottschalk et al., 2022b, 2019). The IMM is further compartmentalized into the inner boundary membrane (IBM), which is the membrane that separates the IMS from the mitochondrial matrix, and the invaginations called cristae. These structures are separated by the CJ, which further separates the IMS from the CL. The CJ is a construct that is built by several proteins including MICU1, OPA1, and the MICOS complex, and guarantees proper mitochondrial function. The spatial propagation of the $\Delta\psi_M$ depends on the tightness of the CJ, which in turn was shown to be modulated by UCP2 and UCP3 in HeLa cells. Gottschalk et al. also showed that the localization of MCU changes from the CL to the IBM under high Ca^{2+} conditions. When they recorded transients in different submitochondrial compartments they found that the first phase of mtCU happens in the CL were the high $\Delta\psi_M$ drives a fast and strong Ca^{2+} influx into the matrix, which is followed by a slower second phase, in which the MCUC is translocated to the IBM were the $\Delta\psi_M$ gradualy decreases and with it the transient kinetics. The participation of UCP2 and UCP3 in this whole process relies on the interaction with methylated MICU1, which leads to an opening of the CJ followed by Ca^{2+} influx to the CL and so forth. The knockdown of UCP2 led to a reduced opening of the CJ, a restriction of TMRM to the CL and a delayed translation of cytosolic to mitochondrial matrix Ca^{2+}. This effect on the CJ and overall mitochondrial Ca^{2+} homeostasis explains how UCP2 and UCP3 fulfil the two functions that have been proposed for the proteins. On the one hand, the increase in Ca^{2+} uptake, and the following metabolic boost, and on the other hand limiting the $\Delta\psi_M$, by loosening the CJ, allowing protons (H^+) to escape from the CL, thus acting like an uncoupler and therefore protecting cells under high energy demand situations (Gottschalk et al., 2022b).

Through the combination of these various proteins with specific effects on the mtCU, the MCUC becomes a versatile tool to adjust to cellular energy needs. By changes in the stoichiometry, localization and posttranslational modifications, cells can change this complex to match their metabolic needs and optimize the MCUC to fulfil specific mitochondrial functions in Ca^{2+} signalling.

1.3.6 Regulator of the MCUC: Annexin V

A very recent addition to the family of proteins that are capable of modulating the mitochondrial Ca^{2+} homeostasis is Annexin-AV (Oflaz et al., 2025). In 2025, Oflaz et al presented their work that showed a reduced mitochondrial Ca^{2+} uptake in Annexin-AV ko cells. While they found a reduction of Ca^{2+} in the IMS, the cytosolic and ER Ca^{2+} levels were unchanged. These findings led to the investigation of the localization of Annexin-AV, showing that under histamine stimulation, the protein accumulates in the close vicinity of VDAC1, and generally close to the OMM. This suggests a role of this protein in the oligomerization of VDAC1 and the subsequent steps in mitochondrial Ca^{2+} influx. Furthermore, these findings were supported by data showing reduced cristae dynamics, and an unchanged MCU IBM association index upon histamine stimulation. Since Annexin-AV is known to participate in apoptotic cell death, the group additionally investigated cisplatin induced cell death and found that the cisplatin mediated elevation of mitochondrial Ca^{2+} was reduced in Annexin-AV ko cells, nonetheless the cells were more susceptible to cispaltin mediated apoptosis.

1.4 Mitochondria associated ER membranes / mitochondria-ER contact sites, where the endoplasmic reticulum meets mitochondria

The ER serves, among other functions, as the cells primary Ca^{2+} store. Through orchestration of the proteins Stim1, Orai and SERCA it gets supplied with Ca^{2+} from the extracellular space, and channels like the IP_3 Receptors or Ryanidine receptors allow the directed release. To enable an efficient transfer of Ca^{2+} from the ER to the mitochondria, these two organelles form domains of proximity, so-called Mitochondria associated ER membranes (MAMs) or

mitochondria-ER contact sites (MERCS). These structures were first described when scientists studied the genesis of phospholipids, like phosphatidylserine or phosphatidylethanolamin, and their distribution in different fractions isolated by gradient centrifugation. They found a fraction X that showed high activity of key enzymes. This fraction X was also found in yeast cells and renamed into MAMs since the fraction contained ER as well as mitochondrial fragments.

Today we know that MAMs are the contact sites between the ER and mitochondria. They are highly organized, dynamic and versatile contact sites and they are a crucial part of cell physiology and pathologies like neurodegeneration, aging or cancer (Chen et al., 2021; Janikiewicz et al., 2018; Madreiter-Sokolowski et al., 2019a; Sathyamurthy et al., 2024) (Bartok et al., 2019a; Csordás et al., 2018). These contact sites can vary in distance between the two organelles. While in the rough ER the distance is bigger than 20 nm, simply due to the size of the ribosomes, the distance can be less than 10 nm in areas of the smooth ER (Csordás et al., 2006). But creating artificial links between the organelles with less than 5 nm distance also limits the functionality in Ca^{2+} signaling (Csordás et al., 2010). Due to the morphological heterogeneity of the MAMs/MERCS, dynamic molecular tools have been created to study contact sites with different distances between the organelles, using linker and spacer sequences (Vallese et al., 2020).

A few years after their discovery, first theories were born that these organelles contact sites also serve as hubs for Ca^{2+} transfer (Bachkoenig et al., 2022; Hajnóczky et al., 2002; Rizzuto et al., 1998). One family of proteins that is particularly involved in this interorganellar Ca^{2+} transfer are the IP_3 receptors (IP_3R). All three isoforms locate on the ER membrane and especially in the MAM regions/MERCS (Bartok et al., 2019b). They release Ca^{2+} from the ER in response to IP_3 binding towards the mitochondria (Bachkoenig et al., 2022). In 2019 Bartok et al. characterized the receptors and identified IP_3R isoform 2 to release Ca^{2+} most efficiently into the cytosol and further in the mitochondria. The tethering of the two organelles happens via the chaperone glucose-regulated protein 75 (GRP75), which binds to the IP_3R and voltage-dependent anion carrier (VDAC) on the mitochondrial side, which allows the passage of ions like Ca^{2+} over the OMM (Szabadkai et al., 2006). A recent publication by Pilic et al. found an elegant solution to bypass artefacts caused by fluorescent tags of VDAC1 in HeLa cells, allowing them to visualize the localization of the protein in the OMM which shows that the protein is primarily localized in the MAM/MERC regions (Pilic et al., 2024).

Also, mitofusin 2 (Mfn2) participates in the establishment of MAMs. Especially under cellular stress, this protein forms interorganellar contacts which are stable for an extended period of time, and higher expression of Mfn2 is correlated with increases in the basal mitochondrial

Ca^{2+} levels, $\Delta\psi_M$, and OCR (Gottschalk et al., 2022a). Interestingly, during aging or senescence, cells undergo high energy demands to counteract stress factors. For the purpose of this research, pulmonary artery endothelial cells (PAECs) are an established model to study these molecular changes since they develop a senescent phenotype in the course of a few serial passages. Madreiter-Sokolowsi et al. showed that the number of MAMs are increased in higher passages of PAECs, which is associated with higher levels of reactive oxygen species (ROS), basal OCR and higher mitochondrial Ca^{2+} uptake under histamine stimulation (Madreiter-Sokolowski et al., 2019b).

Overall, the interaction of the two organelles, ER and mitochondria, via MAMs/MERCS plays a crucial role in cellular physiology. In this work, I aim to investigate mitochondrial Ca^{2+} uptake from various sources (ER and SOCE) at different intensities. To study Ca^{2+} signals at different magnitudes, I will compare two approaches. First, I will use different concentrations of the agonist histamine to simulate physiologic conditions. As a second approach I chose risperidone, a mild antagonist of the H1R. As the coupling of the two organelles ER and mitochondria is very important for the transport of Ca^{2+} to the surface of mitochondria, which allows the exceeding of the MICU-mediated (**fig.5**) threshold, it is questionable how efficiently mitochondria can take up attenuated Ca^{2+} signals. This work will give further insight into the correlation of cytosolic and mitochondrial Ca^{2+} signals under two conditions. One that is closer to physiologic conditions, and one that uses a pharmacological tool. Since 100 µM histamine, a concentration often used in laboratories to stimulate the generation of IP_3, is also an unphysiologically high concentration, I would expect that even under lower concentrations of histamine, efficient mitochondrial Ca^{2+} uptake is guaranteed. On the other hand, inhibition of the H1R to attenuate the signal, could modulate the whole signalling cascade in an unknown way. I expect to find differences in the release of Ca^{2+} from the ER into the cytosol that will affect the tightly regulated mechanism of mitochondrial Ca^{2+} uptake. The aim of this study is to investigate the correlation of cytosolic and mitochondrial Ca^{2+} signals at different magnitudes. Further, we hypothesise that the use of a chemical antagonist to attenuate signals evoked by 100µM histamine changes the release of Ca^{2+} from the ER in a way that disrupts the tight coupling of the ER and mitochondria. These changes are expected to modulate the uptake of Ca^{2+} into the mitochondrial matrix, since proper formation of Ca^{2+} microdomains on the mitochondrial surface is needed to trigger MICU1 and MCU translocation into the IBM, where the major part of Ca^{2+} uptake under IP_3-triggered release from the ER takes place.

2 Material and Methods:

2.1 Materials and compounds:

I used Desfluoro Risperidone (Cat. D290065) from Toronto Research Chemicals (Toronto, Canada), dissolved in DMSO in a concentration of 100 mM, stored at -20°C in 50 µl aliquots (Bachkoenig et al., 2022). Salts for Buffers, ATP (Art.No. HN35.2), and histamine dihydrochloride (Art. No. 4017.6) were bought from Carl Roth (Karlsruhe, Germany). For Transfections, the Reagent (Polyjet^{TM}; SL100688) was used from SigmaGen Laboratories (Fredrick, MD, USA). For cytosolic Ca^{2+} measurements, Fura-2/AM was used (Abcam, Cambridge, UK; Cat. Ab120873). Plasticware used for cell culture purposes was obtained from Greiner Bio-One (Reinbach im Mühlkreis, Austria). Fetal calf serum (FCS), DMEM, and medium supplements were bought from ThermoFisher Scientific (Karlsruhe, Germany) and Sigma Aldrich (Vienna, Austria).

2.2 Cell culture:

The endothelial cell line EA.hy926 (Edgell et al., 1983) was used for the experiments in this work. Cells were grown in DMEM, containing 10% Fetal calf serum (FCS), 100U/ml penicillin, 100µg/ml streptomycin, and 1.25 µg/ml amphotericin B at 37°C, 5% CO_2. Prior to microscopic measurements, cells were seeded on 30 mm glass coverslips (VWR, Vienna, Austria) fitting to be mounted in a perfusion chamber (PC30; NGFI, Graz, Austria; https://www.ngfi.eu)

2.3 Transfection:

Before transfection, cells were seeded in six-well plates and grown to a confluency of 80% under standard conditions. Prior to incubation with the transfection mix, the medium was removed and 1 ml of fresh DMEM medium containing FCS and penicillin/streptomycin (P/S) per well was added. The transfection mix was prepared with DMEM without FCS and P/S 100 µl per well, 0.5 µg of plasmid DNA, and 2.5 µl of polyjet reagent. After thorough mixing using a pipette, the mix was incubated for 15 minutes and added to the cells. The cells were incubated for three hours in the transfection mix, and then the medium was changed to 2 ml of fresh DMEM, 10%FCS and P/S (Bachkoenig et al., 2022).

2.4 Buffers and solutions:

	Loading buffer	2 Ca^{2+} buffer	0 Ca^{2+} buffer
$CaCl_2$ [mM]	2	2	-
EGTA [mM]	-	-	0.1
NaCl [mM]	138	138	138
KCl [mM]	5	5	5
$MgCl_2$ [mM]	1	1	1
HEPES [mM]	1	1	1
$NaHCO_3$ [mM]	2.6	-	-
KH_2PO_4 [mM]	0.44	-	-
Na_2HPO_4 [mM]	0.34	-	-
L-Glutamine [mM]	2	-	-
D-glucose [mM]	10	10	10
Vitamins [%]	0.1	-	-
Essential amino acids [%]	0.2	-	-
Penicillin/streptomycin [%]	1	-	-
Amphotericin B [%]	1	-	-
pH (adjusted using NaOH)	7.45	7.4	7.4

Loading buffer was used for cell storage before measurements and fura-2 loading; for perfusion during experiments either the 2 Ca^{2+} or the 0 Ca^{2+} buffer was used.

2.5 Fura-2/am loading:

To investigate cytosolic Ca^{2+} Fura-2/AM was used. Before cells were loaded with the dye, they were seeded in six-well plates on 30 mm glass coverslips 40 – 48 h before the measurement and cultured under standard conditions. Fura2-AM stock solution was stored at a concentration of 1 M at -80°C in aliquots of 20µl. To dilute the stock solution, loading buffer was used. 12 ml loading buffer was warmed to 37°C before adding 20 µl of Fura2-AM stock, resulting in a 1.6 µM solution. This solution was immediately used to load the cells, 2 ml per well of a six-well plate. Cells were incubated at room temperature for about 200 minutes. In the next step, cells

were washed twice with loading buffer, and stored in the same until measurement at room temperature protected from light (Bachkoenig et al., 2022).

2.6 Genetically-encoded fluorescent sensors

To observe Ca^{2+} levels in different subcellular compartments, I used genetically encoded fluorescent sensors.

	Subcellular localization	Excitation/Emission	Expression vector	Reference
4mtD3cpv	Mitochondrial matrix	Ex: 430, Em: 480/535	pcDNA3.1	(Palmer et al., 2006)
IMS-GemGeco	Inner Boundary Membrane	Ex: 430, Em: 480/535	pcDNA3.1	(Waldeck-Weiermair et al., 2019a)
D1ER	Endplasmic retikulum	Ex: 430, Em: 480/550	pcDNA3.1	(Palmer et al., 2004)
D3cpv	Cytosol	Ex: 430, Em: 480/535	pcDNA3.1	(Palmer et al., 2006)

Transfection was used to introduce plasmids in cells as reported previously (Bachkoenig et al., 2022).

2.7 Microscopes and acquisition

I used two microscopic devices in this work for measurements. The Anglerfish (NGFI, Graz, Austria; www.ngfi.eu) equipped with a Nikon CFI Super Fluor 48x oil immersion NA1.3 (Nikon, Vienna, Austria), 2 CMOS cameras (acA1920-40µm, Basler, Ahrensburg, Germany), 3 LEDs (345 nm/55mW; 380 nm/>1500 mW; 470 nm/>900 mW; NGFI), and the respective set of filters (340/26, 380/14, and 480/17 nm; Semrock from AHF, Tuebingen, Germany) and dichroics (F38-366 and F38-495 dichroics; Semrock) was used. The second microscope was a conventional inverted microscope (Olympus IX73, Olympus, Vienna, Austria) equipped with han ApoN340 40x oil immersion objective (Olympus), CCD QImaging Retiga R1 camera (Teledyne Photometrics, Tucson, AZ, USA), a LedHUB (Omicron Laserage Laserprodukte, Rodgau-Dudenhofen, Germany) with a 385 and 455 LED in Combination with a CFP/YFP/RFP

filter set (Olympus). For FRET measurements, the emission was split onto two halves of the camera using a dual-channel beam splitter DV2 (Teledyne Photometrics) and a CFP/YFP beamsplitter (505DCXR, Chroma Technologies, Bellows Falls, VT, USA). For fura-2 measurements, cells were sequentially illuminated with 340 nm and 380 nm and emission was recorded at 510 nm. VisiView 4.2.01 (Visitron Systems, Puchheim, Germany) or AnglerFish Acquisition Software 4/22 (NGFI) were used for data acquisition at the Olympus and AnglerFish, respectively. Both devices were linked with a gravity-based perfusion system (PS-9D, NGFI).

2.8 Data analysis

In all measurements, a background ROI was included, for background subtraction, and data were corrected for bleaching using an exponential decay fit. ImageJ (NIH, Bethesda, MA, USA) and Microsoft Excel (Microsoft) were used for the image analysis, data extraction, and calculations.

Area under the curve quantification

To quantify the single cells response to histamine, the mean and the standard deviation of the stable basal signal before stimulation were calculated. A deviation from the mean ratio plus five times the standard deviation was chosen as the beginning and end of the histamine-triggered Ca2+ signal. In the next step the difference between the mean basal ratio and each chosen time point was calculated. To quantify the area for all timepoints, the respective deltas were multiplied by 2, since the interval of the measurements was 2 seconds. Finally, all the values were added to get the AUC value.

Slope Calculation

Like in my AUC calculation method, I used the mean basal ratio plus five times the standard deviation to determine the start of the Ca^{2+} transient. Since I were only interested in the first rise in the signal, the first time-point that showed a negative slope was chosen as the end of the time of interest. Next, I calculated the slope, using the corresponding Microsoft office Excel function, between the ratio of each time-point until the turn-point was reached and the slope

turned negative. Next, I calculated the average value for each cell, which was then used for further analysis.

2.9 Statistics

All experiments were repeated on at least three different days in triplicates, data shown represent the mean ±SEM, and numbers indicate the numbers of wells/single cells. Analysis of variance (ANOVA) with Tukey post hoc test was performed. GraphPad Prism software version 9.3.1 (GraphPad Software, San Diego, CA, USA) was used for the analysis and presentation of the data.

3 Results

3.1 Characterization of histamine-triggered cytosolic Ca^{2+} elevations

When I started to study Ca^{2+} signals in EA.hy926 cells I first used different concentrations of histamine, measured $[Ca^{2+}]_{cyto}$ and created a concentration-response curve. For these measurements I used the cytosolic Ca^{2+} indicator dye Fura2-AM. After seeding the cells in 6-well plates on 30 cm glass plates, I cultured the cells for approximately 48 h under standard cell culture conditions. Immediately before the measurements the cells were loaded with the dye and kept in EH- loading buffer in the dark at room-temperature to avoid bleaching. When the measurements were started, healthy cells were selected according to size, shape and density, and perfusion with 2CaNa buffer was started. After selection of cells the recording was started. In case of steady signals the cells were kept in presence of extracellular Ca^{2+} for another two minutes, before the perfusion buffer was changed to a $0Ca^{2+}$ buffer. Again the cells were perfused for about two minutes to allow complete removal of extracellular Ca^{2+}, before the cells were stimulated with histamine for two minutes. After the stimulation phase, perfusion was changed to $0Ca^{2+}$ buffer, and the recording was continued until the ratio returned to the basal ratio. In **figure 7a** you can find representative traces for all concentrations of histamine tested. Based on these data I calculated the area under the curve (AUC), representing the total $[Ca^{2+}]_{cyto}$ (**fig. 7b**). The data were then normalized to 100 µM histamine and the concentration-response curve was created by calculation of a sigmoidal concentration-response curve, which unveiled an EC_{50} value of 2.01 (1.29 – 3.18) µM (**fig. 7c**). Additionally, I calculated the average slope in the on-kinetics of the transients, and the linear regression including all concentrations of histamine tested (**fig. 7d**). These data demonstrated that the change in the on-kinetics of histamine induced Ca^{2+} transients in EA.hy926 cells did not follow a linear decline ($R^2 = 0.5616$) (**fig. 7d**). I also quantified the ΔRatio (**fig. 7e**) by subtracting the average basal ratio of one minute before the stimulation from the maximum ratio during stimulation. Since the change in the ΔRatio was not linear under different concentrations of histamine, I choose the AUC values to create the concentration response curve.

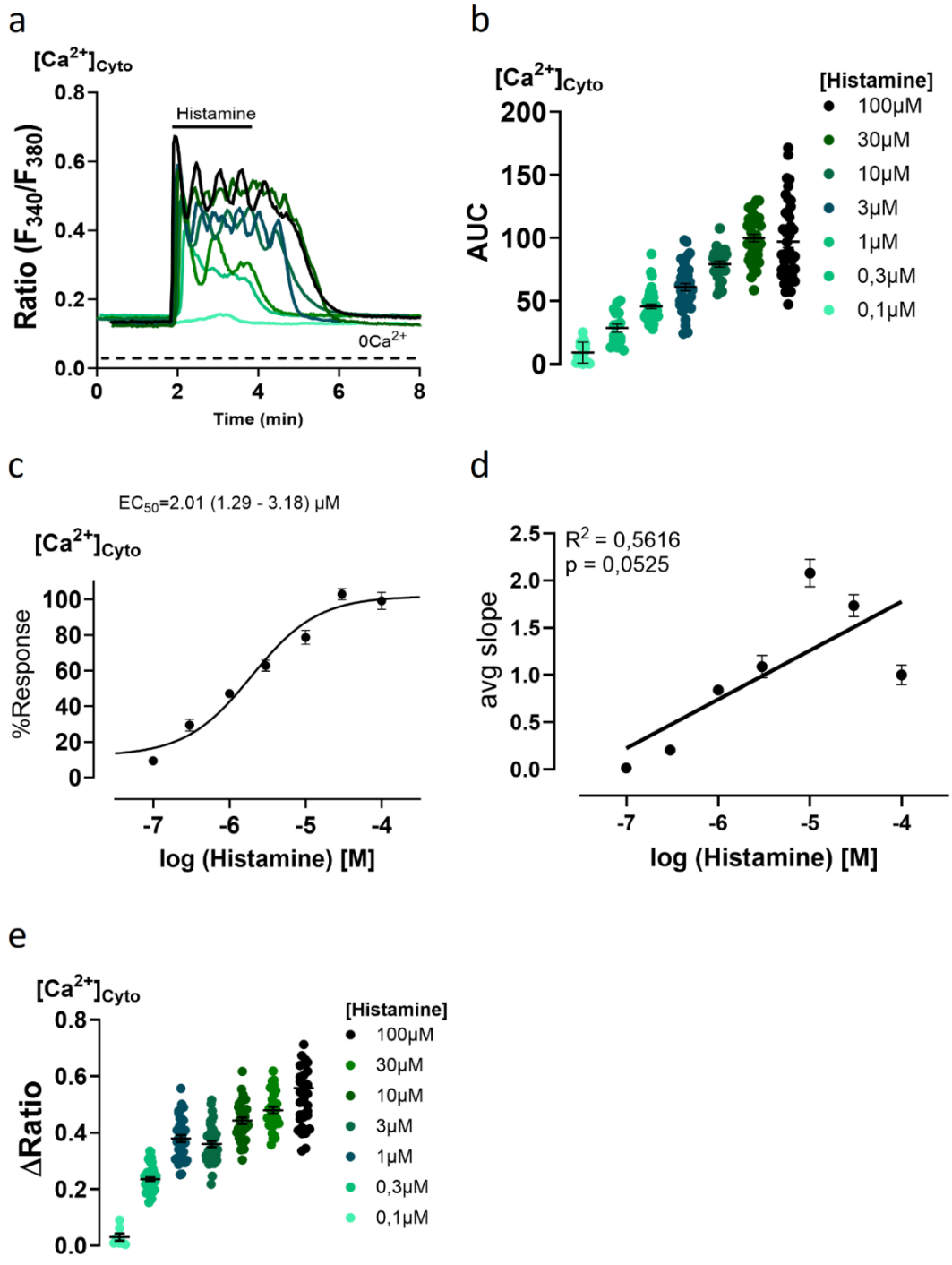

Figure 7 Cytosolic Ca^{2+} transients induced with different concentrations of histamine. (a) Representative traces of EA.hy926 cells loaded with Fura2 and stimulated with 100 nM – 100 µM histamine. (b) concentration-response curve for histamine, AUC values were used to calculate this linear regression, (c) Cellular response to histamine was quantified by calculating the AUC (n = cells/well: histamine: 100 µM 44/5, 30 µM 38/6, 10 µM 26/6, 3 µM 39/6, 1 µM 44/8, 0,3 µM 16/4, 0,1 µM 18/4) (d) linear regression of the average slope in the on-kinetics of histamine-triggered Ca^{2+} transients, (e) Quantification of cellular response to histamine by calculation of the ΔRatio. Reproduced from Bachkoenig et al, 2022 with permission of publisher Elsevier (Bachkoenig et al., 2022)

3.2 Cytosolic Ca^{2+} transients get efficiently translated into the mitochondrial matrix

I continued my experiments with EA.hy926 cells expressing 4mtD3cpv, a genetically encoded FRET sensor for Ca^{2+}, located in the mitochondrial matrix, and stimulated the cells with the same concentrations of histamine as I did while measuring $[Ca^{2+}]_{cyto}$ (**fig. 7**). Again, I started the perfusion in presence of extracellular Ca^{2+} and continued the perfusion for two minutes when the signal was stable. I then changed to the nominal absence of extracellular Ca^{2+} for two minutes before I stimulated the cells with histamine (100 nM – 100 µM). **Fig. 8a** shows representative traces for each concentration of histamine used. To quantify the cellular response to histamine I calculated the ∆Ratio by subtracting the average basal ratio of one minute before stimulation from the maximum Ratio during histamine stimulation (**fig. 8b**). In order to create a concentration-response curve, I normalized the data to the average ∆Ratio of 100 µM histamine. Then I transformed the data to a non-logarithmic scale, and used those transformed data to calculate a non-linear regression. The EC_{50} value that I calculated in this way was 3.53 (3.09 – 4.05) µM (**fig. 8c**) Finally, I compared my findings from the cytosolic measurements (**fig 7**) with my findings in the mitochondrial matrix and put the concentration-response curves in one graph (**fig 8d**). Comparison of the dose-response curves in the two subcellular compartments points out the tight tethering between the ER and the mitochondria in Ca^{2+} signaling, since the EC_{50} values were similar (Cyto: 2.01 vs. Mito. 3.53). But when I normalized the cellular response evoked with 3 µM histamine to the maximum response, using 100 µM histamine, I found a significant difference between the two organelles (**fig.8e**), confirming the regulated uptake of Ca^{2+} by mitochondria, mediated by the MCUC.

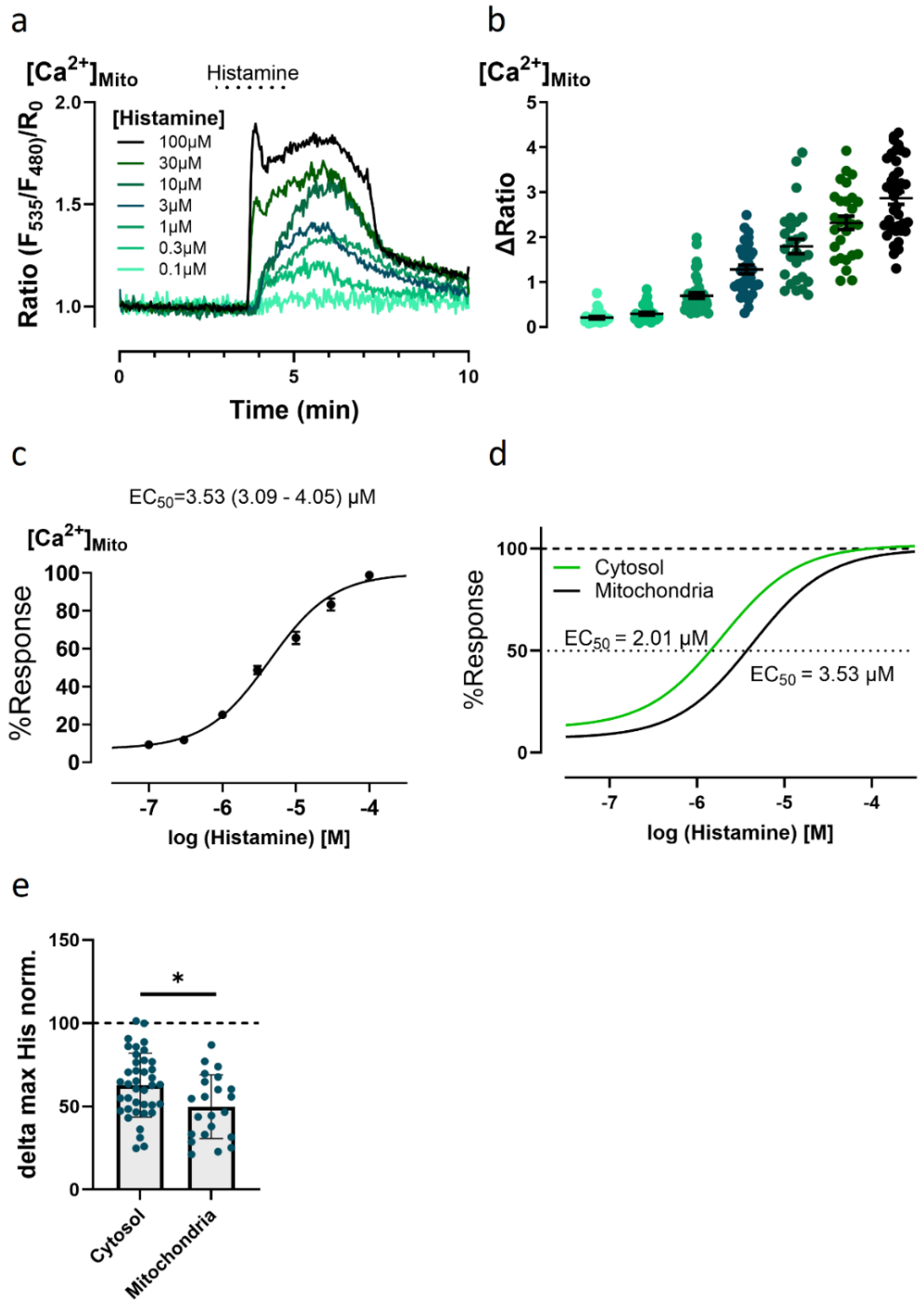

Figure 8: Cytosolic Ca^{2+} transients get efficiently transformed into the mitochondrial matrix independent of agonist concentration. (a) Representative traces of EA.hy926 cells expressing the Ca^{2+} sensor 4mtD3cpv getting stimulated with histamine in several concentrations (100 nM – 100 µM). (b) Quantification of the cell's response to histamine by calculation of ΔRatio. (n = cells/wells: histamine: 100 µM 38/14, 30 µM 28/11, 10 µM 27/12, 3 µM 32/12, 1 µM 42/15, 0.3 µM 35/12, 0.1 µM 31/11) (c) Concentration-response curve created from the ΔRatio of cells stimulated with 100 nM – 100 µM histamine. (d) Comparison of cytosolic vs mitochondrial concentration-response curve for histamine in EA.hy926 cells. (e) Comparison 3 µM histamine evoked elevations in the cytosol vs. mitochondrial matrix, data from fig.7/c and fig.8/b were used. Data were normalized to average of 100 µM histamine of the respective organelle

3.3 Attenuation of cytosolic histamine-induced Ca^{2+} transients with Risperidone

In my next experiment I wanted to investigate the antihistaminic potency of risperidone in EA.hy926 cells (Bachkoenig et al., 2022). Therefore, I continued my cytosolic measurements with Fura2 loaded cells. I prolonged the phase after the 2Ca buffer with 0Ca buffer to five minutes to allow risperidone to reach the desired concentration within the chamber containing my cells. After this five-minute pre-incubation period, I stimulated the cells with 100 µM histamine. In **fig 9a** I present representative traces for my recordings of Fura2-loaded EA.hy926 cells in the presence of different concentrations of risperidone. To quantify the cellular response to 100 µM histamine in the presence of risperidone (1 – 300 µM) I quantified the AUC with the same method that I used in my previous experiments (**fig.7c**), normalized the data to those in the absence of risperidone, transformed them to a non-logarithmic scale and calculated a non-linear regression to create a concentration-response curve (**fig.9b**). The IC_{50} value I found for risperidone in histamine-triggered cytosolic Ca^{2+} transients in EA.hy926 cells was 35.74 (27.42 – 46.58) µM. As I did in my cytosolic experiments with different concentrations of histamine, I quantified the changes in the kinetics of the signals when I inhibited the histamine receptor with risperidone. I used the same way to calculate the average slope as before, and when I created the non-linear regression, I found that with increasing concentrations of risperidone, the average slope in the on-kinetics of histamine-stimulated cells decreased in a linear way (R^2 = 0.9932) (**fig.9d**). Since I calculated the ∆Ratio in my previous experiments (**fig.7**), where I found a non-linear decrease with decreasing concentrations of the used agonist, I calculated it in these experiments as well (**fig.9d**), and found that the height of the signal changed comparably.

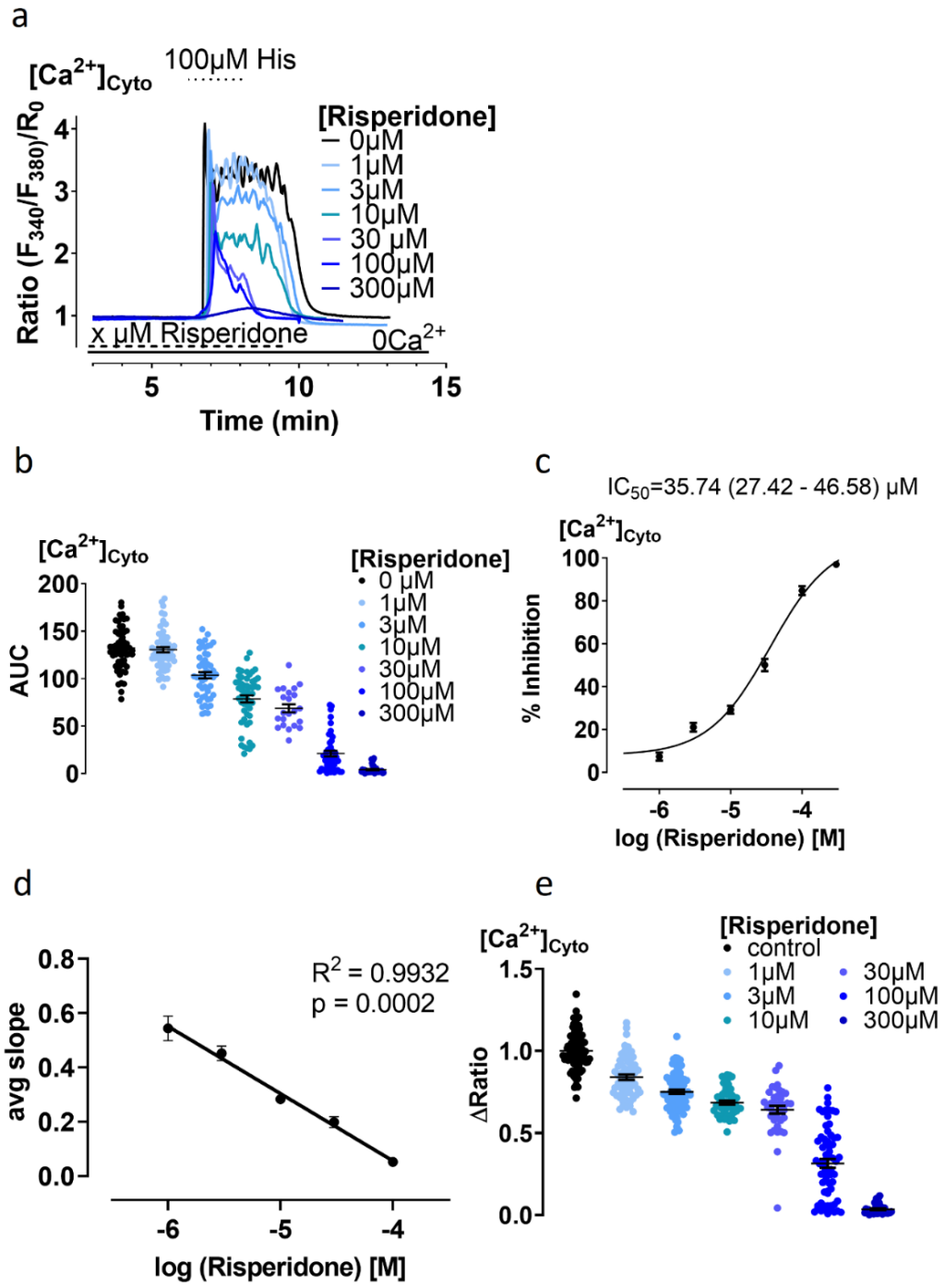

Figure 9: Attenuation of cytosolic histamine-induced Ca^{2+} transients with risperidone.

(a) Representative traces of cells stimulated with 100 µM histamine in the presence of 1 – 300 µM risperidone. (b) Concentration-response curve of risperidone on cytosolic Ca^{2+} release calculated from the AUC in single EA.hy926 cells. (c) Quantification of the cellular response to histamine in the presence of risperidone by calculation of the AUC. (n = cells/wells: 0 µM = 58/16; 1 µM = 36/9; 3 µM = 36/15; 10 µM = 33/10; 30 µM = 22/10; 100 µM = 45/11; 300 µM = 35/6). (d) Linear regression of the average slope in the on-kinetics of histamine-induced Ca^{2+} signals. (e) Quantification (ΔRatio) of the cellular response to 100 µM histamine in the presence of risperidone. Reproduced from Bachkoenig et al, 2022 with permission of publisher Elsevier (Bachkoenig et al., 2022)

3.4 Establishing a protocol for the double stimulation of a single cell with IP_3-generating agents

Since I felt enthusiastic to further investigate the observed effect of risperidone, I wanted to establish a protocol in which I stimulate the cells twice in the nominal absence of Ca^{2+} (Bachkoenig et al., 2022). I kept the first part of my protocol and added a five minute wash-out phase after histamine. After the wash-out, I re-added extracellular Ca^{2+} for eight minutes to refill the ER with Ca^{2+} and thus allow a second stimulation. Five minutes before I added histamine for the second time, I switched the perfusion again to $0Ca^{2+}$ buffer, then added histamine for two minutes again, washed histamine out for five minutes, and finally added extracellular Ca^{2+} to allow SOCE. A representative trace is shown in **fig 10a**. I quantified the response of the cells to histamine stimulation by calculating the ∆Ratio, and found that the fist peak was reduced in the second stimulation, but there was no significant difference in the plateau phase that followed the initial peak (**fig.10b**). Since I knew now that the protocol gave the cells sufficient time to recover from the first stimulation and that the cells responded comparably in the second stimulation, I continued with this protocol and added 10 µM risperidone, either in the first or the second stimulation (**fig. 10c**). When I quantified the cellular response from this recordings I found that 10µM risperidone significantly reduced the cytosolic Ca^{2+} signal in response to stimulation with 100µM histamine under both scenarios, while the uninhibited response to histamine showed no difference, and the effect of risperidone was also unchanged, independent on the sequence of administration (**fig. 10d**).

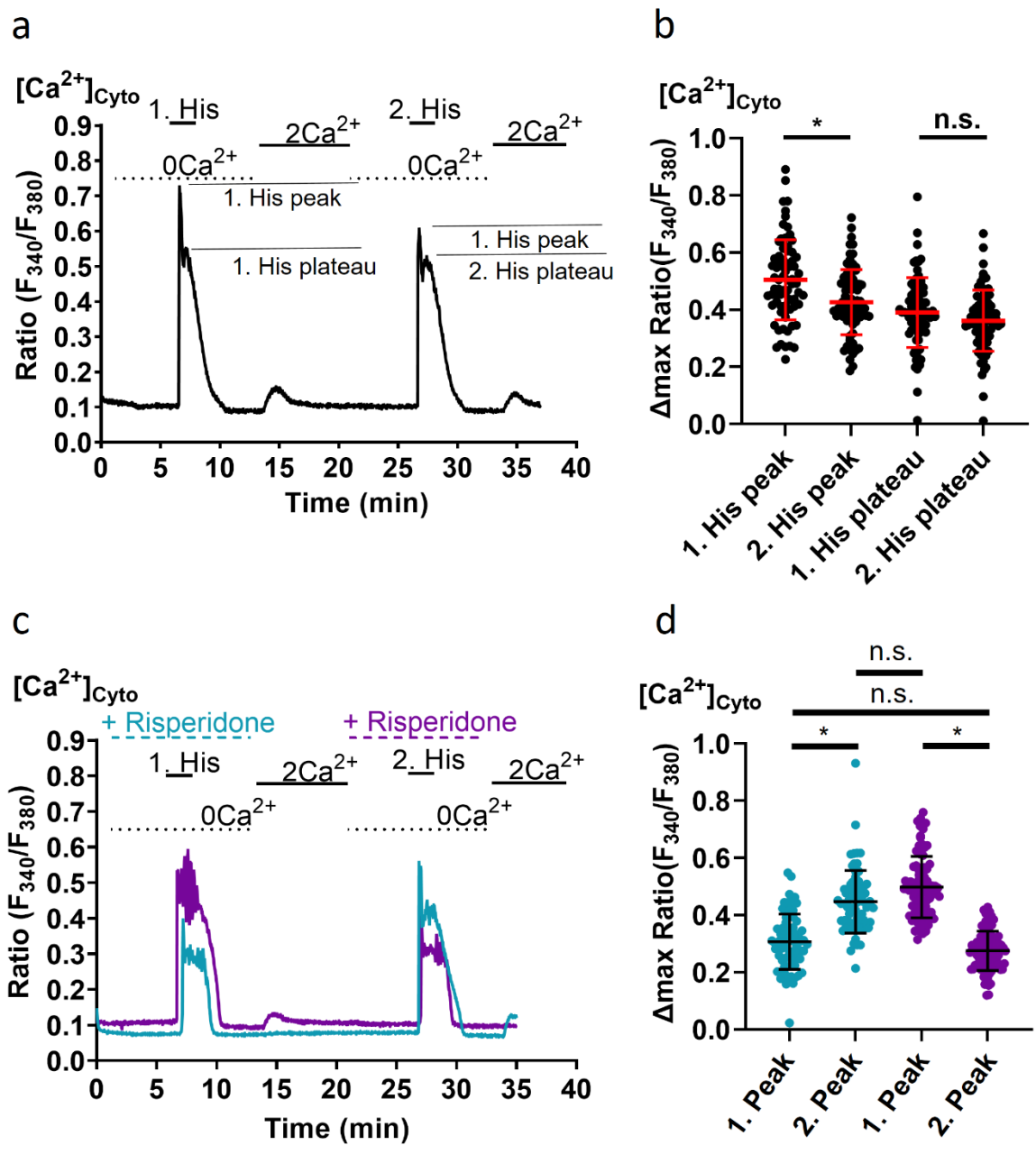

Figure 10: Establishing a protocol for double stimulation of a cell with histamine.

(a) Representative trace of a cell stimulated twice with histamine, the quantified responses are indicated. (b) Quantification of cellular response to the histamine stimulations by calculation of the Δmax Ratios in the first peak and the following plateau phase. (n = cell/wells: 73/4) (c) Representative traces in the absence or presence of 10µM risperidone. In the turquoise trace risperidone was added in the first stimulation, in the purple trace it was added during the second stimulation with 100µM histamine. (d) Quantification of the effect of 10µM risperidone either during the first or the second stimulation phase (1. Peak + risperidone: cells/wells 71/4; 2. Peak risperidone 91/5) Reproduced from Bachkoenig et al, 2022 with permission of publisher Elsevier (Bachkoenig et al., 2022)

3.5 Risperidone inhibits histamine- but not ATP-triggered ER Ca^{2+} release

After establishing the sequential stimulation protocol, I wanted to identify whether the effect of risperidone is specific for histamine, or if it also affects other IP_3-generating agents (Bachkoenig et al., 2022). Therefore, I adjusted my protocol and changed the agonist in the second stimulation phase to 100 µM ATP, which acts on the plasma membrane via the purinergic receptor, a G-protein coupled receptor similar to the histamine receptor. **Figure 11a** shows representative traces of cells from this protocol. When I reintroduced extracellular Ca^{2+} in the perfusion buffers after the stimulation I were able to detect a SOCE-induced peak. I calculated the ∆max of it and correlated it to the ∆max of the preceding IP_3-generating agent-induced peak. I found no significant correlation in my data, most likely since the SOCE peak in my data does not represent the actual amount of Ca^{2+} influx. (**fig. 11b-e**). Under control conditions, ATP seemed to show a trend towards higher Ca^{2+} release and subsequent SOCE, but there was no significant difference found (**fig. 11b**). When I used risperidone, the ∆max of the histamine peak and its following SOCE was significantly lower than the ATP induced transients (**fig. 11c**). When I compared the ATP triggered Ca^{2+} signals in the absence and presence of 10 µM risperidone, I found no significant difference (**fig. 11d**), while when histamine was used to stimulate cells, both peaks were significantly decreased (**fig. 11e**).

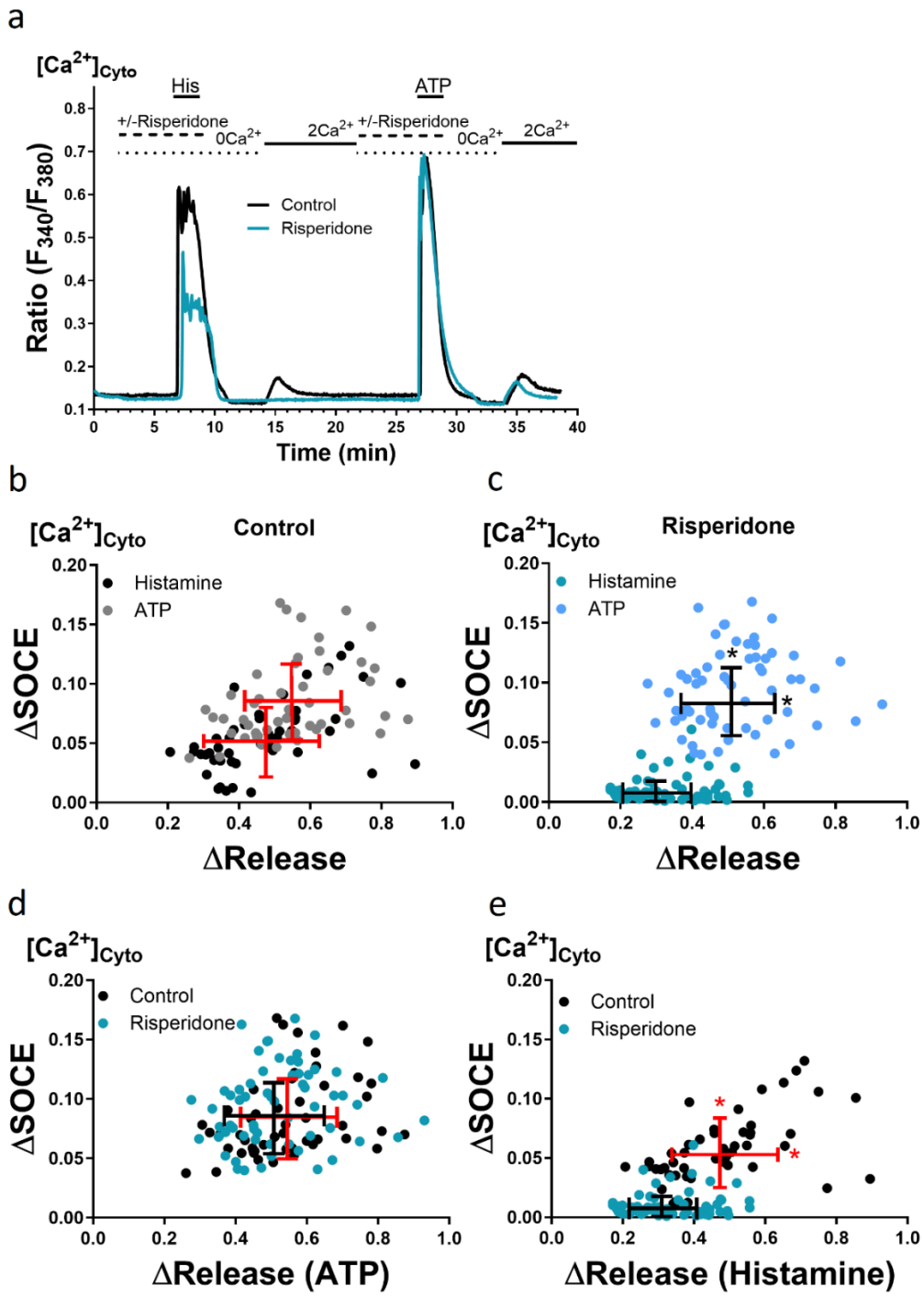

Figure 11 Risperidone inhibits histamine- but not ATP-triggered ER Ca^{2+} release.

(a) Representative traces of cells sequentially stimulated with 100µM histamine and 100µM ATP in the absence and presence of 10 µM risperidone. (b-e) Correlation of the IP_3-triggered ER Ca^{2+} release with the subsequent ΔSOCE. (b) Comparison of deltas from control cells histamine vs ATP (c) Comparison of 10 µM risperidone treated cells histamine vs ATP. (d) Comparison of ATP-triggered Ca^{2+} peaks in control vs risperidone. (e) Comparison of histamine triggered Ca^{2+} peaks control vs. risperidone (n = cells/wells: control 49/9; risperidone 63/9), Reproduced from Bachkoenig et al, 2022 with permission of publisher Elsevier (Bachkoenig et al., 2022)

3.6 Risperidones effect on histamine-induced Ca^{2+} elevations is pronounced in the mitochondrial matrix

After I studied the effect of risperidone in the cytosol, I were eager to find out how it affects the mitochondrial Ca^{2+} homeostasis. To do this I used the same protocol that I used in Fura2-loaded cells (**fig. 11**) in EA.hy926 cells expressing 4mtD3cpv (Bachkoenig et al., 2022). Representative traces are shown in **figure 12a**. For analysis, I again calculated the ∆max from ER Ca^{2+} release and from SOCE (**fig. 12b and c**). 10µM showed a stronger effect on histamine-triggered Ca^{2+} transients in the mitochondrial matrix than it did in the cytosol, while the ATP-induced Ca^{2+} signals remained unaffected (**fig. 12b**). Since the ER Ca^{2+} release by histamine was affected, also the subsequent SOCE peak was decreased (**fig. 12c**). Like in the cytosolic measurements, in the mitochondrial matrix, 10 µM risperidone did neither affect the ATP-triggered Ca^{2+} release (**fig. 12b**) nor the following SOCE induced peak (**fig. 12c**)

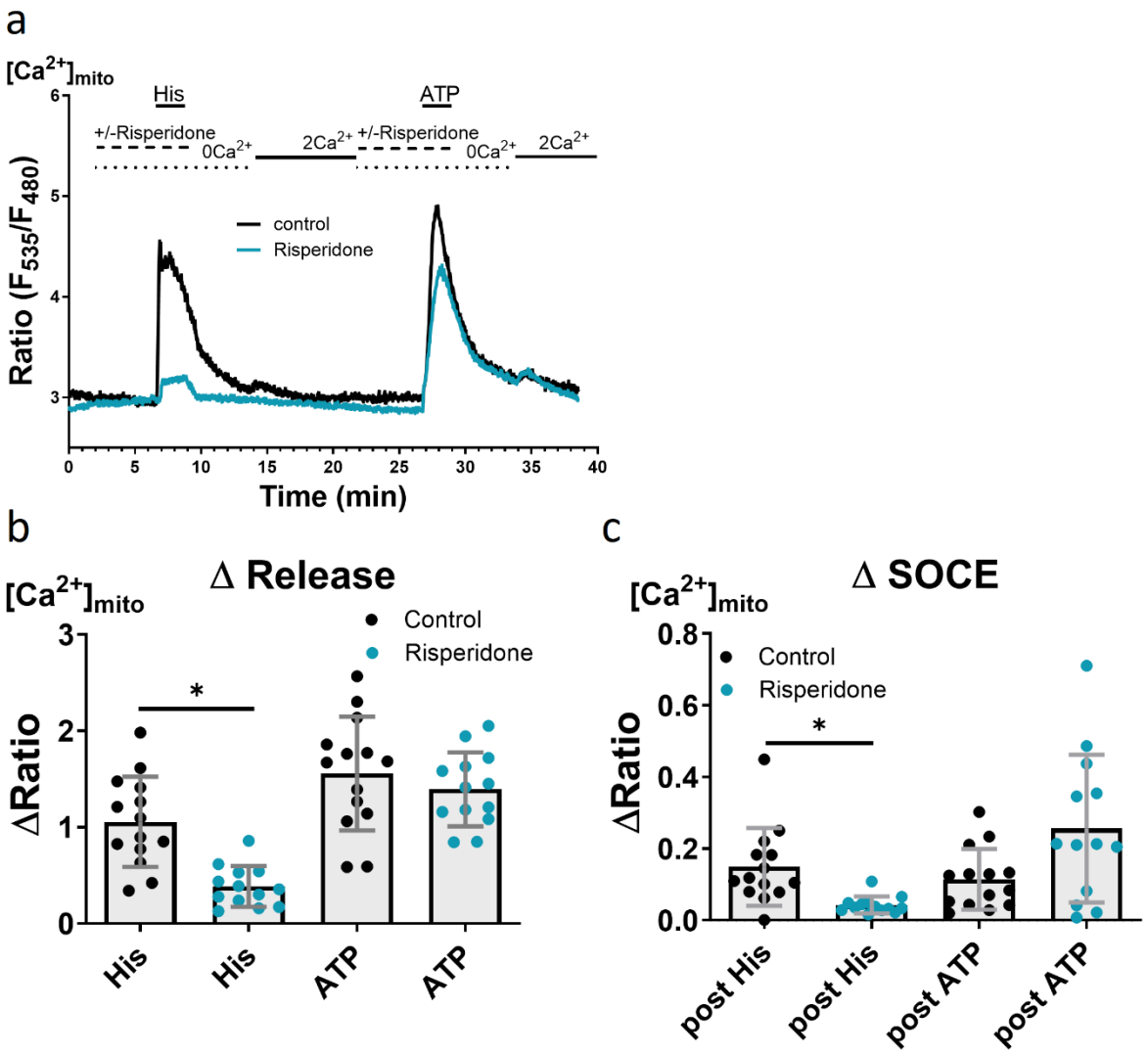

Figure 12 Risperidone induces a pronounced effect on histamine-induced Ca^{2+} elevation in the mitochondrial matrix.

(a) Representative traces of EA.hy926 cells expressing 4mtD3cpv stimulated sequentially with histamine and ATP in the absence or presence of 10 µM risperidone. (b) Statistical analysis of the cells response to IP_3-generating agents histamine and ATP. (c) Statistical analysis of the SOCE induced peak after re-addition of extracellular Ca^{2+} (n = cells/wells: Control 14/9; 10 µM Risperidone 13/9). Reproduced from Bachkoenig et al, 2022 with permission of publisher Elsevier (Bachkoenig et al., 2022)

3.7 The discrepancy between the cytosolic and the mitochondrial effect of risperidone does not rely on an artifact

After I found out that 10 µM risperidone inhibited the histamine triggered Ca^{2+} release stronger within the mitochondrial matrix compared to the cytosol, I wanted to exclude that this discrepancy was due to an artifact based on a different affinity of the two sensors used to measure Ca^{2+}, i.e. Fura2 and 4mtD3cpV. Hence, I utilized a sensor that could omit this error. I utilized cytosolic D3cpv, which is a Ca^{2+} sensor that shares nearly complete sequence homology with 4mtD3cpv, however, lacks the mitochondrial targeting sequence derived from cytochrome c oxidase subunit 8. By repeating the cytosolic Ca^{2+} measurements with this sensor, I can directly compare my data from both subcellular compartments. **Figure 13a** shows representative traces of EA.hy926 cells expressing D3cpv, using the same protocol as before. I again calculated the ∆Ratios to analyze the recordings and I found results similar to my experiments with Fura2-loaded cells. 10 µM risperidone reduced the histamine-triggered transients to approximately 60%, while the ATP-triggered signals were unchanged (**fig. 13b**). This trend was the same for SOCE-induced Ca^{2+} signals. After histamine stimulation in the presence of risperidone I observed a strong decrease, while after ATP stimulation, both, in the absence and presence of risperidone, the deltas were unchanged (**fig. 13c**). To summarize my findings of the last experiments with different sensors that are located in different subcellular compartments, I normalized the risperidone inhibited histamine-induced peaks to the average deltas of the control cells of each experiment and compared the effect (**fig. 13d**).

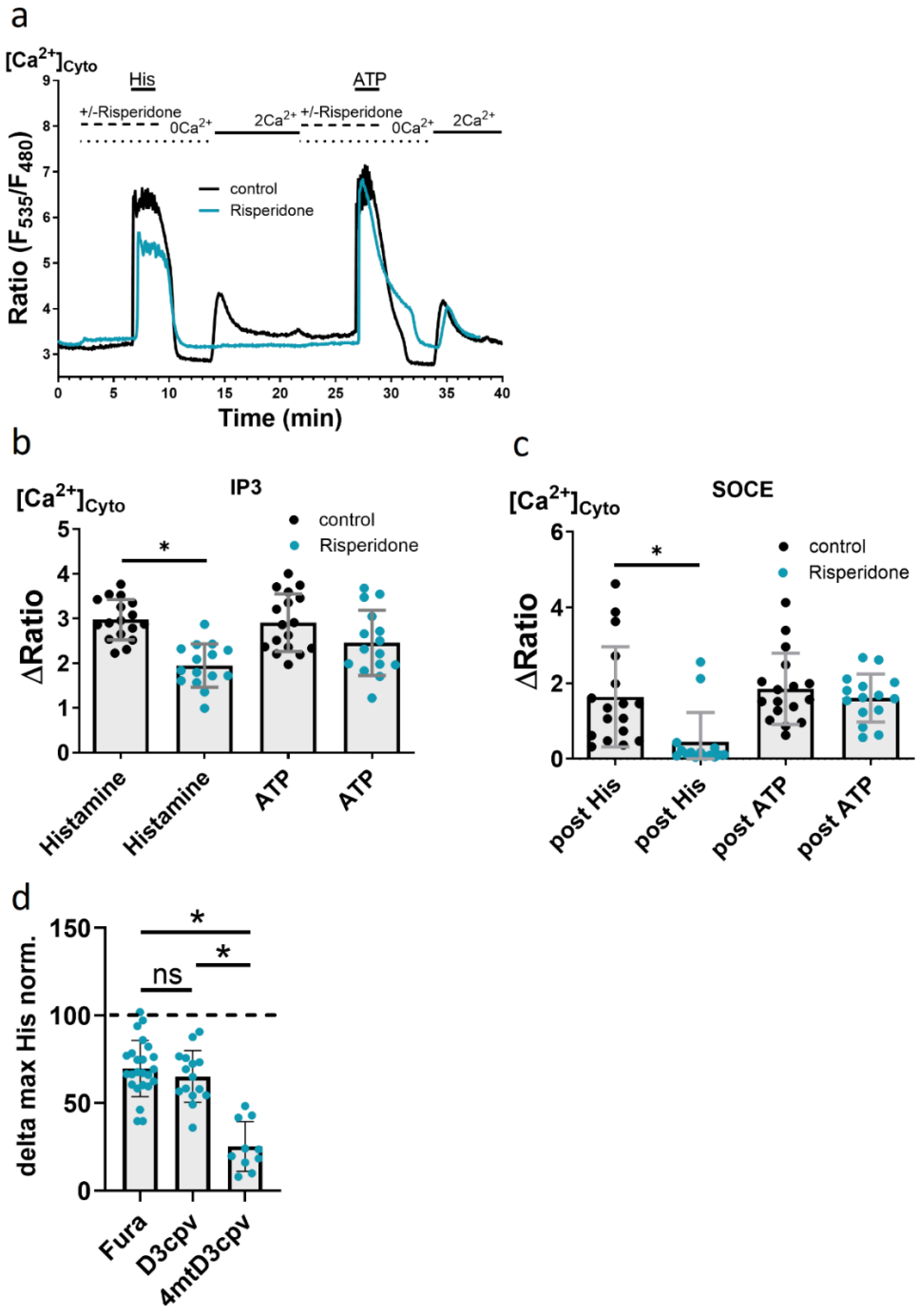

Figure 13 The discrepancy between the cytosolic and the mitochondrial effect of risperidone does not rely on an artifact.

(a) Representative traces of cells expressing D3cpv, stimulated twice, once with 100 µM histamine once with 100 µM ATP, risperidone was used at a concentration of 10 µM. (b & c) Statistical analysis of cellular response to IP_3-generating agents and subsequent SOCE activation. (d) Summary of the effect of 10 µM risperidone in cytosol and mitochondria with different sensors. (n = cells/wells: Control = 17/9; 10 µM Risperidone = 15/9). Reproduced from Bachkoenig et al, 2022 with permission of publisher Elsevier (Bachkoenig et al., 2022)

3.8 The disturbing effect on the translation of cytosolic to mitochondrial Ca^{2+} signals is not specific to risperidone

As my results emphasize that risperidone may have an additional effect on mitochondrial Ca^{2+} uptake I aimed to use a different histamine antagonist to figure out whether the effect was specific to risperidone or a common effect of histamine antagonists. Mepyramine is a potent well-established, first-generation antihistaminic, so I chose it for my experiments. In order to find a concentration that gives similar inhibition like 10 µM risperidone does, I titrated mepyramine in my perfusion buffers. I found that 100 nM of Mepyramine reduced the cytosolic Ca^{2+} signal in Fura2-loaded EA.hy926 cells to roughly 60% compared to control cells (**fig. 14a and b**), which gave similar results as the usage of 10 µM risperidone. I continued my experiments with Ca^{2+} measurements in the mitochondrial matrix. For these measurements I used again my protocol with double stimulation. Representative single cell responses are shown in in **figure 14c**. Again, I calculated the deltas of the IP_3-generating agents and detected a strong inhibition in the histamine peaks, while the ATP-induced peaks remained unchanged (**fig. 14d**). To summarize my findings with mepyramine, I normalized the inhibited histamine-induced transients to the respective control cells, and presented the different degree of inhibition in different subcellular compartments upon using 100 nM Mepyramine (**fig. 14e**)

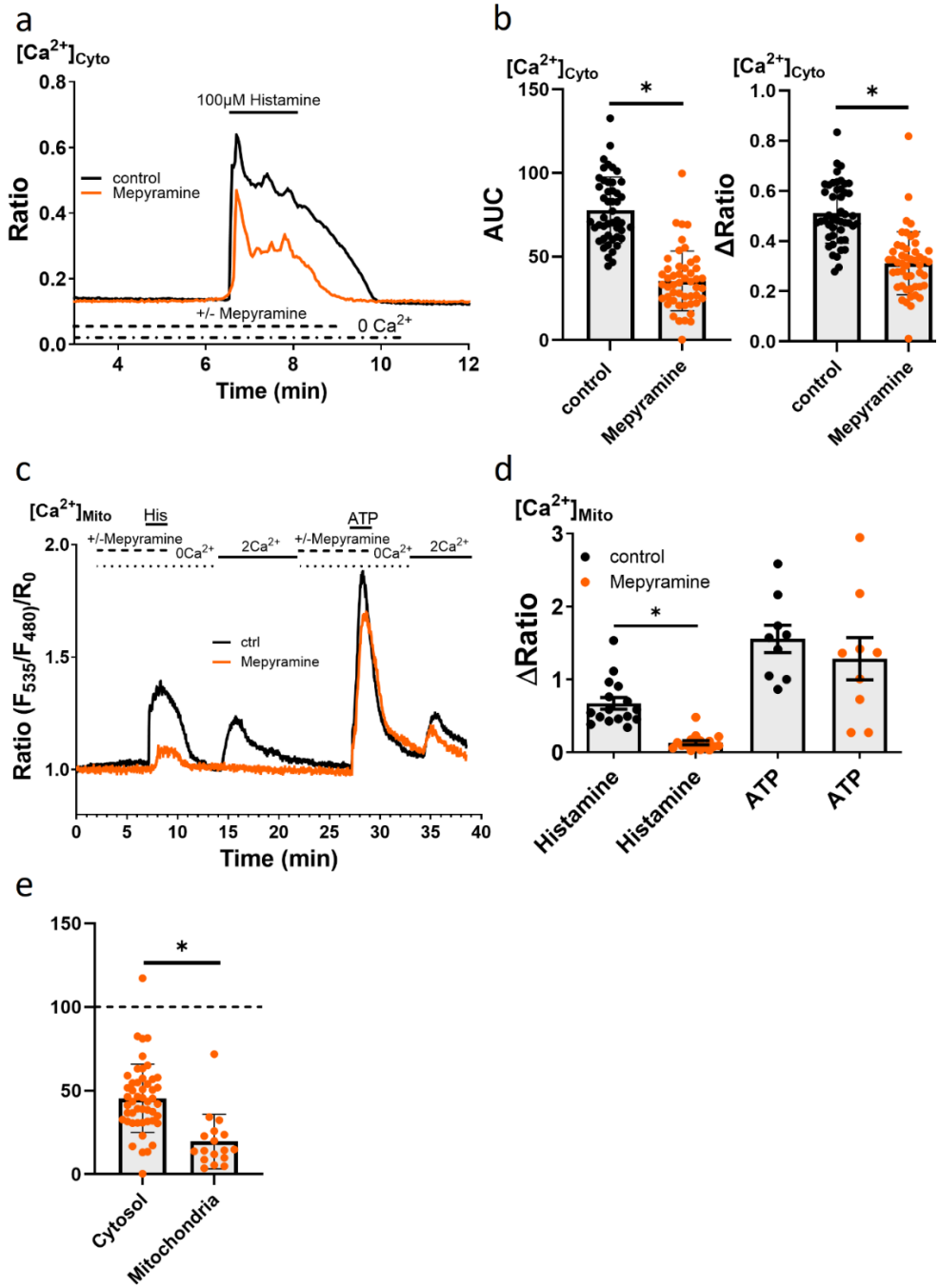

Figure 14 The disturbing effect on the translation of cytosolic to mitochondrial Ca^{2+} signals is not specific to risperidone.

(a) Representative traces of EA.hy926 cell loaded with fura2 and stimulated with 100 µM histamine +/- 100 nM Mepyramine. (b) Quantification of the inhibitory effect of 100 nM mepyramine on histamine-induced Ca^{2+} release AUC and ΔRatio (n = cells/wells; control = 47/6; Mepyramine = 49/6) (c) Representative traces of cells expressing 4mtD3cpv perfused with the double stimulation protocol +/- 100 nM mepyramine. (d) Statistical analysis of cellular response to IP_3-generating agents. (n = cells/wells: control = 16/9; Mepyramine = 17/9) (e) Summary of the inhibitory effect of 100 nM mepyramine in the cytosol and the mitochondria.

3.9 Characterization of risperidones inhibitory effect on mitochondrial Ca^{2+} elevations

After I excluded that risperidone itself interferes with mtCU and thus potentiates its effect by modulating the translation of cytosolic Ca^{2+} signals to mitochondrial ones, I wanted to further explore the impact of risperidone on mtCU. To do this I used EA.hy926 cells expressing 4mtD3cpv. The protocol that I used during the recording was the same that I used for my cytosolic measurements for the concentration-response curve, with a five minute pre-incubation in nominal absence of extracellular Ca^{2+} (Bachkoenig et al., 2022). **Figure 15a** displays representative traces of cells treated with different concentrations of risperidone (100 nM – 100 µM). I quantified the degree of inhibition by calculation of the ∆Ratio of 100 µM histamine triggered Ca^{2+} transients in the presence of different risperidone concentrations (**fig. 15c**). After normalization of the data to control cells which were not treated with risperidone, they were transformed and used to calculate a non-linear regression. The resulting concentration-response curve showed that the IC_{50} value for risperidone in the mitochondrial matrix was 2.23 (1.51 – 3.30) µM (**fig. 15b**). To compare the concentration-response curve of risperidone in the cytosol and in the mitochondria, I put them in one graph to illustrate the loss of efficient translation of Ca^{2+} signals from one organelle to the other (**fig. 15d**). Especially when considering the striking similarity in cells stimulated with different concentrations of histamine (**fig. 8d**)

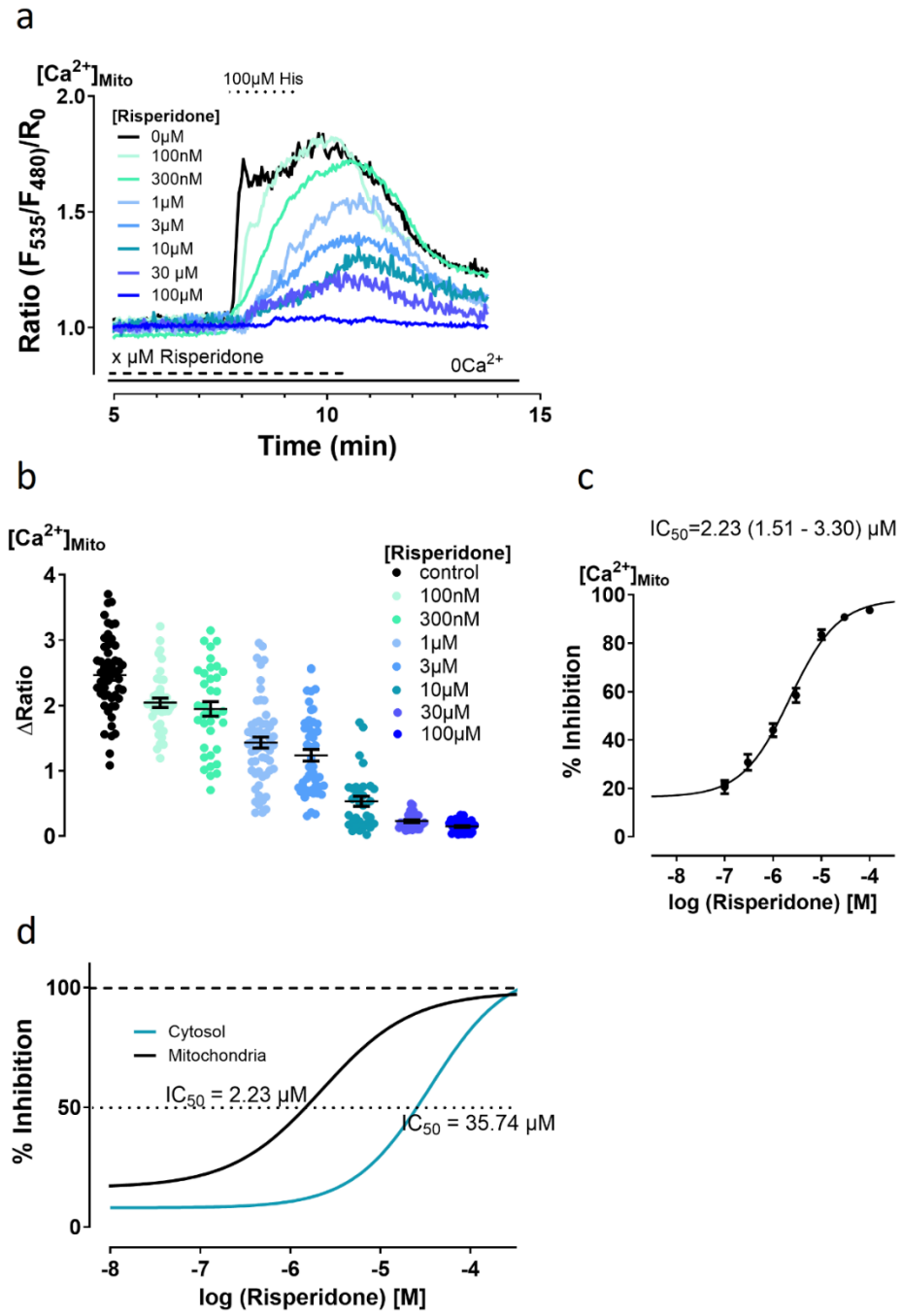

Figure 15 Characterization of the inhibitory effect of risperidone effect on mitochondrial Ca^{2+} elevations.

(a) Representative traces of EA.hy926 cells expressing 4mtD3cpv treated with different concentrations of risperidone (0.1 – 100 µM). (b) Concentration-response curve on risperidone in mitochondrial matrix calculated from ΔRatio (b) Quantification of risperidone-mediated inhibition on 100 µM histamine-triggered Ca^{2+} transients.(n = cells/wells; risperidone 0µM = 53/11; 0.1 µM = 40/9; 0.3 µM = 36/6; 1 µM = 58/9; 3 µM = 47/10; 10 µM = 32/9; 30 µM = 30/9; 100 µM = 34/6) (d) Comparison of risperidone-mediated inhibition of cytosolic versus mitochondrial Ca^{2+} signals. Reproduced from Bachkoenig et al, 2022 with permission of publisher Elsevier (Bachkoenig et al., 2022)

3.10 Describing the relation between mitochondrial and cytosolic Ca^{2+} signals under attenuation with risperidone

In my project, I studied the translation of cytosolic to mitochondrial Ca^{2+} signals, and I found a close connection between the ER and the mitochondria, which led to very efficient transmissions of Ca^{2+} signals (**fig. 8d**). This efficiency was not expected due to the MICU-mediated gatekeeping, but can be explained by the non-linear course of slope in the on-kinetics of Ca^{2+} transients, triggered by different histamine concentrations (**fig. 7d**). When I used risperidone to fine-tune IP_3-mediated Ca^{2+} release, I found the opposite. The slope of the on-kinetics in cytosolic Ca^{2+} transients declined linear to increasing concentrations of risperidone, while the translation of the signal into the mitochondria was disturbed. The experiments with different concentrations of histamine gave us the impression that this translation follows an all or nothing principle, which makes it hard to study processes that happen along this signaling cascade. Since a gradual change in the intensity of a mechanism can help to study it, I thought that inhibition of the histamine receptor with risperidone might help to achieve this in the transmission of Ca^{2+} from the ER to the mitochondria. To prove this, I ultimately correlated the ΔRatio from the mitochondria with the ΔRatio from the cytosol, both inhibited by risperidone, and looked for a regression model that fits best (**fig. 16a**). I found that linear regression was not able to fit ($R^2 = 0.63$), but a bi-linear regression did ($R^2 = 0.96$). I also correlated the ΔRatio from the mitochondria under risperidone, with the slope of cytosolic Ca^{2+} transients under risperidone. In this correlation also the bi-linear model gave the best fit ($R^2 = 0.99$), but the linear regression also exhibited a significant fit ($R^2 = 0.97$) (**fig. 16b**) (Bachkoenig et al., 2022).

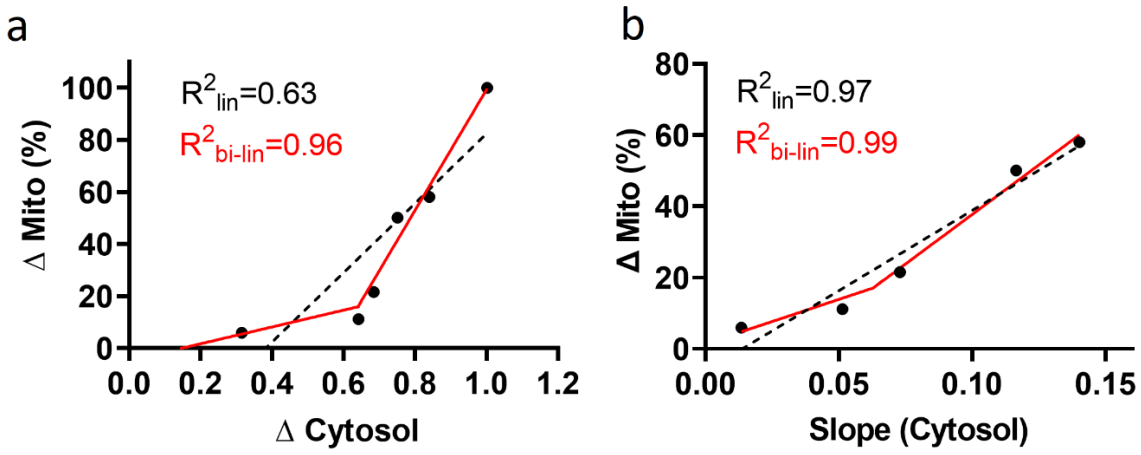

Figure 16 Describing the relation between mitochondrial and cytosolic Ca^{2+} signals under attenuation with risperidone

(a+b) Correlation of IP_3-triggered mitochondrial Ca^{2+} transients normalized to the average ΔRatio with 100 µM histamine with the corresponding cytosolic Ca^{2+} transients (a) and with the average slope of cytosolic Ca^{2+} transient (b) in the presence of risperidone. Graphs were generated with data shown in figure 8 a+c and 14 a, c and d. Data used for the creation of these graphs were extracted from fig. 9 d and e and fig. 15c. Reproduced from Bachkoenig et al, 2022 with permission of publisher Elsevier (Bachkoenig et al., 2022)

4 Discussion

In the present thesis I studied the interdependences of cytosolic to mitochondrial Ca^{2+} elevations, and how a cytosolic Ca^{2+} signal is translated into the mitochondrial matrix. The two organelles, ER and mitochondria, are tightly connected, and Ca^{2+} signals are transmitted efficiently. The cytosolic and mitochondrial Ca^{2+} signals show a correlation, but due to a threshold concentration of Ca^{2+} to be reached prior mitochondrial Ca^{2+} uptake, the mitochondrial Ca^{2+} signal is reduced. To study this atypical correlation between the cytosolic and mitochondrial matrix Ca^{2+}, the establishment of stable and reproducible elevations in cytosolic Ca^{2+} were necessary, which cannot be easily achieved by using various concentrations of an IP_3-generating agonist (e.g. histamine). Instead, I utilized an inhibitor, risperidone. In the course of this work, I quantified risperidones strong inhibitory potency against the histamine 1 receptor. Accordingly, I was able to develop stable and controlled cytosolic Ca^{2+} elevations by using histamine and various concentrations of the H1R antagonist, risperidone. This method disturbed the translation of cytosolic Ca^{2+} signals, and the amplitude of the signal arriving in the mitochondria got strongly diminished. These results point to a tightly directed signaling cascade, starting at the H1R continued via IP_3 to the ER and ending with Ca^{2+} at the mitochondria.

The main goal in this project was to establish a model that resembles physiologic conditions as close as possible, as previously used models that used chelators or selective ionophores to control intracellular ion concentrations disrupt cellular integrity and the ion homeostasis (Sneyers et al., 2024; Yoshida et al., 2010). These changes have major effects and affect the subcellular ultrastructure. Ever since BAPTA was introduced as a tool to study the subcellular Ca^{2+} homeostasis, it has proved to be very useful for the modulation of cytosolic Ca^{2+} levels as an analytical tool to study Ca^{2+} signals (You et al., 1997), or as a buffer to reduce Ca^{2+} signals and study its effect (Kang et al., 2021). BAPTA is capable of specifically binding Ca^{2+}, and its high affinity and rapid dynamics perfectly match the requirements to study subcellular Ca^{2+} signalling. Over the years, however, scientists uncovered Ca^{2+} independent off-target effects, including consequences on mitochondrial respiration, the cytoskeleton or other cytosolic proteins (DIETER et al., 1993; Hardie, 2005; Richardson and Taylor, 1993; Saoudi et al., 2004). Another popular method to control cytosolic ion levels are selective ionophores, like ionomycin or gramicidin. The major problem of these reagents is that mostly the global cellular ion homeostasis gets disrupted. Usually, a plethora of transporters allows the cell to control its ion homeostasis, representing the basis for functional cell signaling and metabolic

pathways (Bachkoenig et al., 2022; Gottschalk et al., 2022a; Koshenov et al., 2022; Madreiter-Sokolowski et al., 2016b). Upon the usage of ionophores, the level of the respective subcellular ion relies on the concentration present in the buffer. This results in the same concentration of the ion of interest within the intra- and extracellular space, which is highly unphysiologic. Moreover, by changing the ion concentrations in the buffer, several transporters in the PM will be affected, and their function and activity will be changed. In this way, the experiment and its results can be affected, potentially introducing a bias to all findings and leading to misinterpretations. The model we introduced in this work does not suffer from these drawbacks, as it took advantage of the highly specific effects of risperidone on the H1R. Additionally, combining inhibitors with a fixed concentration of an agonist allows to titrate cytosolic Ca^{2+} signals in a stable linear way, without affecting subcellular ultrastructures (Bachkoenig et al., 2022). A weakness in our model is the cells that we used. Since EA.hy926 is an immortalised cell line, to strengthen our findings, it would have been a valuable addition to repeat the experiments in freshly isolated endothelial cells. HUVEC or PAEC cells are easily harvested primary endothelial cells that serve as an established model for in vitro studies, more closely resembling physiological conditions.

In this work, we show that the ER Ca^{2+} release via the IP_3 receptors is primarily transferred to the mitochondria. My data describing the on-kinetics of cytosolic Ca^{2+} signals show that the complex machinery of ER to mitochondria Ca^{2+} transfer is adjusted to efficiently create Ca^{2+} hotspots in MERCs, independent of agonist concentration. The proper function of this mechanism is essential to overcome the MICU1-dependent threshold of the MCUC. When I changed this non-linear decline in the on-kinetics to a linear one, using an H1R inhibitor, I changed the correlating translation of cytosolic to mitochondrial Ca^{2+} transients to a non-correlating course. Attenuation of signals allows scientists to study physiological processes, and to get insights into their functionality. Since I found that cytosolic and mitochondrial Ca^{2+} signals to some extent do not follow a linear correlation, I aimed to propose the inhibition of the H1R as an additional tool to modulate cellular Ca^{2+} signals, especially in regard of mitochondrial Ca^{2+} signal processing.

My findings showing the non-linear behavior in the on-kinetics of histamine-triggered Ca^{2+} elevations, which are a valuable addition to the understanding of the MICU-mediated gating of the MCUC. Since the identification of MICU1 as a protein of the MCUC, its Ca^{2+}-dependent opening of the pore and following Ca^{2+} influx into the matrix has been the object of interest of many scientists (Ahuja and Muallem, 2014; Gottschalk et al., 2022b, 2019; Kamer and Mootha,

2014a; Madreiter-Sokolowski et al., 2016b). Differences between the three paralogues of the MICU-proteins are still not clear yet. What we know so far is that MICU1 and 2 are the most abundant and expressed isoforms in most tissues, while MICU3 is expressed in neurons exclusively (Patron et al., 2019b). Only MICU1 directly interacts with the MCUC, while MICU2 and 3 bind to MICU1 (Paillard et al., 2018; Phillips et al., 2019b; Wu et al., 2020; Xing et al., 2019). A lot of reports show that the proteins form heterodimers, while MICU1 can also form homodimers and hexamers (Waldeck-Weiermair et al., 2015; Wang et al., 2014). Since all three proteins have EF-hand domains, I can assume that they act in a Ca^{2+}-dependent way. There have been reports that show differences in the gatekeeping mediated by MICU1 and 2, highlighting that both proteins have distinct effects on mitochondrial Ca^{2+} homeostasis (Kamer and Mootha, 2014b; Patron et al., 2014). These publications support the theory that the stoichiometry of the MCUC is a fine-tuned tool that allows the regulation of mitochondrial Ca^{2+} homeostasis. On the other hand, the reports from Gottschalk et al. that focus on the localization of MICU1 in the CJ under basal conditions show that the gatekeeping of MICU1 is partly mediated by controlling the localization of MCU within the IMM, and the dynamic changes in the distribution of the MCUC proteins deliver an explanation how Ca^{2+} in different concentrations follow different paths, with different characteristics (Gottschalk et al., 2022b, 2019). Moreover, the data on MICU1 draw two quiet different pictures of the functionality of the protein. While we know that it is important for the structure of the CJ by forming homohexamers (Gottschalk et al., 2022b, 2019), we also know that it interacts with the MCUC as a homo- or heterodimer. Moreover, it is also known that there are dynamic changes in the distribution of this protein in the IMM (Gottschalk et al., 2022b, 2019). An explanation for controversial reports about its effect on mitochondrial Ca^{2+} could be that the localization, and its interaction partners, determine its function. While it is in its hexameric form in the CJ, MICU1 contains the MCU apart from minor Ca^{2+} elevations. But through high, fast Ca^{2+} signals, exceeding the MICU1 mediated threshold, this changes. It separates into dimers, releases MCU into the IBM where it interacts with EMRE, and has a stimulating effect on the capacity of the channel. This transition of MICU1 happens during IP_3-mediated Ca^{2+} signals in non-excitable cells, and is independent of the concentration of the stimulant. In excitable cells, Hirtl et al found some differences (Hirtl et al., 2025). While under basal conditions MCU was evenly distributed among the IMM, upon depolarization of AC16 cells MCU moved towards the cristae membrane. Inhibition of the H1R disturbs this translation severely (Bachkoenig et al., 2022), pointing strongly towards a diminished reorganization of MICU1 molecules in the IMM which results in MCU being not able to re-localize into the IBM, thus decreasing mitochondrial Ca^{2+} uptake.

When I started my experiments to investigate the cytosolic [Ca^{2+}], I decided to use Fura2 since it is a well-established, easy-to-use Ca^{2+} dye with high reliability. It allowed us to detect Ca^{2+} signals over a wide range of histamine concentrations used and by calculation of the AUC I was able to calculate a concentration-response curve that represented the actual cellular reaction to histamine stimulation, despite the quantification of the cellular response to histamine by analyzing the AUC was not my first choice. Usually, the ΔRatio (basal to maximal) is the commonly chosen parameter to describe the cells' reaction to histamine stimulation. In my hands, however, analysis of the ΔRatio did not fit an expected linear decline of the signal by decreasing the agonist concentration. Therefore, I next calculated the AUC, and found the continuous decrease that I expected upon decreasing histamine concentrations. As observed from the representative curves, it is visible that the initial peak did not significantly differ between different histamine concentrations used. In the later phase, however, transients were slowly declining to a more stable plateau phase with some oscillations visible. Such a non-linear decline in the ΔRatio could be caused by a saturation of the Fura2, which has a reported K_d for Ca^{2+} at roughly 200 nM. Under basal conditions, the cytosolic [Ca^{2+}] is around 100 nM (Clapham, 2007), indicating the K_d of Fura2 for Ca^{2+} is almost reached already under basal conditions. Contrary, my experiments using two sequential stimulations with histamine and ATP showed that the ATP-triggered elevations had a trend to be higher compared to the histamine-triggered ones, indicating that even a stimulation with 100 µM of histamine did not cause maximal Fura2 saturation. To ensure that my signals lie within the linear part of the used sensor, I would, however, need to permeabilize my cells and titrate extracellular Ca^{2+} to determine the detection rate in my experimental setting.

Moreover, the slopes of the on-kinetics of the Ca^{2+} elevations show that there was no linear decline with decreasing histamine concentrations. This explains why the ΔRatio was not fitting to create the dose-response curve. Since the elevations do not decrease evenly, the ΔRatio did not either. To quantify the average slope of the on-kinetics induced by histamine has been a challenge. I needed a standardized tool to determine the point of transient initiation. My macro that calculated the average ratio, and the standard deviation from one minute of the recorded signal of every single cell before it got stimulated, proved to be a suitable tool to objectively determine a significant change in the signal, thus the beginning of the IP_3-triggered elevation.

When I recorded these measurements, the delay between two time-points was chosen to be two seconds. This might raise doubt about the quality of the data and the possibility to determine the slope in the on-kinetics, since the spacing between two time-points might be too big to accurately follow the kinetics of a Ca^{2+} elevation. On the other hand, first the obtained data matched the course of the ΔRatios, and second, one could observe the oscillatory pattern of the Ca^{2+} transient in the plateau phase, pointing towards an acquisition speed that matched the kinetics of the Ca^{2+} signals. If this imaging settings were too slow, I would not be able to determine a reliable quantification of the maximum response of the cell, or were able to follow the repetitive increases during the oscillatory pattern. Moreover, Gottschalk et al recorded differences in the spatial and temporal patterns across different mitochondrial substructures and their imaging pace was with a delay of one second (Gottschalk et al., 2022b). Hence, they imaged faster, but they also imaged the flow of Ca^{2+} in a narrower spatial area, within different substructures of the mitochondria, while in this work, I only observed the rise of a Ca^{2+} elevation in the mitochondrial matrix. In this regard, it might have been a valuable addition to repeat the measurements using an ER-targeted Ca^{2+} sensor, e.g. D1ER, to observe the changes in the organellar Ca^{2+} release. But so far, cytosolic Ca^{2+} measurements have been a reliable tool to display ER Ca^{2+} release. Even upon changing mtCU, cytosolic Ca^{2+} transients remain stable independent of diminishing or activating mtCU using inhibitors or activators, respectively. This can, of course, be due to SERCA activity that constantly pumps Ca^{2+} into the ER, or by NCX activity that exports Ca^{2+} from the cell in exchange for Na^{2+}. In case of the experiments in this work, the cytosolic clearance of excess Ca^{2+} should mainly be due to NCX, because if SERCA were to take the Ca^{2+} back up into the ER, there would be no SOCE-induced peaks. This means that the cycling of Ca^{2+} within a cell follows strict routes, and the refilling process of the ER happens mainly from the extracellular space, which has been shown to be mediated by Orai and NCX in EA.hy926 cells and in primal cortical neurons (Di Giuro et al., 2017; Sisalli et al., 2014).

The sensor that was used for the mitochondrial Ca^{2+} measurements was 4mtD3cpv. It was published in 2006, nearly 20 years ago, but still, it is a valuable and reliable tool to investigate Ca^{2+} signals and homeostasis in the mitochondrial matrix. It allowed us to create a concentration-response curve for histamine that revealed a slightly higher EC_{50} value than I found in the cytosol. This could of course, be due to the higher K_d value of the two sensors used (200 nM vs. 600 nM), but since my cytosolic measurements with D3cpv reproduced my findings with Fura2, I can still trust my observations using the mitochondrial-targeted sensor. To repeat my cytosolic measurements with D3cpv was not only a valuable addition to this work because of the different affinities for Ca^{2+}, but also because of another difference between

Fura2 and 4mtD3cpv. Fura2 is a dye that was used to incubate the cells immediately before the measurements were started, while D3cpv and 4mtD3cpv are genetically encoded sensors. The cells need to be transfected approximately 40 hours before the measurement, which is already a stress factor for the cells, and they express an artificial protein in a high abundance, which also contains a Ca^{2+} binding site. These factors could have changed the findings between the two organelles, leading to an artefact mediating the described effect of risperidone. But since this was not true for my measurements with histamine concentrations, and the subsequent experiments with risperidone, I can exclude that.

After I created the concentration-response curve, I tried to find a way to compare them. The most objective way to do this is to look at the EC_{50} values since this is the most important parameter to characterize an agonist. Since these values lie in a very narrow range, I can already conclude that the two curves are similar. Moreover, by putting them in one graph, you can see that the linear increase in the relation between agonist concentration and cellular response happens in a comparable concentration range. Finally, I chose the concentration of histamine that is close to the EC_{50} for both compartments, normalized them to the maximum cellular response, and compared them. Even though the difference appeared not big, the statistical evaluation using a t-test gave a significant result. This points to the regulation of mtCU by the MCUC and the threshold mediated by MICU proteins for activation of MCU opening. A valuable addition to these measurements would have been to use a Ca^{2+} sensor targeted to the IMS (Waldeck-Weiermair et al., 2019b) to illustrate the regulatory step to be within the IMM but not the OMM. Since VDAC creates big pores that can be easily passed by ions (Colombini et al., 1996; Heslop et al., 2021), the OMM should not create a barrier that changes the concentration-response curves. But, the opening of the CJ and MCU translocation are the expected steps to cause this shift (Gottschalk et al., 2022b, 2019).

Risperidone was first reported in 1988 (Janssen et al., 1988). It was introduced as a new neuroleptic drug that shows both, serotonin as well as dopamine antagonism, and higher efficacy compared to standard medication for schizophrenia at that time, ritanserin and haloperidol. Already in the first publication, the anti-histaminic side effect was detected, while the strength of this effect was not completely assessable. But soon after this, in a second publication, the affinity for several receptors were further studied with radioligand binding assays in tissue-membrane preparations, and $-\log IC_{50}$ = 8.3 M and a K_d of 2.23 nM for the histamine-H1 receptor (Leysen et al., 1988) was reported. The potency of risperidone was further strengthened by showing that risperidone inhibited effects induced by Lysergic acid

diethylamid (LSD) (Meert et al., 1989), which showed that its affinity for 5-HT2 receptors was stronger than LSDs, pointing out that even in a competitive setting for ligation, risperidone showed strong effects. Soon, the first clinical trials were conducted, and promising results were found (Castelão et al., 1989; Claus et al., 1992; Gelders et al., 1990). Risperidone treatment even led to a reduction of hospital days in chronic schizophrenia patients (Addington et al., 1993). In 1995, one year after the FDA approved the prescription of risperidone, a study was released that displayed the impact of risperidone on the treatment of schizophrenia, becoming already the second most used antipsychotic in the clinic (Carter et al., 1995), and, in 2013, risperidone was added to the WHO Model List of Essential Medicines. Even though this medication has become a widely used therapeutic for people who suffer from schizophrenia, my data show that the antihistaminic side effect was probably underestimated due to its low affinity for the H1R, but since even low cytosolic inhibition of histamine-triggered Ca^{2+} signals are dramatically potentiated in the mitochondria, I want to highlight that this side-effect should not be neglected.

The H1R is expressed in various tissues and fulfills multiple physiological functions in the body (Andersson et al., 2017; Hasenöhrl, 2001; Niijima-Yaoita et al., 2012; Thangam et al., 2018). Since the receptor is participating in neurological processes, histamine can be categorized as neurotransmitter. It is an important agonist in the regulation of the sleep-wake rhythm (Thakkar, 2011), and inhibition of the H1R leads to sleepiness. The primary effect of risperidone during manic episodes is to attenuate the effect of increased dopamine and noradrenalin concentrations. Due to its inhibitory effect on the H1R, this effect is further enhanced. However, this induction of sleepiness and sedation leads to a restricted lifestyle in patients and highlights the need for a more specific treatment that allows patients with schizophrenia to live with fewer limitations. To achieve this goal, the dosage of any treatment needs to be properly adjusted, and more importantly, our understanding of neuronal signaling needs to be further deepened. The complexity of neuronal signaling can be explained with the following example. Success during learning gets rewarded with dopamine release, and attenuated by histamine release (Hasenöhrl, 2001). This attenuation is necessary to focus, as the inhibition of H1R in this setting leads to the dopamine releasing effect.

But the H1R is not only essential in neuro-signaling, but has also an important effect in skeletal muscle during training and recovery (Niijima-Yaoita et al., 2012; Sieck et al., 2025; Van der Stede et al., 2021). After training sessions, skeletal muscles release histamine. This histamine affects surrounding endothelial cells in the vasculature, leading to vasodilatation and increased

permeability. This ensures that the muscle is provided with sufficient nutrients during the recovery phase. Since it has been shown that physical exercise is an effective part of the therapy in patients suffering from schizophrenia (Guo et al., 2024), the side effect on the H1R has a tremendously limiting effect on the lifestyle of patients. On the one hand the tiring effect makes it harder for patients to exercise, and the negative effect during the recovery phase reduces the effectiveness of the training. Since risperidones affinity for the histamine receptor was not very strong, I decided to use it in my study, because I expected it to allow us to mildly attenuate histamine-triggered signals. My assumption was confirmed by my cytosolic experiments, and the IC_{50} value I found was rather high, 35.74 (27.42 – 46.58) µM. Similar to my findings derived upon reduction of the histamine concentration used for stimulation, I used the AUC to find a steady decline in the cellular response, while the ∆Ratio changed in a non-linear way. Moreover, since the ∆Ratio behaved comparable to when I decreased the agonist concentration, I can only conclude that the fast rise in the on-kinetics of cytosolic transients is essential for the proper translation into the mitochondria, and only small deceleration is sufficient to disturb it. My data suggest that this temporal delay disrupts the formation of microdomains of high calcium at the MCUC, leading to less efficient MCUC activation/opening, resulting in the decrease of mtCU.

My later experiments with Mepyramine revealed a comparable effect, both in the cytosol and in the mitochondria. In order to be sure that the two compounds act in the same way, it would have been necessary to create a concentration-response curve for mepyramine in EA.hy926 cells too, at least for measuring [Ca^{2+}] in the cytosol. The recordings needed to create the concentration response curve would also have allowed us to determine the decay of the slope in the on-kinetics, and further measurements would have allowed us to choose a concentration more comparable to the effect of 10 µM risperidone. But since 100 nM showed an increased effect in the mitochondria compared to the cytosol, I can conclude that inhibition of the H1R leads to a drastic decrease in mitochondrial Ca^{2+}, independent of the H1R antagonist used, which is associated with a decrease in mitochondrial respiration rate (Madreiter-Sokolowski et al., 2019a). Moreover, since Mepyramine shows a comparable effect on the translation of cytosolic to mitochondrial Ca^{2+} signals as risperidone, the data represent a strong argument against the assumption that risperidone has an inhibitory effect on the MCUC.

When I tested my protocol for the sequential stimulation, I found only in the initial peak, but not in the following plateau phase a decrease in the signal. This could be due to receptor internalization, insufficient restoration of Phosphatidylinositol-4,5-biphosphate (PIP_2) in the

PM, or insufficient ER Ca^{2+} refilling (Burghi et al., 2021; Tropmann et al., 2021). In my first experiment, in the absence of risperidone, I found a decrease in the initial spike, from 0.5 ± 0.14 to 0.43 ± 0.11, which is a 15.6% decrease. When I added 10 µM risperidone to my experiments, I found a decrease from 0.45 ± 0.11 to 0.31 ± 0.1 (31.3%) when I added risperidone in the first phase of histamine, and a decrease from 0.5 ± 0.11 to 0.28 ± 0.1 (44.8%) when I added it in the second phase. Whenever I added risperidone to my measurements I saw a stronger decrease in the 100 µM histamine triggered signal. If I assume that the 15.6% decrease without risperidone was an artefact caused by the reasons mentioned before, I can see that these factors also apply to the measurements in the presence of 10 µM risperidone. When I added risperidone during the first histamine stimulation, the cells were not able to recover completely because the ∆Ratio of the second peak showed a trend to be lower than the ∆Ratio of the first peak without risperidone. On the other hand, the inhibitory effect of risperidone was stronger when I added it only during the second stimulation phase (31.3 vs. 44.8%). When I later changed the protocol to stimulation with two different IP_3-generating agents, histamine and ATP, I excluded at least the factor of receptor internalization that influences the signals. Moreover, this change allowed us to compare the effect of risperidone to uninhibited ER Ca^{2+} release within one cell. Since the ∆Release and the subsequent ∆SOCE induced by ATP showed the trend to be higher than the ones induced by histamine in control cells, one can speculate that either the restoration of PIP_2 in the inner leaflet of the PM happens fast enough so the second stimulation is not diminished due to lack of substrate for Phospholipase C (PLC), or the distribution of histamine receptors and purinergic receptors in the PM is spatially different so they do not share the same reservoir of PIP_2.

Another aspect raising interest was the fact that ATP-triggered transients showed a different shape compared to histamine-triggered ones. This can not only be observed in Fura2-loaded cells, but also in cells expressing 4mtD3cpv or D3cpv. Although I did not characterize these differences since they had no obvious impact on my work, it appears that there is a difference in the transients evoked by these two agonists. It is hard to argue that, since both receptors share the same signaling cascade (MAGUIRE and DAVENPORT, 2005; Wang et al., 2015), and both are involved in inflammatory processes and vaso-constriction and -dilation (Guns et al., 2006). Since H1R is mainly involved in allergic reactions and P2Y receptors are majorly involved in multiple other mechanisms, including thrombocyte aggregation or neurotransmission, however, the hypothesis that they transmit different Ca^{2+} signals to the cell is not far. Nevertheless, the difference between those signals could simply be explained by the expression level of the two receptors. So, quantifying expression levels on the mRNA and

protein levels would be an easy step to support this theory. Moreover, the localization of the receptors on the PM could lead to a difference in the evoked Ca^{2+} elevations, depending on their location in a more central or peripheral part of the cell.

Proteins that are known to be differently distributed within a cell are the four isoforms of the IP_3 - receptor. While types 1a and 1b are located close to the PM, types 2 and 3 are more evenly distributed within 1 to 7 µm from the PM of DT40 cells (Bartok et al., 2019b). Moreover, there is a difference in the Ca^{2+} release through all types of IP_3 receptors, with type two showing the most efficient transfer of Ca^{2+} into the mitochondria (Bartok et al., 2019b). This also allows us to speculate on the molecular basis for my findings of diminished Ca^{2+} transfer in the presence of histamine antagonists. If the inhibition of the H1R would create a shift in coupling from one specific isoform of the IP_3 receptor towards another isoform, this could explain why the translation of the signal gets strongly disturbed. I could investigate this with the help of siRNA-mediated KD of IP_3 receptor subtypes. If I would find that the KD of one specific isoform mimic the effect of histamine receptor inhibition, I could assume that this isoform is tightly coupled to the corresponding G-protein coupled receptor. On top, overexpression experiments could be included, since a higher abundance of the isoform could rescue the inhibitory effect. Additionally, tracking the propagation of the cytosolic Ca^{2+} elevations spatially in the cell using line scans (Hammer et al., 2015) could give valuable information on the signal transduction across the cell, and how it is changed by inhibition of the H1R or IP_3 receptor-KD. Since Bartok et al. also found differences in the spatial distribution of IP_3 receptor subtypes in their experiments, this data would support the theory (Bartok et al., 2019b). My data show that the most important aspect that is affected by risperidone are the kinetics of the cytosolic Ca^{2+} elevations. Since the inhibitory effect starts already in the first step of the signaling cascade, it is most likely that this delay begins already at this step, and is then continued in the activation of PLC and thus in the release of IP_3 from the PM. Assuming that the distribution of IP_3 receptors follows a similar pattern in EA.hy926 cells as it does in DT40 cells, a slower release of IP_3 could be associated with a more superficial signal, thus reaching IP_3 receptors of the type 1, which would explain the reduced transfer of Ca^{2+} into the mitochondrial matrix.

When I looked for a model to describe my findings, I found that the correlation between mitochondrial and cytosolic Ca^{2+} signals followed a non-linear decline under attenuation with risperidone. This was even more pronounced in the absence of risperidone, when I titrated histamine in EA.hy926 cells (**fig. 7+8**). Although the inhibition using H1R antagonists disrupted the translation of Ca^{2+} elevations from the cytosol to the mitochondria, the reduction of

histamine showed a comparable decrease in both organelles. I showed that the kinetics in the early phase of Ca^{2+} elevations represent the basis for the efficient translation of Ca^{2+} from the ER to the mitochondria, and a delay disturbs the signaling cascade fundamentally, which has tremendous effects on the bioenergetic household of the cell. The difference in the translation efficacy between different concentrations of histamine and the inhibition of the signaling cascade right at the beginning points out how important the tight coupling of the two organelles, ER and mitochondria, in Ca^{2+} signaling is. An additional way to study IP_3-mediated Ca^{2+} signals is to load cells with caged IP_3 and release it via photolysis (Bartlett et al., 2020; Matsu-ura et al., 2019b). As the amount of released IP_3 could be changed by adjustments in the intensity and duration of the ultraviolet light signal, the intensity of the evoked signals in the studied cells can be regulated. This approach could have been used as an additional way to study cellular IP_3-triggered Ca^{2+} signals in different quantities and could have further deepened my insights into crucial aspects of the efficient translation of cytosolic to mitochondrial Ca^{2+} signals. Since this artificial introduction of IP_3 into the cytosol skips the activation of PLC, regulatory steps in the generation of IP_3 are omitted. This could result in a shortened presence of IP_3 and thus more transient opening of the corresponding receptors. In this scenario, the speed of IP_3 recycling could have a major impact on sustained ER Ca^{2+} release. By releasing IP_3 in the cytosol, I could start the signaling cascade directly before the release of Ca^{2+} from the ER. It has been shown before that uncaging IP_3 allows to initiate cytosolic Ca^{2+} oscillations in primary hepatocytes (Bartlett et al., 2020). But by skipping the activation of PLC via a G-protein-coupled receptor, an essential part of the signaling cascade is missing. The G-protein $G_{q/11}$ activates the isoform β of PLC (Berstein et al., 1992; Hubbard and Hepler, 2006). This isoform contains a C2 domain, which is a Ca2+-dependent lipid-binding domain. This domain is important, as the release of the Ca^{2+} from the ER mediated by IP_3 negatively influences the enzymes activity since it leads to a translocation from the PM to the cytosol (Yilmaz et al., 2011). Via this mechanism, the enzyme is separated from its substrate, and the generation of IP_3 and DAG is reduced. Another mechanism to regulate IP_3–mediated Ca^{2+} release from the ER is the effect of Ca^{2+} on IP_3-receptors (Paknejad and Hite, 2018; Emily A. Schmitz et al., 2022). While IP_3-receptors need Ca^{2+} to be activated, high Ca^{2+} concentrations have an inhibitory effect. Consequently, after a quick rise in cytosolic Ca^{2+} levels, the release from the ER gets slowed down, the Ca^{2+} is buffered by mitochondria, extruded from the cell via NCX (WHEATLY et al., 2007) and taken back up into the ER via SERCA (Inoue et al., 2019). These are a few prominent examples, how the cell is able to cope with the rapid Ca^{2+} elevations and how the concentration of Ca^{2+} in the cytosol is lowered again. Since the self-limitation of the Ca^{2+} signal is then attenuated again, the release of Ca^{2+} from the ER re-increases, resulting in

an oscillatory pattern. (Bartlett et al., 2020; Matsu-ura et al., 2019b). These oscillations are high and fast elevations in cytosolic Ca^{2+}, hence, it can be expected that they are able to overcome the mitochondrial threshold of Ca^{2+} uptake, thus rearranging the CJ structure (Gottschalk et al., 2022b, 2019) and allowing the entry of Ca^{2+} into the mitochondrial matrix. So, the question arises whether risperidone has an effect on cytosolic oscillations, which then influences the uptake of Ca^{2+} into the mitochondria. Since these oscillations are the result of the synergistic interplay of several mechanisms (Giorgi et al., 2018; Hubbard and Hepler, 2006; Inoue et al., 2019; Emily A. Schmitz et al., 2022; WHEATLY et al., 2007), it would be hard to point out one specific effect. To investigate this, one would need to increase the resolution in the monitoring and recording of Ca^{2+} signals (Bartlett et al., 2020). The release of Ca^{2+} from the ER is facilitated by immobilized patches of IP_3-receptors (Atakpa-Adaji et al., 2024; Ivanova et al., 2024). The signals emanating from these patches are spatially limited events (Bartlett et al., 2020). That means, to record the dynamics of the Ca^{2+} signals, I would need to choose a region of interest on the subcellular level. In this way, I could observe the course of Ca^{2+} transients originating from a single patch. These recordings would allow us to study the effect of different concentrations of histamine and risperidone on the dynamics and the spatial expansion of IP_3-mediated Ca^{2+} release.

In this work, I studied the tethering of the ER and the mitochondria in Ca^{2+} signaling. I found confirmation for the threshold of MCUC activation and a strong connection between these two organelles, allowing efficient translation of Ca^{2+} fluxes from the ER to the mitochondrial matrix. Moreover, I found that this efficient translation got disrupted by the inhibition of the H1R, pointing out the bioenergetic burden represented by the side effects of risperidone and antihistamines. The effect described in this work could especially be used for *in-vitro* studies to titrate the amount of Ca^{2+} transferred to the mitochondrial matrix, which is a useful tool for studying mitochondrial Ca^{2+} homeostasis and the complex mechanisms underlying mitochondrial Ca^{2+} uptake. Moreover, my study raises an interesting off-target effect of risperidone, which could further be investigated in various disease models in the future.

Bibliography

Addington, D.E., Jones, B., Bloom, D., Chouinard, G., Remington, G., Albright, P., 1993. Reduction of hospital days in chronic schizophrenic patients treated with risperidone: a retrospective study. Clin Ther 15, 917–26.

Ahuja, M., Muallem, S., 2014. The gatekeepers of mitochondrial calcium influx: MICU1 and MICU2. EMBO Rep 15, 205–206. https://doi.org/10.1002/embr.201438446

Andersson, R., Galter, D., Papadia, D., Fisahn, A., 2017. Histamine induces KCNQ channel-dependent gamma oscillations in rat hippocampus via activation of the H1 receptor. Neuropharmacology 118, 13–25. https://doi.org/10.1016/j.neuropharm.2017.03.003

Antony, A.N., Paillard, M., Moffat, C., Juskeviciute, E., Correnti, J., Bolon, B., Rubin, E., Csordás, G., Seifert, E.L., Hoek, J.B., Hajnóczky, G., 2016. MICU1 regulation of mitochondrial Ca2+ uptake dictates survival and tissue regeneration. Nat Commun 7, 10955. https://doi.org/10.1038/ncomms10955

Atakpa-Adaji, P., Ivanova, A., Kujawa, K., Taylor, C.W., 2024. KRAP regulates mitochondrial Ca2+ uptake by licensing IP3 receptor activity and stabilizing ER–mitochondrial junctions. J Cell Sci 137. https://doi.org/10.1242/jcs.261728

Bachkoenig, O.A., Gottschalk, B., Malli, R., Graier, W.F., 2022. An unexpected effect of risperidone reveals a nonlinear relationship between cytosolic Ca2+ and mitochondrial Ca2+ uptake. pp. 13–35. https://doi.org/10.1016/bs.ctm.2022.09.001

Baradaran, R., Wang, C., Siliciano, A.F., Long, S.B., 2018. Cryo-EM structures of fungal and metazoan mitochondrial calcium uniporters. Nature 559, 580–584. https://doi.org/10.1038/s41586-018-0331-8

Bartlett, P.J., Cloete, I., Sneyd, J., Thomas, A.P., 2020. IP3-Dependent Ca2+ Oscillations Switch into a Dual Oscillator Mechanism in the Presence of PLC-Linked Hormones. iScience 23, 101062. https://doi.org/10.1016/j.isci.2020.101062

Bartok, A., Weaver, D., Golenár, T., Nichtova, Z., Katona, M., Bánsághi, S., Alzayady, K.J., Thomas, V.K., Ando, H., Mikoshiba, K., Joseph, S.K., Yule, D.I., Csordás, G., Hajnóczky, G., 2019a. IP3 receptor isoforms differently regulate ER-mitochondrial contacts and local calcium transfer. Nat Commun 10, 3726. https://doi.org/10.1038/s41467-019-11646-3

Bartok, A., Weaver, D., Golenár, T., Nichtova, Z., Katona, M., Bánsághi, S., Alzayady, K.J., Thomas, V.K., Ando, H., Mikoshiba, K., Joseph, S.K., Yule, D.I., Csordás, G., Hajnóczky, G., 2019b. IP3 receptor isoforms differently regulate ER-mitochondrial contacts and local calcium transfer. Nat Commun 10, 3726. https://doi.org/10.1038/s41467-019-11646-3

Baughman, J.M., Perocchi, F., Girgis, H.S., Plovanich, M., Belcher-Timme, C.A., Sancak, Y., Bao, X.R., Strittmatter, L., Goldberger, O., Bogorad, R.L., Koteliansky, V., Mootha, V.K., 2011. Integrative genomics identifies MCU as an essential component of the mitochondrial calcium uniporter. Nature 476, 341–345. https://doi.org/10.1038/nature10234

Baumgartner, H.K., Gerasimenko, J. V, Thorne, C., Ferdek, P., Pozzan, T., Tepikin, A. V, Petersen, O.H., Sutton, R., Watson, A.J.M., Gerasimenko, O. V, 2009. Calcium elevation in mitochondria is the main Ca2+ requirement for mitochondrial permeability transition pore (mPTP) opening. J Biol Chem 284, 20796–803. https://doi.org/10.1074/jbc.M109.025353

Berstein, G., Blank, J.L., Jhon, D.-Y., Exton, J.H., Rhee, S.G., Ross, E.M., 1992. Phospholipase C-β1 is a GTPase-activating protein for Gq/11, its physiologic regulator. Cell 70, 411–418. https://doi.org/10.1016/0092-8674(92)90165-9

Bonora, M., Bononi, A., De Marchi, E., Giorgi, C., Lebiedzinska, M., Marchi, S., Patergnani, S., Rimessi, A., Suski, J.M., Wojtala, A., Wieckowski, M.R., Kroemer, G., Galluzzi, L., Pinton, P., 2013. Role of the c subunit of the FO ATP synthase in mitochondrial permeability transition. Cell Cycle 12, 674–683. https://doi.org/10.4161/cc.23599

Bootman, M.D., Berridge, M.J., 1996. Subcellular Ca2+ signals underlying waves and graded responses in HeLa cells. Current Biology 6, 855–865. https://doi.org/10.1016/S0960-9822(02)00609-7

Brierley, G.P., Murer, E., Bachmann, E., 1964. Studies on ion transport: III. The accumulation of calcium and inorganic phosphate by heart mitochondria. Arch Biochem Biophys 105, 89–102. https://doi.org/10.1016/0003-9861(64)90239-5

Brustovetsky, N., Klingenberg, M., 1996. Mitochondrial ADP/ATP Carrier Can Be Reversibly Converted into a Large Channel by Ca2+. Biochemistry 35, 8483–8488. https://doi.org/10.1021/bi960833v

Burghi, V., Echeverría, E.B., Zappia, C.D., Díaz Nebreda, A., Ripoll, S., Gómez, N., Shayo, C., Davio, C.A., Monczor, F., Fernández, N.C., 2021. Biased agonism at histamine H1 receptor: Desensitization, internalization and MAPK activation triggered by antihistamines. Eur J Pharmacol 896, 173913. https://doi.org/10.1016/j.ejphar.2021.173913

Carafoli Ernesto, Rossi Carlo Stefano, Lehninger Albert, 1965. Uptake of Adenine Nucleotides by Respiring Mitochondria during Active Accumulation of Ca++ and Phosphate - PIIS0021925818974557.

Carraro, M., Giorgio, V., Šileikytė, J., Sartori, G., Forte, M., Lippe, G., Zoratti, M., Szabò, I., Bernardi, P., 2014. Channel Formation by Yeast F-ATP Synthase and the Role of

Dimerization in the Mitochondrial Permeability Transition. Journal of Biological Chemistry 289, 15980–15985. https://doi.org/10.1074/jbc.C114.559633

Carsten, M.E., 1969. Role of Calcium Binding by Sarcoplasmic Reticulum in the Contraction and Relaxation of Uterine Smooth Muscle.

Carsten, M.E., 1964. THE CARDIAC CALCIUM PUMP*.

Carter, C.S., Mulsant, B.H., Sweet, R.A., Maxwell, R.A., Coley, K., Ganguli, R., Branch, R., 1995. Risperidone use in a teaching hospital during its first year after market approval: economic and clinical implications. Psychopharmacol Bull 31, 719–25.

Castelão, J., Ferreira, L., Gelders, Y.G., Heylen, S.L.E., 1989. The efficacy of the D2 and 5-HT2 antagonist risperidone (R 64 766) in the treatment of chronic psychosis. Schizophr Res 2, 411–415. https://doi.org/10.1016/0920-9964(89)90034-0

Chaudhuri, D., Artiga, D.J., Abiria, S.A., Clapham, D.E., 2016. Mitochondrial calcium uniporter regulator 1 (MCUR1) regulates the calcium threshold for the mitochondrial permeability transition. Proceedings of the National Academy of Sciences 113. https://doi.org/10.1073/pnas.1602264113

Chen, J., Bassot, A., Giuliani, F., Simmen, T., 2021. Amyotrophic Lateral Sclerosis (ALS): Stressed by Dysfunctional Mitochondria-Endoplasmic Reticulum Contacts (MERCs). Cells 10, 1789. https://doi.org/10.3390/cells10071789

Clapham, D.E., 2007. Calcium Signaling. Cell 131, 1047–1058. https://doi.org/10.1016/j.cell.2007.11.028

Claus, A., Bollen, J., Cuyper, H. De, Eneman, M., Malfroid, M., Peuskens, J., Heylen, S., 1992. Risperidone versus haloperidol in the treatment of chronic schizophrenic inpatients: a multicentre double-blind comparative study. Acta Psychiatr Scand 85, 295–305. https://doi.org/10.1111/j.1600-0447.1992.tb01473.x

Colombini, M., Blachly-Dyson, E., Forte, M., 1996. VDAC, a Channel in the Outer Mitochondrial Membrane, in: Ion Channels. Springer US, Boston, MA, pp. 169–202. https://doi.org/10.1007/978-1-4899-1775-1_5

Connern, C.P., Halestrap, A.P., 1992. Purification and N-terminal sequencing of peptidyl-prolyl cis-trans-isomerase from rat liver mitochondrial matrix reveals the existence of a distinct mitochondrial cyclophilin. Biochem J 284 (Pt 2), 381–5. https://doi.org/10.1042/bj2840381

Contreras, L., Gomez-Puertas, P., Iijima, M., Kobayashi, K., Saheki, T., Satrústegui, J., 2007. Ca2+ Activation Kinetics of the Two Aspartate-Glutamate Mitochondrial Carriers, Aralar and Citrin. Journal of Biological Chemistry 282, 7098–7106. https://doi.org/10.1074/jbc.M610491200

Csordás, G., Renken, C., Várnai, P., Walter, L., Weaver, D., Buttle, K.F., Balla, T., Mannella, C.A., Hajnóczky, G., 2006. Structural and functional features and significance of the physical linkage between ER and mitochondria. J Cell Biol 174, 915–921. https://doi.org/10.1083/jcb.200604016

Csordás, G., Várnai, P., Golenár, T., Roy, S., Purkins, G., Schneider, T.G., Balla, T., Hajnóczky, G., 2010. Imaging Interorganelle Contacts and Local Calcium Dynamics at the ER-Mitochondrial Interface. Mol Cell 39, 121–132. https://doi.org/10.1016/j.molcel.2010.06.029

Csordás, G., Weaver, D., Hajnóczky, G., 2018. Endoplasmic Reticulum–Mitochondrial Contactology: Structure and Signaling Functions. Trends Cell Biol 28, 523–540. https://doi.org/10.1016/j.tcb.2018.02.009

D'Arcy, M.S., 2019. Cell death: a review of the major forms of apoptosis, necrosis and autophagy. Cell Biol Int 43, 582–592. https://doi.org/10.1002/cbin.11137

De Stefani, D., Raffaello, A., Teardo, E., Szabò, I., Rizzuto, R., 2011. A forty-kilodalton protein of the inner membrane is the mitochondrial calcium uniporter. Nature 476, 336–340. https://doi.org/10.1038/nature10230

Denton, R.M., 2009. Regulation of mitochondrial dehydrogenases by calcium ions. Biochimica et Biophysica Acta (BBA) - Bioenergetics 1787, 1309–1316. https://doi.org/10.1016/j.bbabio.2009.01.005

Denton, R.M., Richards, D.A., Chin, J.G., 1978. Calcium ions and the regulation of NAD+-linked isocitrate dehydrogenase from the mitochondria of rat heart and other tissues. Biochem J 176, 899–906. https://doi.org/10.1042/bj1760899

Di Giuro, C.M.L., Shrestha, N., Malli, R., Groschner, K., van Breemen, C., Fameli, N., 2017. Na +/Ca2+ exchangers and Orai channels jointly refill endoplasmic reticulum (ER) Ca2+ via ER nanojunctions in vascular endothelial cells. Pflugers Arch 469, 1287–1299. https://doi.org/10.1007/s00424-017-1989-8

DIETER, P., FITZKE, E., DUYSTER, J., 1993. BAPTA Induces a Decrease of Intracellular Free Calcium and a Translocation and Inactivation of Protein Kinase C in Macrophages. Biol Chem Hoppe Seyler 374, 171–174. https://doi.org/10.1515/bchm3.1993.374.1-6.171

Dong, Z., Shanmughapriya, S., Tomar, D., Siddiqui, N., Lynch, S., Nemani, N., Breves, S.L., Zhang, X., Tripathi, A., Palaniappan, P., Riitano, M.F., Worth, A.M., Seelam, A., Carvalho, E., Subbiah, R., Jaña, F., Soboloff, J., Peng, Y., Cheung, J.Y., Joseph, S.K., Caplan, J., Rajan, S., Stathopulos, P.B., Madesh, M., 2017. Mitochondrial Ca2+ Uniporter Is a Mitochondrial Luminal Redox Sensor that Augments MCU Channel Activity. Mol Cell 65, 1014-1028.e7. https://doi.org/10.1016/j.molcel.2017.01.032

Edgell, C.J.S., McDonald, C.C., Graham, J.B., 1983. Permanent cell line expressing human factor VIII-related antigen established by hybridization. Proc Natl Acad Sci U S A 80. https://doi.org/10.1073/pnas.80.12.3734

Fan, C., Fan, M., Orlando, B.J., Fastman, N.M., Zhang, J., Xu, Y., Chambers, M.G., Xu, X., Perry, K., Liao, M., Feng, L., 2018. X-ray and cryo-EM structures of the mitochondrial calcium uniporter. Nature 559, 575–579. https://doi.org/10.1038/s41586-018-0330-9

Gelders, Y., Heylen, S., Bussche, G., Reyntjens, A., Janssen, P., 1990. Pilot Clinical Investigation of Risperidone in the Treatment of Psychotic Patients. Pharmacopsychiatry 23, 206–211. https://doi.org/10.1055/s-2007-1014509

Giacomello, M., Drago, I., Bortolozzi, M., Scorzeto, M., Gianelle, A., Pizzo, P., Pozzan, T., 2010. Ca2+ Hot Spots on the Mitochondrial Surface Are Generated by Ca2+ Mobilization from Stores, but Not by Activation of Store-Operated Ca2+ Channels. Mol Cell 38, 280–290. https://doi.org/10.1016/j.molcel.2010.04.003

Giorgi, C., Marchi, S., Pinton, P., 2018. The machineries, regulation and cellular functions of mitochondrial calcium. Nat Rev Mol Cell Biol 19, 713–730. https://doi.org/10.1038/s41580-018-0052-8

Giorgio, V., von Stockum, S., Antoniel, M., Fabbro, A., Fogolari, F., Forte, M., Glick, G.D., Petronilli, V., Zoratti, M., Szabó, I., Lippe, G., Bernardi, P., 2013. Dimers of mitochondrial ATP synthase form the permeability transition pore. Proceedings of the National Academy of Sciences 110, 5887–5892. https://doi.org/10.1073/pnas.1217823110

Gottschalk, B., Klec, C., Leitinger, G., Bernhart, E., Rost, R., Bischof, H., Madreiter-Sokolowski, C.T., Radulović, S., Eroglu, E., Sattler, W., Waldeck-Weiermair, M., Malli, R., Graier, W.F., 2019. MICU1 controls cristae junction and spatially anchors mitochondrial Ca2+ uniporter complex. Nat Commun 10, 3732. https://doi.org/10.1038/s41467-019-11692-x

Gottschalk, B., Koshenov, Z., Bachkoenig, O.A., Rost, R., Malli, R., Graier, W.F., 2022a. MFN2 mediates ER-mitochondrial coupling during ER stress through specialized stable contact sites. Front Cell Dev Biol 10. https://doi.org/10.3389/fcell.2022.918691

Gottschalk, B., Koshenov, Z., Waldeck-Weiermair, M., Radulović, S., Oflaz, F.E., Hirtl, M., Bachkoenig, O.A., Leitinger, G., Malli, R., Graier, W.F., 2022b. MICU1 controls spatial membrane potential gradients and guides Ca2+ fluxes within mitochondrial substructures. Commun Biol 5, 649. https://doi.org/10.1038/s42003-022-03606-3

Guns, P.D.F., Van Assche, T., Fransen, P., Robaye, B., Boeynaems, J., Bult, H., 2006. Endothelium-dependent relaxation evoked by ATP and UTP in the aorta of P2Y2 -deficient mice. Br J Pharmacol 147, 569–574. https://doi.org/10.1038/sj.bjp.0706642

Guo, J., Liu, K., Liao, Y., Qin, Y., Yue, W., 2024. Efficacy and feasibility of aerobic exercise interventions as an adjunctive treatment for patients with schizophrenia: a meta-Analysis. Schizophrenia 10, 2. https://doi.org/10.1038/s41537-023-00426-0

Hajnóczky, G., Csordás, G., Yi, M., 2002. Old players in a new role: mitochondria-associated membranes, VDAC, and ryanodine receptors as contributors to calcium signal propagation from endoplasmic reticulum to the mitochondria. Cell Calcium 32, 363–377. https://doi.org/10.1016/S0143416002001872

Halestrap, A., Brenner, C., 2003. The Adenine Nucleotide Translocase: A Central Component of the Mitochondrial Permeability Transition Pore and Key Player in Cell Death. Curr Med Chem 10, 1507–1525. https://doi.org/10.2174/0929867033457278

Halestrap, A.P., 2004. Dual role for the ADP/ATP translocator? Nature 430, 984–984. https://doi.org/10.1038/nature02816

Halestrap, A.P., Davidson, A.M., 1990. Inhibition of Ca2+-induced large-amplitude swelling of liver and heart mitochondria by cyclosporin is probably caused by the inhibitor binding to mitochondrial-matrix peptidyl-prolyl *cis-trans* isomerase and preventing it interacting with the adenine nucleotide translocase. Biochemical Journal 268, 153–160. https://doi.org/10.1042/bj2680153

Hammer, K.P., Hohendanner, F., Blatter, L.A., Pieske, B.M., Heinzel, F.R., 2015. Variations in local calcium signaling in adjacent cardiac myocytes of the intact mouse heart detected with two-dimensional confocal microscopy. Front Physiol 5. https://doi.org/10.3389/fphys.2014.00517

Hardie, R.C., 2005. Inhibition of phospholipase C activity in Drosophila photoreceptors by 1,2-bis(2-aminophenoxy)ethane N,N,N′,N′-tetraacetic acid (BAPTA) and di-bromo BAPTA. Cell Calcium 38, 547–556. https://doi.org/10.1016/j.ceca.2005.07.005

Hasenöhrl, R., 2001. Comparison of intra-accumbens injection of histamine with histamine H1-receptor antagonist chlorpheniramine in effects on reinforcement and memory parameters. Behavioural Brain Research 124, 203–211. https://doi.org/10.1016/S0166-4328(01)00214-5

Heslop, K.A., Milesi, V., Maldonado, E.N., 2021. VDAC Modulation of Cancer Metabolism: Advances and Therapeutic Challenges. Front Physiol 12. https://doi.org/10.3389/FPHYS.2021.742839/FULL

Hirtl, M., Gottschalk, B., Bachkoenig, O.A., Oflaz, F.E., Madreiter-Sokolowski, C., Høydal, M.A., Graier, W.F., 2025. A novel super-resolution STED microscopy analysis approach to observe spatial MCU and MICU1 distribution dynamics in cells. Biochimica et Biophysica Acta (BBA) - Molecular Cell Research 1872, 119900. https://doi.org/10.1016/j.bbamcr.2025.119900

Horne, J.H., Meyer, T., 1997. Elementary Calcium-Release Units Induced by Inositol Trisphosphate. Science (1979) 276, 1690–1693. https://doi.org/10.1126/science.276.5319.1690

Huang, B., Gudi, R., Wu, P., Harris, R.A., Hamilton, J., Popov, K.M., 1998. Isoenzymes of Pyruvate Dehydrogenase Phosphatase. Journal of Biological Chemistry 273, 17680–17688. https://doi.org/10.1074/jbc.273.28.17680

Hubbard, K.B., Hepler, J.R., 2006. Cell signalling diversity of the Gqα family of heterotrimeric G proteins. Cell Signal 18, 135–150. https://doi.org/10.1016/j.cellsig.2005.08.004

Inoue, M., Sakuta, N., Watanabe, S., Zhang, Y., Yoshikaie, K., Tanaka, Y., Ushioda, R., Kato, Y., Takagi, J., Tsukazaki, T., Nagata, K., Inaba, K., 2019. Structural Basis of Sarco/Endoplasmic Reticulum Ca2+-ATPase 2b Regulation via Transmembrane Helix Interplay. Cell Rep 27, 1221-1230.e3. https://doi.org/10.1016/j.celrep.2019.03.106

Ivanova, A., Atakpa-Adaji, P., Rao, S., Marti-Solano, M., Taylor, C.W., 2024. Dual regulation of IP3 receptors by IP3 and PIP2 controls the transition from local to global Ca2+ signals. Mol Cell 84, 3997-4015.e7. https://doi.org/10.1016/j.molcel.2024.09.009

Janikiewicz, J., Szymański, J., Malinska, D., Patalas-Krawczyk, P., Michalska, B., Duszyński, J., Giorgi, C., Bonora, M., Dobrzyn, A., Wieckowski, M.R., 2018. Mitochondria-associated membranes in aging and senescence: structure, function, and dynamics. Cell Death Dis 9, 332. https://doi.org/10.1038/s41419-017-0105-5

Janssen, P.A., Niemegeers, C.J., Awouters, F., Schellekens, K.H., Megens, A.A., Meert, T.F., 1988. Pharmacology of risperidone (R 64 766), a new antipsychotic with serotonin-S2 and dopamine-D2 antagonistic properties. J Pharmacol Exp Ther 244, 685–93.

Kamer, K.J., Mootha, V.K., 2014a. MICU1 and MICU2 play nonredundant roles in the regulation of the mitochondrial calcium uniporter. EMBO Rep 15, 299–307. https://doi.org/10.1002/embr.201337946

Kamer, K.J., Mootha, V.K., 2014b. MICU1 and MICU2 play nonredundant roles in the regulation of the mitochondrial calcium uniporter. EMBO Rep 15, 299–307. https://doi.org/10.1002/embr.201337946

Kang, K., Kim, J., Ryu, B., Lee, S., Oh, M., Baek, J., Ren, X., Canavero, S., Kim, C., Chung, H.M., 2021. BAPTA, a calcium chelator, neuroprotects injured neurons in vitro and promotes motor recovery after spinal cord transection in vivo. CNS Neurosci Ther 27, 919–929. https://doi.org/10.1111/cns.13651

Karch, J., Kwong, J.Q., Burr, A.R., Sargent, M.A., Elrod, J.W., Peixoto, P.M., Martinez-Caballero, S., Osinska, H., Cheng, E.H.-Y., Robbins, J., Kinnally, K.W., Molkentin, J.D., 2013. Bax and

Bak function as the outer membrane component of the mitochondrial permeability pore in regulating necrotic cell death in mice. Elife 2. https://doi.org/10.7554/eLife.00772

Kokoszka, J.E., Waymire, K.G., Levy, S.E., Sligh, J.E., Cai, J., Jones, D.P., MacGregor, G.R., Wallace, D.C., 2004. The ADP/ATP translocator is not essential for the mitochondrial permeability transition pore. Nature 427, 461–465. https://doi.org/10.1038/nature02229

Koshenov, Z., Oflaz, F.E., Hirtl, M., Bachkoenig, O.A., Rost, R., Osibow, K., Gottschalk, B., Madreiter-Sokolowski, C.T., Waldeck-Weiermair, M., Malli, R., Graier, W.F., 2020. The contribution of uncoupling protein 2 to mitochondrial Ca2+ homeostasis in health and disease – A short revisit. Mitochondrion 55, 164–173. https://doi.org/10.1016/j.mito.2020.10.003

Koshenov, Z., Oflaz, F.E., Hirtl, M., Gottschalk, B., Rost, R., Malli, R., Graier, W.F., 2022. Citrin mediated metabolic rewiring in response to altered basal subcellular Ca2+ homeostasis. Commun Biol 5, 76. https://doi.org/10.1038/s42003-022-03019-2

Lawlis, V.B., Roche, T.E., 1981. Regulation of bovine kidney .alpha.-ketoglutarate dehydrogenase complex by calcium ion and adenine nucleotides. Effects on S0.5 for .alpha.-ketoglutarate. Biochemistry 20, 2512–2518. https://doi.org/10.1021/bi00512a023

Leysen, J.E., Gommeren, W., Eens, A., de Chaffoy de Courcelles, D., Stoof, J.C., Janssen, P.A., 1988. Biochemical profile of risperidone, a new antipsychotic. J Pharmacol Exp Ther 247, 661–70.

Madreiter-Sokolowski, C.T., Gottschalk, B., Parichatikanond, W., Eroglu, E., Klec, C., Waldeck-Weiermair, M., Malli, R., Graier, W.F., 2016a. Resveratrol Specifically Kills Cancer Cells by a Devastating Increase in the Ca2+ Coupling Between the Greatly Tethered Endoplasmic Reticulum and Mitochondria. Cellular Physiology and Biochemistry 39, 1404–1420. https://doi.org/10.1159/000447844

Madreiter-Sokolowski, C.T., Győrffy, B., Klec, C., Sokolowski, A.A., Rost, R., Waldeck-Weiermair, M., Malli, R., Graier, W.F., 2017. UCP2 and PRMT1 are key prognostic markers for lung carcinoma patients. Oncotarget 8, 80278–80285. https://doi.org/10.18632/oncotarget.20571

Madreiter-Sokolowski, C.T., Klec, C., Parichatikanond, W., Stryeck, S., Gottschalk, B., Pulido, S., Rost, R., Eroglu, E., Hofmann, N.A., Bondarenko, A.I., Madl, T., Waldeck-Weiermair, M., Malli, R., Graier, W.F., 2016b. PRMT1-mediated methylation of MICU1 determines the UCP2/3 dependency of mitochondrial Ca2+ uptake in immortalized cells. Nat Commun 7, 12897. https://doi.org/10.1038/ncomms12897

Madreiter-Sokolowski, C.T., Waldeck-Weiermair, M., Bourguignon, M.-P., Villeneuve, N., Gottschalk, B., Klec, C., Stryeck, S., Radulovic, S., Parichatikanond, W., Frank, S., Madl,

T., Malli, R., Graier, W.F., 2019a. Enhanced inter-compartmental Ca2+ flux modulates mitochondrial metabolism and apoptotic threshold during aging. Redox Biol 20, 458–466. https://doi.org/10.1016/j.redox.2018.11.003

Madreiter-Sokolowski, C.T., Waldeck-Weiermair, M., Bourguignon, M.-P., Villeneuve, N., Gottschalk, B., Klec, C., Stryeck, S., Radulovic, S., Parichatikanond, W., Frank, S., Madl, T., Malli, R., Graier, W.F., 2019b. Enhanced inter-compartmental Ca2+ flux modulates mitochondrial metabolism and apoptotic threshold during aging. Redox Biol 20, 458–466. https://doi.org/10.1016/j.redox.2018.11.003

MAGUIRE, J., DAVENPORT, A., 2005. Regulation of vascular reactivity by established and emerging GPCRs. Trends Pharmacol Sci. https://doi.org/10.1016/j.tips.2005.07.007

Mallilankaraman, K., Cárdenas, C., Doonan, P.J., Chandramoorthy, H.C., Irrinki, K.M., Golenár, T., Csordás, G., Madireddi, P., Yang, J., Müller, M., Miller, R., Kolesar, J.E., Molgó, J., Kaufman, B., Hajnóczky, G., Foskett, J.K., Madesh, M., 2012a. MCUR1 is an essential component of mitochondrial Ca2+ uptake that regulates cellular metabolism. Nat Cell Biol 14, 1336–1343. https://doi.org/10.1038/ncb2622

Mallilankaraman, K., Doonan, P., Cárdenas, C., Chandramoorthy, H.C., Müller, M., Miller, R., Hoffman, N.E., Gandhirajan, R.K., Molgó, J., Birnbaum, M.J., Rothberg, B.S., Mak, D.-O.D., Foskett, J.K., Madesh, M., 2012b. MICU1 Is an Essential Gatekeeper for MCU-Mediated Mitochondrial Ca2+ Uptake that Regulates Cell Survival. Cell 151, 630–644. https://doi.org/10.1016/j.cell.2012.10.011

Marchi, S., Corricelli, M., Branchini, A., Vitto, V.A.M., Missiroli, S., Morciano, G., Perrone, M., Ferrarese, M., Giorgi, C., Pinotti, M., Galluzzi, L., Kroemer, G., Pinton, P., 2019. Akt-mediated phosphorylation of MICU1 regulates mitochondrial Ca 2+ levels and tumor growth. EMBO J 38. https://doi.org/10.15252/embj.201899435

Mármol, P., Pardo, B., Wiederkehr, A., del Arco, A., Wollheim, C.B., Satrústegui, J., 2009. Requirement for Aralar and Its Ca2+-binding Sites in Ca2+ Signal Transduction in Mitochondria from INS-1 Clonal β-Cells. Journal of Biological Chemistry 284, 515–524. https://doi.org/10.1074/jbc.M806729200

Matsu-ura, T., Shirakawa, H., Suzuki, K.G.N., Miyamoto, A., Sugiura, K., Michikawa, T., Kusumi, A., Mikoshiba, K., 2019a. Dual-FRET imaging of IP3 and Ca2+ revealed Ca2+-induced IP3 production maintains long lasting Ca2+ oscillations in fertilized mouse eggs. Sci Rep 9, 4829. https://doi.org/10.1038/s41598-019-40931-w

Matsu-ura, T., Shirakawa, H., Suzuki, K.G.N., Miyamoto, A., Sugiura, K., Michikawa, T., Kusumi, A., Mikoshiba, K., 2019b. Dual-FRET imaging of IP3 and Ca2+ revealed Ca2+-

induced IP3 production maintains long lasting Ca2+ oscillations in fertilized mouse eggs. Sci Rep 9, 4829. https://doi.org/10.1038/s41598-019-40931-w

McCormack, J.G., Denton, R.M., 1979. The effects of calcium ions and adenine nucleotides on the activity of pig heart 2-oxoglutarate dehydrogenase complex. Biochemical Journal 180, 533–544. https://doi.org/10.1042/bj1800533

Meert, T.F., de Haes, P., Janssen, P.A.J., 1989. Risperidone (R 64 766), a potent and complete LSD antagonist in drug discrimination by rats. Psychopharmacology (Berl) 97, 206–212. https://doi.org/10.1007/BF00442251

MITCHELL, P., 1961. Coupling of Phosphorylation to Electron and Hydrogen Transfer by a Chemi-Osmotic type of Mechanism. Nature 191, 144–148. https://doi.org/10.1038/191144a0

Mnatsakanyan, N., Llaguno, M.C., Yang, Y., Yan, Y., Weber, J., Sigworth, F.J., Jonas, E.A., 2019. A mitochondrial megachannel resides in monomeric F1FO ATP synthase. Nat Commun 10, 5823. https://doi.org/10.1038/s41467-019-13766-2

Morciano, G., Preti, D., Pedriali, G., Aquila, G., Missiroli, S., Fantinati, A., Caroccia, N., Pacifico, S., Bonora, M., Talarico, A., Morganti, C., Rizzo, P., Ferrari, R., Wieckowski, M.R., Campo, G., Giorgi, C., Trapella, C., Pinton, P., 2018. Discovery of Novel 1,3,8-Triazaspiro[4.5]decane Derivatives That Target the c Subunit of F1/FO -Adenosine Triphosphate (ATP) Synthase for the Treatment of Reperfusion Damage in Myocardial Infarction. J Med Chem 61, 7131–7143. https://doi.org/10.1021/acs.jmedchem.8b00278

Nakagawa, T., Shimizu, S., Watanabe, T., Yamaguchi, O., Otsu, K., Yamagata, H., Inohara, H., Kubo, T., Tsujimoto, Y., 2005. Cyclophilin D-dependent mitochondrial permeability transition regulates some necrotic but not apoptotic cell death. Nature 434, 652–658. https://doi.org/10.1038/nature03317

Neginskaya, M.A., Solesio, M.E., Berezhnaya, E. V., Amodeo, G.F., Mnatsakanyan, N., Jonas, E.A., Pavlov, E. V., 2019. ATP Synthase C-Subunit-Deficient Mitochondria Have a Small Cyclosporine A-Sensitive Channel, but Lack the Permeability Transition Pore. Cell Rep 26, 11-17.e2. https://doi.org/10.1016/j.celrep.2018.12.033

Nguyen, N.X., Armache, J.-P., Lee, C., Yang, Y., Zeng, W., Mootha, V.K., Cheng, Y., Bai, X., Jiang, Y., 2018. Cryo-EM structure of a fungal mitochondrial calcium uniporter. Nature 559, 570–574. https://doi.org/10.1038/s41586-018-0333-6

Niijima-Yaoita, F., Tsuchiya, M., Ohtsu, H., Yanai, K., Sugawara, S., Endo, Y., Tadano, T., 2012. Roles of Histamine in Exercise-Induced Fatigue: Favouring Endurance and Protecting against Exhaustion. Biol Pharm Bull 35, 91–97. https://doi.org/10.1248/bpb.35.91

Novials, A., Vidal, J., Franco, C., Ribera, F., Sener, A., Malaisse, W.J., Gomis, R., 1997. Mutation in the Calcium-Binding Domain of the Mitochondrial Glycerophosphate Dehydrogenase Gene in a Family of Diabetic Subjects. Biochem Biophys Res Commun 231, 570–572. https://doi.org/10.1006/bbrc.1997.6147

Oflaz, F.E., Bondarenko, A.I., Trenker, M., Waldeck-Weiermair, M., Gottschalk, B., Bernhart, E., Koshenov, Z., Radulović, S., Rost, R., Hirtl, M., Pilic, J., Karunanithi Nivedita, A., Sagintayev, A., Leitinger, G., Brachvogel, B., Summerauer, S., Shoshan-Barmatz, V., Malli, R., Graier, W.F., 2025. Annexin A5 controls VDAC1-dependent mitochondrial Ca2+ homeostasis and determines cellular susceptibility to apoptosis. EMBO J 44, 3413–3447. https://doi.org/10.1038/s44318-025-00454-9

Ou, X., Ji, C., Han, X., Zhao, X., Li, X., Mao, Y., Wong, L.-L., Bartlam, M., Rao, Z., 2006. Crystal Structures of Human Glycerol 3-phosphate Dehydrogenase 1 (GPD1). J Mol Biol 357, 858–869. https://doi.org/10.1016/j.jmb.2005.12.074

Paillard, M., Csordás, G., Huang, K.-T., Várnai, P., Joseph, S.K., Hajnóczky, G., 2018. MICU1 Interacts with the D-Ring of the MCU Pore to Control Its Ca2+ Flux and Sensitivity to Ru360. Mol Cell 72, 778-785.e3. https://doi.org/10.1016/j.molcel.2018.09.008

Paknejad, N., Hite, R.K., 2018. Structural basis for the regulation of inositol trisphosphate receptors by Ca2+ and IP3. Nat Struct Mol Biol 25, 660–668. https://doi.org/10.1038/s41594-018-0089-6

Palmer, A.E., Giacomello, M., Kortemme, T., Hires, S.A., Lev-Ram, V., Baker, D., Tsien, R.Y., 2006. Ca2+ Indicators Based on Computationally Redesigned Calmodulin-Peptide Pairs. Chem Biol 13, 521–530. https://doi.org/10.1016/j.chembiol.2006.03.007

Palmer, A.E., Jin, C., Reed, J.C., Tsien, R.Y., 2004. Bcl-2-mediated alterations in endoplasmic reticulum Ca 2 analyzed with an improved genetically encoded fluorescent sensor.

Pan, X., Liu, J., Nguyen, T., Liu, C., Sun, J., Teng, Y., Fergusson, M.M., Rovira, I.I., Allen, M., Springer, D.A., Aponte, A.M., Gucek, M., Balaban, R.S., Murphy, E., Finkel, T., 2013. The physiological role of mitochondrial calcium revealed by mice lacking the mitochondrial calcium uniporter. Nat Cell Biol 15, 1464–1472. https://doi.org/10.1038/ncb2868

Parker, I., Choi, J., Yao, Y., 1996. Elementary events of InsP3-induced Ca2+ liberation in Xenopus oocytes: hot spots, puffs and blips. Cell Calcium 20, 105–121. https://doi.org/10.1016/S0143-4160(96)90100-1

Parker, I., Yao, Y., 1996. Ca2+ transients associated with openings of inositol trisphosphate-gated channels in Xenopus oocytes. J Physiol 491, 663–668. https://doi.org/10.1113/jphysiol.1996.sp021247

Patron, M., Checchetto, V., Raffaello, A., Teardo, E., Vecellio Reane, D., Mantoan, M., Granatiero, V., Szabò, I., De Stefani, D., Rizzuto, R., 2014. MICU1 and MICU2 Finely Tune the Mitochondrial Ca2+ Uniporter by Exerting Opposite Effects on MCU Activity. Mol Cell 53, 726–737. https://doi.org/10.1016/j.molcel.2014.01.013

Patron, M., Granatiero, V., Espino, J., Rizzuto, R., De Stefani, D., 2019a. MICU3 is a tissue-specific enhancer of mitochondrial calcium uptake. Cell Death Differ 26, 179–195. https://doi.org/10.1038/s41418-018-0113-8

Patron, M., Granatiero, V., Espino, J., Rizzuto, R., De Stefani, D., 2019b. MICU3 is a tissue-specific enhancer of mitochondrial calcium uptake. Cell Death Differ 26, 179–195. https://doi.org/10.1038/s41418-018-0113-8

Perocchi, F., Gohil, V.M., Girgis, H.S., Bao, X.R., McCombs, J.E., Palmer, A.E., Mootha, V.K., 2010. MICU1 encodes a mitochondrial EF hand protein required for Ca2+ uptake. Nature 467, 291–296. https://doi.org/10.1038/nature09358

Petrungaro, C., Zimmermann, K.M., Küttner, V., Fischer, M., Dengjel, J., Bogeski, I., Riemer, J., 2015. The Ca2+-Dependent Release of the Mia40-Induced MICU1-MICU2 Dimer from MCU Regulates Mitochondrial Ca2+ Uptake. Cell Metab 22, 721–733. https://doi.org/10.1016/j.cmet.2015.08.019

Phillips, C.B., Tsai, C.-W., Tsai, M.-F., 2019a. The conserved aspartate ring of MCU mediates MICU1 binding and regulation in the mitochondrial calcium uniporter complex. Elife 8. https://doi.org/10.7554/eLife.41112

Phillips, C.B., Tsai, C.-W., Tsai, M.-F., 2019b. The conserved aspartate ring of MCU mediates MICU1 binding and regulation in the mitochondrial calcium uniporter complex. Elife 8. https://doi.org/10.7554/eLife.41112

Pilic, J., Oflaz, F.E., Gottschalk, B., Erdogan, Y.C., Graier, W.F., Malli, R., 2024. Visualizing VDAC1 in live cells using a tetracysteine tag. PLoS One 19, e0311107. https://doi.org/10.1371/journal.pone.0311107

Putney, J.W., 1986. A model for receptor-regulated calcium entry. Cell Calcium 7, 1–12. https://doi.org/10.1016/0143-4160(86)90026-6

Raffaello, A., De Stefani, D., Sabbadin, D., Teardo, E., Merli, G., Picard, A., Checchetto, V., Moro, S., Szabò, I., Rizzuto, R., 2013. The mitochondrial calcium uniporter is a multimer that can include a dominant-negative pore-forming subunit. EMBO J 32, 2362–2376. https://doi.org/10.1038/emboj.2013.157

Richardson, A., Taylor, C.W., 1993. Effects of Ca2+ chelators on purified inositol 1,4,5-trisphosphate (InsP3) receptors and InsP3-stimulated Ca2+ mobilization. Journal of Biological Chemistry 268, 11528–11533. https://doi.org/10.1016/S0021-9258(19)50232-0

Rizzuto, R., Pinton, P., Carrington, W., Fay, F.S., Fogarty, K.E., Lifshitz, L.M., Tuft, R.A., Pozzan, T., 1998. Close Contacts with the Endoplasmic Reticulum as Determinants of Mitochondrial Ca2+ Responses. Science (1979) 280, 1763–1766. https://doi.org/10.1126/science.280.5370.1763

Rutter, G.A., Denton, R.M., 1989. The binding of Ca2+ ions to pig heart NAD+-isocitrate dehydrogenase and the 2-oxoglutarate dehydrogenase complex. Biochem J 263, 453–62. https://doi.org/10.1042/bj2630453

Rutter, G.A., Denton, R.M., 1988a. Regulation of NAD+-linked isocitrate dehydrogenase and 2-oxoglutarate dehydrogenase by Ca2+ ions within toluene-permeabilized rat heart mitochondria. Interactions with regulation by adenine nucleotides and NADH/NAD+ ratios. Biochem J 252, 181–9. https://doi.org/10.1042/bj2520181

Rutter, G.A., Denton, R.M., 1988b. Regulation of NAD+-linked isocitrate dehydrogenase and 2-oxoglutarate dehydrogenase by Ca2+ ions within toluene-permeabilized rat heart mitochondria. Interactions with regulation by adenine nucleotides and NADH/NAD+ ratios. Biochemical Journal 252, 181–189. https://doi.org/10.1042/bj2520181

Sancak, Y., Markhard, A.L., Kitami, T., Kovács-Bogdán, E., Kamer, K.J., Udeshi, N.D., Carr, S.A., Chaudhuri, D., Clapham, D.E., Li, A.A., Calvo, S.E., Goldberger, O., Mootha, V.K., 2013. EMRE Is an Essential Component of the Mitochondrial Calcium Uniporter Complex. Science (1979) 342, 1379–1382. https://doi.org/10.1126/science.1242993

Saoudi, Y., Rousseau, B., Doussière, J., Charrasse, S., Gauthier-Rouvière, C., Morin, N., Sautet-Laugier, C., Denarier, E., Scaïfe, R., Mioskowski, C., Job, D., 2004. Calcium-independent cytoskeleton disassembly induced by BAPTA. Eur J Biochem 271, 3255–3264. https://doi.org/10.1111/j.1432-1033.2004.04259.x

Sathyamurthy, V.H., Nagarajan, Y., Parvathi, V.D., 2024. Mitochondria-Endoplasmic Reticulum Contact Sites (MERCS): A New Axis in Neuronal Degeneration and Regeneration. Mol Neurobiol 61, 6528–6538. https://doi.org/10.1007/s12035-024-03971-6

Schmitz, Emily A, Takahashi, H., Karakas, E., 2022. Structural basis for activation and gating of IP3 receptors. Nat Commun 13, 1408. https://doi.org/10.1038/s41467-022-29073-2

Schmitz, Emily A., Takahashi, H., Karakas, E., 2022. Structural basis for activation and gating of IP3 receptors. Nat Commun 13, 1408. https://doi.org/10.1038/s41467-022-29073-2

Sieck, D.C., Kobak, S.H., Larson, E.A., Dreyer, H.C., Fogarty, M.J., Sieck, G.C., Minson, C.T., Halliwill, J.R., 2025. Histamine is a molecular transducer of adaptation to endurance exercise training in humans. J Appl Physiol 138, 1398–1410. https://doi.org/10.1152/japplphysiol.00687.2024

Sisalli, M.J., Secondo, A., Esposito, A., Valsecchi, V., Savoia, C., Di Renzo, G.F., Annunziato, L., Scorziello, A., 2014. Endoplasmic reticulum refilling and mitochondrial calcium extrusion promoted in neurons by NCX1 and NCX3 in ischemic preconditioning are determinant for neuroprotection. Cell Death Differ 21, 1142–1149. https://doi.org/10.1038/cdd.2014.32

Sneyers, F., Speelman-Rooms, F., Verhelst, S.H.L., Bootman, M.D., Bultynck, G., 2024. Cellular effects of BAPTA: Are they only about Ca2+ chelation? Biochimica et Biophysica Acta (BBA) - Molecular Cell Research 1871, 119589. https://doi.org/10.1016/j.bbamcr.2023.119589

Streb, H., Irvine, R.F., Berridge, M.J., Schulz, I., 1983. Release of Ca2+ from a nonmitochondrial intracellular store in pancreatic acinar cells by inositol-1,4,5-trisphosphate. Nature 306, 67–69. https://doi.org/10.1038/306067a0

Swann, K., Yu, Y., 2008. The dynamics of calcium oscillations that activate mammalian eggs. Int J Dev Biol 52, 585–594. https://doi.org/10.1387/ijdb.072530ks

Szabadkai, G., Bianchi, K., Várnai, P., De Stefani, D., Wieckowski, M.R., Cavagna, D., Nagy, A.I., Balla, T., Rizzuto, R., 2006. Chaperone-mediated coupling of endoplasmic reticulum and mitochondrial Ca2+ channels. J Cell Biol 175, 901–911. https://doi.org/10.1083/jcb.200608073

Takemura, H., Hughes, A.R., Thastrup, O., Putney, J.W., 1989. Activation of calcium entry by the tumor promoter thapsigargin in parotid acinar cells. Evidence that an intracellular calcium pool and not an inositol phosphate regulates calcium fluxes at the plasma membrane. J Biol Chem 264, 12266–71.

Thakkar, M.M., 2011. Histamine in the regulation of wakefulness. Sleep Med Rev 15, 65–74. https://doi.org/10.1016/j.smrv.2010.06.004

Thangam, E.B., Jemima, E.A., Singh, H., Baig, M.S., Khan, M., Mathias, C.B., Church, M.K., Saluja, R., 2018. The Role of Histamine and Histamine Receptors in Mast Cell-Mediated Allergy and Inflammation: The Hunt for New Therapeutic Targets. Front Immunol 9. https://doi.org/10.3389/fimmu.2018.01873

Tomar, D., Dong, Z., Shanmughapriya, S., Koch, D.A., Thomas, T., Hoffman, N.E., Timbalia, S.A., Goldman, S.J., Breves, S.L., Corbally, D.P., Nemani, N., Fairweather, J.P., Cutri, A.R., Zhang, X., Song, J., Jaña, F., Huang, J., Barrero, C., Rabinowitz, J.E., Luongo, T.S., Schumacher, S.M., Rockman, M.E., Dietrich, A., Merali, S., Caplan, J., Stathopulos, P., Ahima, R.S., Cheung, J.Y., Houser, S.R., Koch, W.J., Patel, V., Gohil, V.M., Elrod, J.W., Rajan, S., Madesh, M., 2016. MCUR1 Is a Scaffold Factor for the MCU Complex Function and Promotes Mitochondrial Bioenergetics. Cell Rep 15, 1673–1685. https://doi.org/10.1016/j.celrep.2016.04.050

Trenker, M., Malli, R., Fertschai, I., Levak-Frank, S., Graier, W.F., 2007. Uncoupling proteins 2 and 3 are fundamental for mitochondrial Ca2+ uniport. Nat Cell Biol 9, 445–452. https://doi.org/10.1038/ncb1556

Tropmann, K., Seibel-Ehlert, U., Littmann, T., Strasser, A., 2021. Shining light on the histamine H2 receptor: Synthesis of carbamoylguanidine-type agonists as a pharmacological tool to study internalization. Bioorg Med Chem Lett 52, 128388. https://doi.org/10.1016/j.bmcl.2021.128388

Tsai, M.-F., Phillips, C.B., Ranaghan, M., Tsai, C.-W., Wu, Y., Williams, C., Miller, C., 2016. Dual functions of a small regulatory subunit in the mitochondrial calcium uniporter complex. Elife 5. https://doi.org/10.7554/eLife.15545

Vais, H., Tanis, J.E., Müller, M., Payne, R., Mallilankaraman, K., Foskett, J.K., 2015. MCUR1, CCDC90A, Is a Regulator of the Mitochondrial Calcium Uniporter. Cell Metab 22, 533–5. https://doi.org/10.1016/j.cmet.2015.09.015

Vallese, F., Catoni, C., Cieri, D., Barazzuol, L., Ramirez, O., Calore, V., Bonora, M., Giamogante, F., Pinton, P., Brini, M., Calì, T., 2020. An expanded palette of improved SPLICS reporters detects multiple organelle contacts in vitro and in vivo. Nat Commun 11, 6069. https://doi.org/10.1038/s41467-020-19892-6

Van der Stede, T., Blancquaert, L., Stassen, F., Everaert, I., Van Thienen, R., Vervaet, C., Gliemann, L., Hellsten, Y., Derave, W., 2021. Histamine H1 and H2 receptors are essential transducers of the integrative exercise training response in humans. Sci Adv 7. https://doi.org/10.1126/sciadv.abf2856

Vasington, F.D., Murphy, J. V, 1962. Ca ion uptake by rat kidney mitochondria and its dependence on respiration and phosphorylation. J Biol Chem 237, 2670–7.

Waldeck-Weiermair, M., Duan, X., Naghdi, S., Khan, M.J., Trenker, M., Malli, R., Graier, W.F., 2010a. Uncoupling protein 3 adjusts mitochondrial Ca2+ uptake to high and low Ca2+ signals. Cell Calcium 48, 288–301. https://doi.org/10.1016/j.ceca.2010.10.004

Waldeck-Weiermair, M., Gottschalk, B., Madreiter-Sokolowski, C.T., Ramadani-Muja, J., Ziomek, G., Klec, C., Burgstaller, S., Bischof, H., Depaoli, M.R., Eroglu, E., Malli, R., Graier, W.F., 2019a. Development and Application of Sub-Mitochondrial Targeted Ca2 + Biosensors. Front Cell Neurosci 13, 449. https://doi.org/10.3389/fncel.2019.00449

Waldeck-Weiermair, M., Gottschalk, B., Madreiter-Sokolowski, C.T., Ramadani-Muja, J., Ziomek, G., Klec, C., Burgstaller, S., Bischof, H., Depaoli, M.R., Eroglu, E., Malli, R., Graier, W.F., 2019b. Development and Application of Sub-Mitochondrial Targeted Ca2 + Biosensors. Front Cell Neurosci 13. https://doi.org/10.3389/fncel.2019.00449

Waldeck-Weiermair, M., Malli, R., Naghdi, S., Trenker, M., Kahn, M.J., Graier, W.F., 2010b. The contribution of UCP2 and UCP3 to mitochondrial Ca2+ uptake is differentially

determined by the source of supplied Ca2+. Cell Calcium 47, 433–440. https://doi.org/10.1016/j.ceca.2010.03.004

Waldeck-Weiermair, M., Malli, R., Naghdi, S., Trenker, M., Kahn, M.J., Graier, W.F., 2010c. The contribution of UCP2 and UCP3 to mitochondrial Ca2+ uptake is differentially determined by the source of supplied Ca2+. Cell Calcium 47, 433–440. https://doi.org/10.1016/j.ceca.2010.03.004

Waldeck-Weiermair, M., Malli, R., Parichatikanond, W., Gottschalk, B., Madreiter-Sokolowski, C.T., Klec, C., Rost, R., Graier, W.F., 2015. Rearrangement of MICU1 multimers for activation of MCU is solely controlled by cytosolic Ca(2.). Sci Rep 5, 15602. https://doi.org/10.1038/srep15602

Wang, L., Yang, X., Li, S., Wang, Z., Liu, Y., Feng, J., Zhu, Y., Shen, Y., 2014. Structural and mechanistic insights into MICU1 regulation of mitochondrial calcium uptake. EMBO J 33, 594–604. https://doi.org/10.1002/embj.201386523

Wang, S., Iring, A., Strilic, B., Albarrán Juárez, J., Kaur, H., Troidl, K., Tonack, S., Burbiel, J.C., Müller, C.E., Fleming, I., Lundberg, J.O., Wettschureck, N., Offermanns, S., 2015. P2Y2 and Gq/G11 control blood pressure by mediating endothelial mechanotransduction. Journal of Clinical Investigation 125, 3077–3086. https://doi.org/10.1172/JCI81067

Wang, Y., Nguyen, N.X., She, J., Zeng, W., Yang, Y., Bai, X., Jiang, Y., 2019. Structural Mechanism of EMRE-Dependent Gating of the Human Mitochondrial Calcium Uniporter. Cell 177, 1252-1261.e13. https://doi.org/10.1016/j.cell.2019.03.050

Watanabe, A., Maeda, K., Nara, A., Hashida, M., Ozono, M., Nakao, A., Yamada, A., Shinohara, Y., Yamamoto, T., 2022. Quantitative analysis of mitochondrial calcium uniporter (MCU) and essential MCU regulator (EMRE) in mitochondria from mouse tissues and HeLa cells. FEBS Open Bio 12, 811–826. https://doi.org/10.1002/2211-5463.13371

WHEATLY, M.G., GAO, Y., STINER, L.M., WHALEN, D.R., NADE, M., VIGO, F., GOLSHANI, A.E., 2007. Roles of NCX and PMCA in Basolateral Calcium Export Associated with Mineralization Cycles and Cold Acclimation in Crayfish. Ann N Y Acad Sci 1099, 190–192. https://doi.org/10.1196/annals.1387.022

WOODFIELD, K., RÜCK, A., BRDICZKA, D., HALESTRAP, A.P., 1998. Direct demonstration of a specific interaction between cyclophilin-D and the adenine nucleotide translocase confirms their role in the mitochondrial permeability transition. Biochemical Journal 336, 287–290. https://doi.org/10.1042/bj3360287

Wu, W., Shen, Q., Zhang, R., Qiu, Z., Wang, Y., Zheng, J., Jia, Z., 2020. The structure of the MICU1-MICU2 complex unveils the regulation of the mitochondrial calcium uniporter. EMBO J 39. https://doi.org/10.15252/embj.2019104285

Xing, Y., Wang, M., Wang, J., Nie, Z., Wu, G., Yang, X., Shen, Y., 2019. Dimerization of MICU Proteins Controls Ca2+ Influx through the Mitochondrial Ca2+ Uniporter. Cell Rep 26, 1203-1212.e4. https://doi.org/10.1016/j.celrep.2019.01.022

Yilmaz, U., Schaefer, M., Kübler, W.M., Schülein, P.-D.R., 2011. Calcium-abhängige Translokation der Phospholipase c-β1a aus der Plasmamembran (dissertation). Medizinische Fakultät Charite, Berlin.

Yoo, J., Wu, M., Yin, Y., Herzik, M.A., Lander, G.C., Lee, S.-Y., 2018. Cryo-EM structure of a mitochondrial calcium uniporter. Science (1979) 361, 506–511. https://doi.org/10.1126/science.aar4056

Yoshida, H., Hirono, C., Shimamoto, C., Daikoku, E., Kubota, T., Sugita, M., Shiba, Y., Nakahari, T., 2010. Membrane potential modulation of ionomycin-stimulated Ca2+ entry via Ca2+/H+ exchange and SOC in rat submandibular acinar cells. The Journal of Physiological Sciences 60, 363–371. https://doi.org/10.1007/s12576-010-0098-7

You, Y., Pelzer, D.J., Pelzer, S., 1997. Modulation of L-type Ca2+ current by fast and slow Ca2+ buffering in guinea pig ventricular cardiomyocytes. Biophys J 72, 175–187. https://doi.org/10.1016/S0006-3495(97)78656-9

Zhou, Y., Jing, S., Liu, S., Shen, X., Cai, L., Zhu, C., Zhao, Y., Pang, M., 2022. Double-activation of mitochondrial permeability transition pore opening via calcium overload and reactive oxygen species for cancer therapy. J Nanobiotechnology 20, 188. https://doi.org/10.1186/s12951-022-01392-y

Zorov, D.B., Juhaszova, M., Yaniv, Y., Nuss, H.B., Wang, S., Sollott, S.J., 2009. Regulation and pharmacology of the mitochondrial permeability transition pore. Cardiovasc Res 83, 213–225. https://doi.org/10.1093/cvr/cvp151

List of Illustrations